PETROLEUM RESEARCH JOURNAL

TECHNICAL PAPERS

Screening of Libyan EOR Candidates (Applying MMP and MMC Criteria).....
M.M. Khazam, M. El Werfalli and A. A. Mesallati 1

Innovative Formation Damage Sample Evaluation Techniques .....
I.S.C. Spark, N. Fleming, M.T. Byrne and I.T.M. Patey 13

Review of Raguba Oil Field Miscibility Project .....
A.H. Al Kafagi 23

A Case History of Attic Oil Recovery of a Unique Multi-layered Bottom Water-drive Carbonate Reservoir .....
AM. Reda, C. Wong, M. Gharsalla and A. Majdoub 37

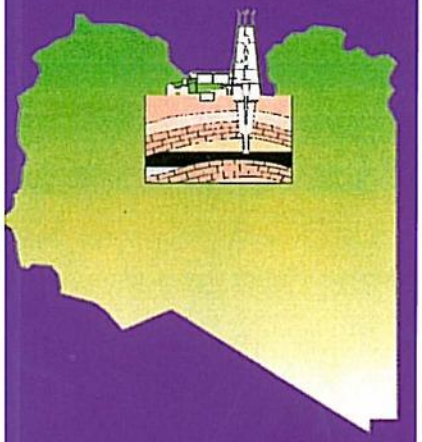
Water Shut Off Field Experiences to Improve Hydrocarbons Recovery in Depleted Reservoirs .....
G. Burrafato, E. Pitoni, G. Vietina and L. Mauri 45

Miscible Gas Displacement of Facha and Gir Reservoir Oils Using Farrud Reservoir Gas (Ghani Field) .....
M.F. Dahab and H.A. Belhaj 59

Abu Attiffel Field: Gas Injection Process to Improve the Final Oil Recovery .....
Emilio Causin, Elio Rossi, Francesco Radaelli and I.S. El Ageli 67

The Mabruk History or How to Develop a Challenging Field .....
Daniel Chaussumier and Benoît Ludot 83

4D Case History in North Kuwait .....
Tim Perrin 93



VOLUME 14 – (2002)

Petroleum Research Journal
P.O. Box 6431 Tripoli
Great Socialist People's Libyan Arab Jamahiriya

Petroleum Res. J. Vol. 14 (2002); P. 1–12, 2 Figs.

Screening of Libyan EOR Candidates (Applying MMP and MMC Criteria)

M.M. Khazam*, M. Werfalli* and A.A. Mesallati*

مسح لحقول النفط الليبية المرشحة لطرق الاسترداد الإضافي باستخدام معيار الضغط الأدنى للامتزاجية والمركبات الأدنى للامتزاجية

محسن م. خزام، و م. الورفلي و عزام أ. المسلاتي

إن كفاءة أو فاعلية طرق الاسترداد الإضافي وخاصة الطرق التي تشمل برامج الحقن بالغاز تتحكم فيها بشكل هام خواص موائع المكمن وكذلك درجة الحرارة والضغط. كما تسيطر عوامل أخرى مثل خواص صخور المكمن والقوة الدافعة في النجاح النهائي لتقنيات الاسترداد الإضافي. وقد تم في هذا العمل التركيز على تأثير خواص موائع المكمن فقط.

تم في هذه الدراسة تسليط الضوء على الأسئلة الأربعة التالية:

1 – ما هو الضغط الأدنى للمكمن الذي يكون عنده مائع المكمن قابل للامتزاج مع ثاني أكسيد الكربون؟ (طريقة الغمر بثاني أكسيد الكربون).

2 – ما هو الضغط الأدنى الذي يصبح عنده غاز الحقل قابل للامتزاجية مع سائل المكمن؟ (طريقة الغمر للامتزاجية بالتبخر الهيدروكربوني).

3 – في حالة عدم توفر إمكانية تشغيل المكمن عند أو أعلى من الضغط اللازم للحصول على الامتزاجية بالإتصال المتعدد مع ثاني أكسيد الكربون، هل يعد الحقن باستخدام ثاني أكسيد الكربون مثمر؟ (الغمر غير القابل للامتزاجية، باستخدام ثاني أكسيد الكربون).

4 – ما هو المائع المشبع المتبقي – مثل مكثفات الغاز المسال – وما هي الكمية المطلوبة إضافتها لغاز الحقل لحدوث الامتزاجية مع مائع المكمن عند درجة الحرارة والضغط الحالي؟ (الغمر عن طريق الامتزاجية بواسطة التكثيف الهيدروكربوني).

للإجابة على الأسئلة المشار إليها أعلاه يمكن استخدام عدة تقنيات إعتماداً على البيانات المتوفرة. فكلما كانت المعلومات أكثر إتاحة كلما قلّت درجة الغموض في إجاباتنا التي نقدمها.

تم في هذا العمل إستعمال العلاقات الرياضية المتوفرة للإجابة على الأسئلة سالفة الذكر، كما تم أيضاً مقارنة النتائج المتحصل عليها (باستخدام هذه العلاقات) ببعض بيانات التجارب المعملية.

هذا بالإضافة إلى توصية بضرورة إنتاج أفضل الطرق للقيام بعملية المسح.

Abstract: *The performance of the EOR methods, particularly those involving gas injection schemes, is governed significantly by the reservoir fluid properties and the reservoir temperature and pressure. Other factors like reservoir rock properties and the drive energy also control the ultimate success of the EOR technique. However, in this work, we concentrate on the influence of the properties of the reservoir fluids only.*

* National Oil Corporation, Tripoli, Libya.

We have also focused our attention on the following four questions:

1. *What is the minimum reservoir pressure at which the reservoir fluid will be miscible with CO_2? (miscible CO_2 flood.)*
2. *What is the minimum pressure at which field gas will become miscible with the reservoir fluid? (vaporising hydrocarbon miscible gas flood.)*
3. *If the reservoir can not be operated at or above the pressure required for achieving multiple contact miscibility with CO_2, could injection of CO_2 still be beneficial? (Immiscible CO_2 flood.)*
4. *What rich fluid stock – like LPG condensate – and how much of it has to be added to field gas to make it miscible with the reservoir fluid at the existing pressure and temperature? (condensing hydrocarbon miscible gas flood.)*

Depending on the information available, several techniques can be used to answer the questions raised above. Naturally, the more information we have at hand, the less will be the degree of uncertainty in the answers we provide. In this work, we have utilized the empirical correlations available in the literature to answer the questions. We have also compared the answers we obtained by the application of these correlations with some experimental data already generated in the laboratories. Based on these, we plan to recommend the best way to carry out the screening process.

INTRODUCTION

The search for tomorrow's oil reserves has directed the efforts of the energy industry to frontiers beyond the conventional exploration and production strategies. This is what is called the enhanced oil recovery (EOR). The results of successful application of this new technology will have a decisive impact on the energy conservation programme of any country.

The first step in formulating an EOR programme is to screen the reservoir using criteria based on past experience. This is done to select one or more possible techniques that are further investigated in more detail. During the last decade, several empirical correlations have been developed to help screen the reservoirs.

Here in Al Jamahiriya (GSPLAJ) a preliminary screening has been carried out using the initial oil in place (IOIP>500 MMSTB) as a first screening criterion to arrive at a preliminary list of 30 possible EOR candidates (Table, 1). Most of these are likely to be economical candidates for application of EOR by gas (CO_2 hydrocarbon and/or N_2 injector).

During 1986, the EOR department of National Oil Corporation (ONC) developed a set of guidelines for the implementation of EOR schemes in the GSPLAJ. These guidelines were drawn based on world-wide experience. Based on the guidelines, the operating companies have initiated several projects mainly concerned with the data gathering required for these schemes. In particular, they are concerned with experimental data generated in the laboratories. In some cases, field data generation, particularly determination of residual oil saturation, has also been initiated. The experimental data being generated by the operating companies consists mainly of reservoir fluid compositions, miscibility limits and core floods. Data is being generated for possible application of miscible or immiscible CO_2 floods and miscible hydrocarbon floods.

Since 1986, the EOR department has carried out two major projects[1,5] which are of particular importance to the selection of the optimum gas injection scheme. The first work is concerned with the compilation of all data pertaining to the gas reserves and their compositions. The gases considered were hydrocarbon gases from associated and non-associated sources and CO_2. The second major work involved the ongoing studies on technical and EOR planning. Part of the work involved the detailed study of the behavior of reservoir fluids of chosen reservoirs. The expertise gained in these two studies enabled us to review the guidelines formulated by the department with particular emphasis on Libyan oils. The present work is one such outcome of this endeavor.

CO_2 injection is known to improve recovery by several mechanisms. These include the generation of miscibility by multiple contact and the reduction of viscosity and the swelling of the oil volume by dissolution. Reduction in the viscosity of the oil will lead to improved mobility ratio which, in turn, can lead to improvement in the vertical and areal sweeps and increased displacement efficiencies. Swelling of the oil will lead to reduction in the amount of oil left behind in the reservoir for the same liquid saturation. Both these factors can improve the performance of the reservoir if the CO_2 injection is followed by water flood.

Except for reservoirs at high pressure, miscible hydrocarbon flood is realized by a condensing drive mechanism. The gas that will achieve this has to be fairly rich in its propane/butane content. Field gases seldom contain these components in sufficient amounts. It is then usually necessary to blend the

field gases with rich fluids like LPG to enable them to achieve miscibility with the reservoir fluid.

The objectives of the study are summarized as follows:

1. To determine the miscibility limits for the reservoir fluids with CO_2 and hydrocarbon gases (vaporizing and condensing drives).
2. To determine the swelling factor and viscosity reduction for immiscible CO_2 injection.
3. Based on 1 and 2, the recommended EOR schemes that will warrant further investigations for the reservoirs, will be decided, and the current EOR programme of the operating companies, in the light of the results generated herein, will be reviewed.
4. The best method to screen reservoir fluid data, to evaluate the feasibility of gas injection schemes, will be recommended.

METHODOLOGY

The detailed compositional analysis of all the reservoir fluids was collected from the PVT reports. This information was input into the empirical correlations listed below to generate the required miscible limits. The empirical correlations used are:

CO_2 MMP Limit

Holm and Josendal, 1974 modified by Mungan, 1981[9]
Cronquist, 1978[10]
Petroleum Recovery Institute, 1979[11]
Yellig and Metcalf, 1980[7]
Johnsons and Pollin, 1981[8]
Alston, 1985[12]
Glaso, 1985[14]
Eakin and Mitch, 1988[15]

Hydrocarbon Vaporising Drive

Glaso, 1985[14]
Glaso, 1990[16]
Firoozabadi and Aziz, 1986[17]

Hydrocarbon Condensing Drive

Benham *et al*, 1960[13]
Glaso, 1985[14]

Immiscible CO_2 Drive

Simon and Graue, 1965[18]

The results generated by these different correlations were analysed for their consistency using statistical methods. They were also compared with the experimental data available. Based on these, a limited number of these correlations was chosen to evaluate the feasibility of the processes.

The results generated, using these correlations, were then compared to other available data from the reservoir to decide on the feasibility of the different gas injection schemes.

RESULTS

The Holm, Josendal and Mungan, Yellig-Metcalfe, Glaso, and Eakin-Mitch correlations perform better than the others for CO_2 MMP prediction.

There is good agreement between the predictions made for rich gas miscibility limits using the correlations of Benham *et al.* and Glaso. Any one of them can be used for screening purposes.

There is poor agreement in the predictions made for vaporizing hydrocarbon miscibility limits using the correlations of Firoozabadi and Aziz and those of Glaso. Since not much experimental data is available it is not possible to assess their relative merits. However, the correlations of Firoozabadi and Aziz were developed based on results with lean hydrocarbon gas. Glaso developed his correlation based on results with nitrogen gas. In this study, we are mainly concerned with the feasibility of using lean gas for EOR. Hence, the correlations of Firoozabadi and Aziz were used for the screening purpose.

Miscible CO_2 flood is feasible in 20 out of the 26 candidates. Abu Attiffel appears to be suitable for CO_2 flood and hydrocarbon vaporizing gas flood using field gas.

Out of the remaining six candidate reservoirs, only Ragubat and Kotlat are suitable for enriched gas injection.

The immiscible CO_2 flood appears attractive in three of the four remaining shallow reservoirs (Bahi PL-7, Gialo Eocene and Dahra PL-7/YPL-7).

No EOR process involving gas injection appears suitable for Dahra-Hofra PL-5 reservoir unit.

Good consistency exists between the operating companies (OPCO's) EOR programme and the results of this study.

DISCUSSION

Database

The database consists of the detailed compositions of reservoir fluids. The pertinent data are summarized in Table 1 with a wide range of PVT properties as summarized in Table 2.

Table 1. Reservoir fluid compositions and properties of Libyan EOR candidates.

Component	Sarir C-Main	Sarir C-North	Sarir L	Messla	N.A..U (TBG))	N.A.U (BAM)	Haram	Kotla	Nasser North	Nasser South		Raguba	Jebel	LDM	Bahi PL7	Dahra-Jofra PL5
N_2	1.050	0.740	1.03	1.760	1.520	1.420	0.920	1.140	0.830	0.600	0.400	0.620	0.290	0.980	0.200	0.110
CO_2	1.120	1.150	0.74	1.240	0.590	1.150	0.800	0.000	1.920	1.510	1.340	1.080	1.410	3.920	.420	0.520
H_2S	0.000	0.000	0.00	0.000	0.000	0.000	0.000	0.000	0.210	0.940	0.650	0.000	0.000	0.000	0.390	0.380
C1	10.820	5.580	4.32	17.710	37.290	38.850	10.480	13.323.	29.610	22.050	18.770	32.510	42.020	49.040	4.350	18.550
C2	4.340	3.180	3.00	7.530	5.420	5.240	2.540	290	10.680	10.760	8.720	10.580	7.440	9.260	3.750	6.990
C3	8.220	4.960	3.55	8.470	4.510	4.300	2.180	6.050	7.280	7.610	5.540	7.520	6.640	5.520	9.260	6.560
C4	8.630	4.650	5.45	7.520	4.540	4.250	2.770	7.000	5.260	5.980	4.440	6.730	5.390	4.550	11.610	7.890
C5	6.400	6.230	6.56	5.100	2.670	3.290	2.720	6.050	3.470	3.540	4.040	5.200	3.990	3.220	9.890	6.700
C6	4.450	6.580	6.25	3.980	3.570	3.300	2.470	4.910	5.330	1.920	4.290	4.410	3.840	3.010	7.130	6.200
C7+	54.970	66.930	69.11	46.690	39.890	38.200	75.120	58.240	35.410	45.090	51.810	31.350	28.980	20.500	53.000	46.100
M.Wt C7+	290	208	210	230	310	308	382	281	214	227	222	201	227	179	195	188
API C7+	32	-	-	36	33	33	22	27	0	36	37	38	34	46	38	39
Oil API gravity	37	40	41	37	34	33	23	32	38	38	37	40	36	50	44	44
PI (psig)	3.909	3.906	4.006	3.970	4.272	4.695	2.012	2.450	2.457	2.457	2.457	2.385	3.375	4.028	1.188	959
Pb (psig)	715	500	544	1.320	3.530	2.790	540	545	2.060	1.395	1.178	2.385	3.310	3.780	222	942
Temp (deg F)	225	230	240	238	230	240	184	164	170	170	178	214	206	262	150	129
Pb density (gm/cc)	0.749	0.745	0.756	0.699	0.716	0.711	0.853	0.790	0.695	0.717	0.735	0.629	0.635	0.507	0.762	0.712
Pb viscosity (cp)	1.120	2.050	0.610	0.713	1.010	1.010	15.690	2.040	0.550	0.620	0.800	0.350	0.310	0.115	1.010	0.600
Pb FVF (RB/STB)	1.232	1.170	1.175	1.456	1.344	1.370	1.094	1.141	1.377	1.335	1.256	1.680	1.710	2.320	1.140	1.278
Diff. Initial GOR (SCF/STB)	192	167	187	460	498	551	78	160	775	528	370	1036	1090	1971	200	427

Component	Samah	Waha North	Waha South	Defa	Gialo Eocene	Gialo Pale.	Dahra Pl7/YPL7	Amal B	Amal E	Amal N	Gahni L-Earrud	Zenad Earrud	Intisar-D	Abu-Attifel Main
N_2	0.710	0.520	0.510	1.390	0.310	0.480	0.760	1.250	0.980	1.560	0.000	0.150	0.000	0.240
CO_2	0.600	0.200	0.140	0.280	1.420	0.970	1.270	0.700	0.900	0.800	2.100	0.270	1.350	3.365
H_2S	0.000	0.000	0.000	0.000	0.490	0.170	2.100	0.000	0.000	0.000	0.000	0.000	0.000	0.000
C1	8.080	17.320	23.060	21.320	1.470	14.620	5.290	26.900	35.790	29.720	33.810	29.720	33.550	58.952
C2	2.230	6.920	6.930	6.210	2.110	6.750	5.120	6.970	7.590	7.670	8.030	6.420	5.350	9.044
C3	3.780	9.460	8.610	8.110	2.930	6.410	3.010	6.800	6.920	6.740	8.900	7.350	4.410	3.138
C4	3/800	7.030	6.400	6.370	4.670	7.500	5.810	6.370	5.600	5.890	7.310	5.490	4.650	2.005
C5	3.510	5.010	4.530	3.840	6.280	5.620	7.300	4.650	4.160	4.140	4.910	4.450	3.654	1.444
C6	3.580	4.420	4..120	5.450	5.900	5.020	4.590	4.340	2.840	3.980	2.910	3.880	5.006	1.630
C7+	73.710	49.120	45.700	47.030	74.420	52.460	64.750	42.120	34.220	39.500	32.030	42.270	42.080	20.784
M.Wt C7+	247	226	227	257	234	222	198	261	262	262	201	202	219	244
API C7+	34	34	34	31	35	36	35	34	35	-	36	-	-	-
Oil API gravity	35	35	35	36	38	39	39	35	38	37	38	37	39	42
PI (psig)	2.705	2.983	2.963	2.490	1.176	2.726	1.129	4.875	4.675	4.675	2.340	2.385	4.257	6.868
Pb (psig)	536	1.075	1.400	1.204	137	910	398	1.921	2.639	2.185	2.093	1.717	2.225	5.746
Temp (deg F)	214	180	180	156	125	209	146	220	234	239	170	180	226	300
Pb density(gm/Co)	0.767	0.733	0.725	0.745	0.796	0.722	0.766	0.707	0.676	0.689	0.669	0.688	0.677	0.585
Pb viscosity (cp)	1.290	0.840	0.800	0.992	2.380	0.680	1.180	0.840	0.555	0.590	0.320	0.590	0.460	0.460
Pb FVF (RB/STB)	1.158	1.315	1.344	1.255	1.067	1.315	1.140	1.393	1.520	1.448	1.603	1.472	1.460	2.009
Diff. Initial GOR (SCF/STB)	133	420	488	352	48	381	149	537	750	602	980	713	525	1.747

Table 2 . Range of PVT data.

	Minimum	Maximum
API of oil	23	50
Temperature, deg F	125	300
Initial GOR, scf/stb	49	1972
Mwt of C7+	179	382
Mwt of C5+	156	363

Evaluation of the Correlations

A. CO_2 MMP

Figure 1 shows the predictions of the correlations. The ordinate is the value of the MMP predicted while the abscissa is the average of the MMPs predicted by the eight correlations. There is a wide scatter in the results. Predicted MMPs vary by as much as 1000 psi from the average values predicted by the correlations. On the basis of this information alone, it was not possible to choose the appropriate correlation for the screening work.

Figure 2 shows the plot of the experimental MMP for these reservoir fluids against the MMP predicted by the correlations. The correlations of Holm, Josendal and Mangan, Yellig-Metcalfe, Glaso, and Eakin-Mitch performed better than others. The predictions deviated from the experimental results by about 400 psi. The standard deviations of these correlations were 16, 13, 17 and 17% respectively. The complete data are given in Table 3.

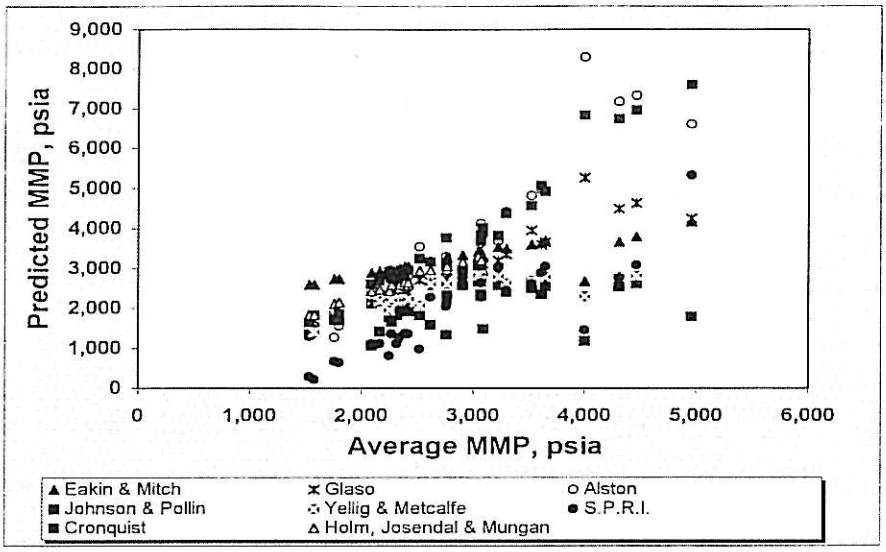


Fig. 1. Comparison of CO_2 MMP predictions by different correlations.

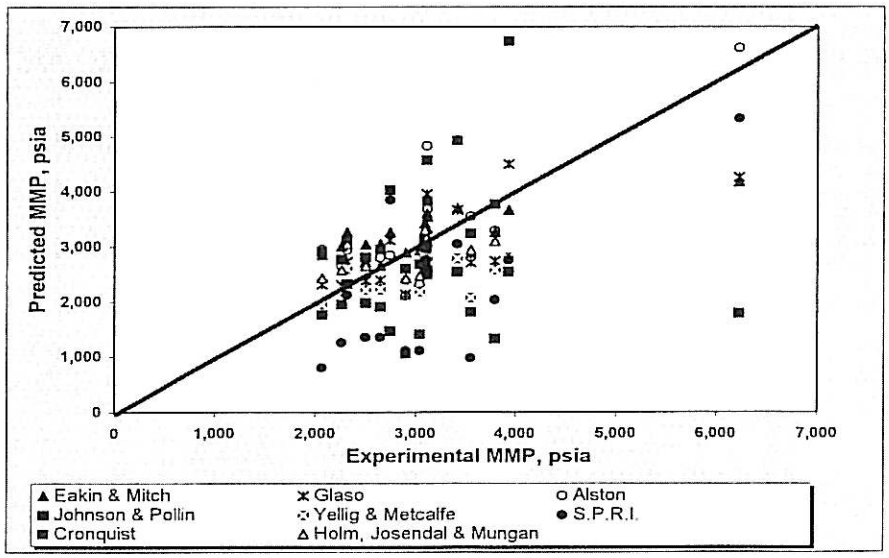


Fig. 2. Comparison between experimental and predicted CO_2 MMP.

Table 3. Predicted and measured Co_2 MMP.

Field	1 Holm, Josendal and Mungan 1974	2 Cronquist 1978	3 S.P.R.I 1979	4 Yellig and Metcalf 1980	5 Johnson and Pollin 1981	6 Alston 1985	7 Glaso 1985	8 Eakin and Mitch 1988	Exper. MMP psia	Current Pressure Psia	Initial Pressure
Sarir C-Main	O.O.R	4,562	2,600	2,690	2,494	4,823	3,948	3,593	3,112	2,919	3,924
Sarir c_North	3,150	2,964	2,756	2,800	2,562	2,782	2,879	3,327	3,104	2,645	3,921
Sarir L	3,300	3,114	3,080	2,820	2,667	2,956	3,021	3,415	3,089	3,141	4,021
Messla	O.O.R	3,817	3,014	2,780	2,573	3,669	3,190	3,531	3,118	2,869	3,985
N.A.U (TBG)	O.O.R	6,738	2,756	2,800	2,543	7,174	4,489	3,657	3,930	2,789	4,287
N.N.U (BAM)	O.O.R	6,956	3,080	2,820	2,622	7,332	4,644	3,793		2,944	4,710
Haram	O.O.R	6,841	1,448	2,300	1,179	8,293	5,270	2,675			2,027
Kotla	2,940	3,233	978	2,070	1,818	3,540	2,710	2,885	3,550	1,620	2,465
Nasser North	2,470	2,680	1,114	2,180	1,413	2,306	2,183	2,929	3,040	2,264	2,472
Nasser South	2,600	2,883	1,114	2,180	1,812	2,719	2,265	2,961		2,308	2,472
Nasser S.E	2,580	2,767	1,255	2,200	1,953	2,653	2,309	2,998	2,258	2,318	2,472
Raguba	2,950	3,157	2,268	2,600	1,583	2,563	2,647	3,177		1,853	2,400
Jebel	3,100	3,756	2,037	2,580	1,331	3,283	2,736	3,255	3,790	2,656	3,390
LDM	O.O.R	4,017	3,842	O.O.R	1,471	2,846	3,117	3,261	2,740	3,612	4,043
Bahi PL7	2,120	1,732	681	1,900	1,703	1,267	1,880	2,736		865	1,203
Dahra Jofra PL5	1,836	1,648	288	1,605	1,347	1,298	1,633	2,584		617	974
Samah	O.O.R	3,689	2,268	2,600	2,363	4,123	3,064	3,396		2,605	2,720
Waha North	2,650	2,800	1,352	2,220	1,977	2,643	2,388	3,040	2,500	2,310	2,978
Waha South	2,650	2,950	1,352	2,220	1,914	2,798	2,396	3,043	2,644	2,322	2,978
Defa	2,430	2,908	805	1,950	1,769	2,948	2,314	2,842	2,065	2,353	2,505
Gialo Eocene	1,840	1,825	220	1,400	1,465	1,574	1,707	2,580		726	1,191
Gialo Paleocene	3,050	3,095	2,123	2,600	2,321	2,942	2,731	3,257	2,315	2,384	2,741
Dahra PL7/YPL7	2,150	1,856	641	1,900	1,697	1,561	1,863	2,732		959	1,144
Amal B	O.O.R	4,371	2,447	2,620	2,388	4,422	3,349	3,494		2,650	4,690
Amal E	O.O.R	5,075	2,884	2,820	2,338	4,974	3,584	3,641		3,200	4,690
Amal N	O.O.R	4,924	3,047	2,780	2,544	4,932	3,654	3,691	3,414	3,050	4,690
Ghani L-Farrud	2,425	2,594	1,114	2,390	1,059	2,103	2,129	2,888	2,900	2,026	2,355
Zenad Farrud	2,580	2,737	1,352	2,220	1,648	2,401	2,250	2,959		1,920	2,400
Intisar – D	3,200	3,830	2,631	2,690	2,291	3,630	2,918	3,370		4,396	4,272
Abu - Attifel	O.O.R	7,595	5,323	O.O.R	1,784	6,613	4,251	4,165	6,224	6,049	6,883

- O.O.R. = Out of range

On the basis of the above discussion, it was concluded that the correlations of Holm, Josendal and Mungan, yellig-Metcalf, Glaso, and Eakin-Mitch are the best for screening purposes compared to others.

B. Miscible HC gas (Vaporising drive)

Firoozabadi and Aziz proposed a simple correlation to estimate MMP for vaporizing drive mechanism. Three parameters seem to affect multiple-contact misciblility of a reservoir fluid: the amount of intermediates in a reservoir fluid (C2 through C5, CO_2 and H_2S), the volatility of the reservoir oil which was represented by the C7+ molecular weight and the reservoir temperature.

Glaso proposed two correlations for N2 gas injection. The first one in 1985 and the other one modified in 1990. Both of Glaso's correlations are function of reservoir temperature, molecular weight of C7+ in stock-tank oil, and the intermediate contents (C2 through C6) in the reservoir oil. However, more additional data (API gravity and C1 content in the reservoir oil) are required for the modified one.

The predictions made with these correlations vary widely. Owing to the limited experimental data for the vaporizing drive, it was not possible to choose between these two correlations.

The correlations of Firoozabadi and Aziz were developed based on results with lean hydrocarbon gases. On the other hand, the correlations of Glaso were developed based on the results with Nitrogen. Hence, it was decided to make predictions using the correlations of Firoozabadi and Aziz. The results are summarized in Table 4.

C. Miscible HC gas (Condensing drive)

Glaso's correlations are given in the form of analytical expression. These give the MMP as a function of "Corrected molecular weight of C7+ in the stock-tank oil", the methane content in the injection gas and the reservoir temperature. These different equations are given corresponding to 34, 44 and 54 of the molecular weight of C2 through C6 in the injection gas. The equations were inverted to predict the MMC at the initial pressure of the reservoirs for gases with C2 through C6 molecular weight of 34, 44 and 54. These were then compared with the prediction made using Benham *et al.*'s correlation.

The results are given in Table 5. It is seen that the predictions made by both correlations are in good agreement with each other. Table 6 confirms this good agreement between the two correlations compared to the existing experimental data.

Based on the discussion above, it is concluded that the correlations of Glaso and Benham *et al.*, are equally good.

Table 4. Predicted lean gas MMP.

Field	1 Glaso 1985	2 Glaso 1990	3 Firoozabadi and Aziz 1986
Sarir C-Main	7,993	9,017	5,562
Sarir c_North	4,891	9,726	5,634
Sarir L	5,027	4,348	5,829
Messla	4,899	6,236	4,781
N.A.U (TBG)	10,937	8,405	6,980
N.N.U (BAM)	11,070	8,374	6,929
Haram	19,376	23,724	8,050
Kotla	6,420	8,687	5,956
Nasser North	4,315	4,906	4,404
Nasser South	4,473	5,840	4,433
Nasser S.E	4,742	6,416	5,021
Raguba	4,361	6,487	4,167
Jebel	4,942	5,193	5,167
LDM	5,134	4,212	4,455
Bahi PL7	4,260	3,123	3,533
Dahra Jofra PL5	4,292	8,871	3,820
Samah	6,630	13,405	6,973
Waha North	4,506	5,957	4,643
Waha South	4,523	5,716	4,881
Defa	5,062	6,441	5,365
Gialo Eocene	5,143	18,680	5,880
Gialo Paleocene	4,566	6,485	4,835
Dahra PL7/YPL7	4,675	8,850	4,549
Amal B	6,002	6,461	5,585
Amal E	6,544	6,226	5,678
Amal N	6,272	6,418	5,680
Ghani L-Farrud	4,273	4,518	3,989
Zenad Farrud	4,554	5,133	4,840
Intisar – D	5,282	6,005	5,878
Abu - Attiffel	7,199	4,953	6,416

EOR PROCESS RECOMMENDATIONS

The second part of this study is to recommend the suitable EOR process for each candidate reservoir. During the last few years,

Table 5. Prediction of HC MMC using different correlations.

Field	Initial Pressure	Temp.	Mwt C5+	Benham's Correlation Pred. MMC C1 Mole % C2-C4 Mwt of Injected Gas			Glaso's Correlation Pred. MMC C1 Mole % C2-C4 Mwt of Injected Gas		
	psia	Deg. F		34	44	58	34	44	54
Sarir C-Main	3,924	225	255	47.0	56.0	66.0	21.5	55.5	55.5
Sarir C_North	3,921	230	187	52.0	61.0	67.0	50.6	64.5	67.0
Sarir L	4,021	240	190	51.0	60.0	63.0	49.0	63.5	66.0
Messla	3,985	238	205	50.0	59.0	65.0	42.5	61.7	63.6
N.A.U (TBG)	4,284	230	279	34.0	52.0	64.0	15.0	54.8	53.6
N.N.U (BAM)	4,710	240	274	37.0	45.0	56.0	17.5	56.5	55.0
Haram	2,027	184	363	12.0	38.0	47.0	-	35.5	35.0
Kotla	2,465	164	249	44.0	57.0	63.0	23.5	53.0	55.4
Nasser North	2,472	170	187	51.0	60.0	66.0	42.5	59.5	63.0
Nasser South	2.472	170	211	50.0	60.0	65.0	39.0	58.0	61.5
Nasser S.E	2,472	176	202	47.0	55.0	63.0	39.0	57.6	61.0
Raguba	2,400	214	172	49.0	61.0	66.0	35.0	53.5	57.5
Jebel	3,390	206	196	56.0	67.0	69.0	43.0	61.5	64.0
LDM	4,043	262	156	62.0	65.0	74.0	53.0	63.3	66.7
Bahi PL7	1,203	150	167	39.0	44.0	57.0	-	35.0	40.0
Dahra Jofra PL5	974	129	164	28.0	44.0	47.0	-	-	-
Samah	2,720	214	232	44.0	50.0	63.0	27.0	52.0	55.5
Waha North	2,978	180	202	55.0	62.0	68.0	44.0	61.5	64.0
Waha South	2,978	180	203	55.0	62.0	68.0	44.0	61.5	64.0
Defa	2,505	156	228	50.0	56.0	66.0	34.0	57.6	60.4
Gialo Eocene	1,191	125	212	32.0	46.0	50.0	23.0	43.5	51.0
Gialo Paleocene	2,741	209	198	45.0	56.0	62.0	36.5	55.5	59.5
Dahra PL7/YPL7	1,144	148	179	23.0	40.0	49.0	3.0	30.0	40.0
Amal B	4,690	220	229	48.0	58.0	66.0	41.0	64.8	64.8
Amal E	4,690	234	231	44.0	56.0	65.0	37.8	62.8	63.0
Amal N	4,690	239	230	44.0	56.0	65.0	37.0	62.0	62.5
Ghani L-Farrud	2,355	170	177	45.0	58.0	64.0	42.5	59.5	62.5
Zenad Farrud	2,400	180	182	48.0	58.0	63.0	41.5	58.5	62.0
Intisar – D	4,272	226	195	56.0	66.0	67.0	51.0	66.0	67.8
Abu - Attifel	6,883	300	223	-	-	-	49.5	68.5	67.5

Table 6. Measured and predicted HC MMC.

Field	Pressure psia	Temp. Deg. F	Mwt C5+	Interm. Mwt of Inj. Gas		LPG Required%	C1 Conc. Inj. Gas (Mole%)		
				C2-C4	C2-C6		Exp	Benham	Glaso
Nasser North	2,300	170	187	44.2	44.6	17.8	51.6	57.6	57.8
Nasser S.E	2,312	170	202	45.7	46.3	20.0	53.6	56.3	56.7
Waha North	2,041	180	183	50.0	50.4	34.3	52.5	55.4	55.7
Waha South	2,314	180	188	50.0	50.4	34.3	52.3	58.4	59.3
Defa	2,200	156	213	48.1	48.9		59.9	58.9	58.1

the EOR department carried out a survey of the availability of gases for EOR processes. Both HC and CO_2 gas reserves were compiled.

A directive was given to OPCOs to give priority to CO_2 injection schemes. Our recommendation follows the same guidelines. First, we checked whether the initial reservoir pressure was greater than the pressure required to achieve miscibility with CO_2. If it is greater, than we conclude that it will be feasible to implement the miscible CO_2 flood for this reservoir and recommend detailed investigations of this scheme. Underlying this is the assumption that it will be possible to operate the reservoir at the initial reservoir pressure. This should be possible for most of the reservoirs, though one must be cautious.

Condensing gas drive requires blending of field gases with rich fluids like LPG or condensate, *etc.* These are expensive and not available in surplus quantities. Hence, we are of the opinion that, wherever feasible, the vaporizing gas process will perform better than the condensing gas process. On this basis, candidate reservoirs, where CO_2 flood is not feasible, are considered for vaporizing HC gas process.

The condensing miscible hydrocarbon flood and immiscible CO_2 injection schemes are evaluated for reservoirs where both the miscible CO_2 and vaporizing hydrocarbon floods are not feasible. It is not easy to evaluate the relative merits of the rich gas miscible floods vis-à-vis the immiscible CO_2 flood.

There is very little information available in the literature to carry out a good evaluation of immiscible CO_2 flood. Hence, we have ranked the immiscible CO_2 flood as the last choice. It must be emphasized that the relative ranking of the two schemes is not governed by process considerations, but rather by the data available to carry out the screening.

The results, given in Table 7, indicate the possibility of using miscible CO_2 for most of our candidates. Twenty out of 26 candidates could be subjected for miscible CO_2 flood. Abu Attiffel field is the only candidate where miscible CO_2 and lean gas injection schemes appear feasible. The lean gas injection is not feasible in any other candidate.

We have evaluated the feasibility of the other gas injection schemes, rich gas miscible flood and CO_2 immiscible flood, for the remaining six candidates. As discussed earlier, the condensing HC gas drive requires blending of field gases with rich fluids. To get a feel for the amount of rich gases required for achieving miscibility, predictions were made using "typical" composition of "field gas" and "LPG" as given in Table 8. The predictions were made for five of the remaining six candidates which are not suitable for miscible CO_2 flood. (The sixth candidate Gialo Eocene, had already been tested experimentally for immiscible CO_2 and condensing gas drive.) The results are given in Table 9. From this Table it appears that Kotla and Raguba fields are likely candidates for rich gas injection. The other three require significant amounts of LPG and hence are unlikely to be candidates for this process.

Table 8. Assumed composition of dry gas (DG) and LPG gas used for the prediction.

Component	DG %	LPG %
CO2	2.69	0.00
H2S	0.59	0.00
N2	1.39	0.00
C1	66.98	0.00
C2	14.24	2.63
C3	9.07	29.09
IC4	1.24	22.72
NC4	2.67	45.56
IC5	0.56	0.00
NC5	0.57	0.00

Table 7. EOR process recommendation.

Field	Misc. CO_2	This Study		IMM. CO_2	OPCO's EOR Program
		Lean Gas	Rich Gas		
Sarir C-Main	Yes				Miscible CO_2
Sarir c_North	Yes				Miscible CO_2
Sarir L	Yes				Miscible CO_2
Messla	Yes				Miscible CO_2
N.A.U (TBG)	Yes				Miscible CO_2
N.N.U (BAM)	Yes				Miscible CO_2
Kotla*			Yes		Miscible CO_2
Nasser North*	Yes				Miscible CO_2 & HC Gas
Nasser South	Yes				Miscible CO_2 & HC Gas
Nasser S.E	Yes				Miscible CO_2 & HC Gas
Raguba			Yes		Miscible CO_2 & HC Gas
Jebel*	Yes				Miscible CO_2 & HC Gas
Bahi PL7				Yes	Miscible HC Gas
Dahra Jofra PL5					Miscible HC Gas
Waha North	Yes				Miscible CO_2 & HC Gas
Waha South	Ys				Miscible CO_2 & HC Gas
Defa	Yes				Miscible CO_2
Gialo Eocene				Yes	Immscible CO_2 & HC Gas
Gialo Paleocene	Yes				Miscible CO_2 & HC Gas
Dahra PL7/YPL7				Yes	Immscible CO_2 & HC Gas
Amal B	Yes				Miscible CO_2
Amal E	Yes				Miscible CO_2
Amal N	Yes				Miscible CO_2
Ghani L-Farrud*	Yes				Miscible CO_2 & HC Gas
Zenad Farrud	Yes				Miscible CO_2 & HC Gas
Abu - Attifel	Yes	Yes			Miscible CO_2 & HC Gas

* Experimental CO_2 MMP is higher than the initial pressure

Table 9. Predicted LPG requirement using the above composition and Benham, *et. al.*, correlation.

Field	Pressure Psia	Temp. Deg. F	Mwt C5+	Benham Correlation @ Intermediate MWt of injected gas = 45	LPG Mole %
Kotla	2465 I 2065 C	164	249	C1 Mole % = 57.4 = 52.5	14.5 21.5
Raguba	2400 I 1865 C	214	172	= 61.2 = 52.0	9.0 22.0
Dahra- Jofra PL5	974 I 636 C	129	164	= 44.0 = 35.0	34.0 47.0
Bahi – PL7	1203 I 897 C	150	167	= 44.0 = 33.0	34.0 50.0
Dahra – PL7/YPL 7	1144 I 1020 C	148	179	= 40.0 = 36.0	40.0 46.0

I = Initial Pressure, C= Pressure as of Dec. 1990

The only choice for these three candidates is the possibility of applying immiscible CO_2 injection. However, we need some guidelines or criteria to decide whether this process can be successfully implemented in these reservoirs. Detailed experimental work carried out for the Gialo Eocene crude and the simulation carried out for the reservoir under CO_2 injection enabled us to get some initial guidelines. The results show that a high degree of enrichment is required for HC gas to achieve the miscibility limits (62.5 mole % of condensate Faregh gas). Compared to this, the reservoir fluid can dissolve a significant amount of CO_2 (730 scf/stb) at the initial pressure (1191 psia). The resulting CO_2-saturated oil viscosity is low (0.634 cp) compared to the initial oil viscosity of 2.25 cp. The resulting swelling factor is 1.35 rb/stb compared to the original FVF of 1.048 rb/stb. Accordingly, a very preliminary criterion for the applicability of immiscible CO_2 flood can be formulated as:

i) low initial solution GOR, and
ii) good solubility of CO_2 in the reservoir fluid.

Simon and Graue's correlations were used to predict the properties of the CO_2- swollen oils for Bahi PL-7, Dahra PL-7, YPL-7 complex and Dahra-Jofra PL-5 unit. The results are given in Table 10. The reservoir fluids of Bahi PL-7 and Dahra PL-7 YPL-7 complex are able to dissolve significant amounts of CO_2 in the reservoir fluid (516 and 439 scf/stb for both reservoirs respectively) and reduce the viscosity of the reservoir fluid.

The case of Dahra-Jofra PL-5 reservoir is different. The bubble point pressure is almost equal to the initial pressure and the viscosity of the original reservoir fluid is low. Therefore, immiscible CO_2 injection is not recommended in this case.

Based on the analysis carried out above, we conclude that Kotla and Raguba are potential candidates for miscible hydrocarbon flood using rich gases, and Bahi PL-7 and Dahra PL7 YPL-7 complex reservoirs are candidates for immiscible CO_2 flood. Dahra-Jofra unit appears to be unsuitable for any of the EOR schemes considered so far.

COMPARISON BETWEEN THE RECOMMENDED EOR PROCESSES AND THE PROGRAMMES OF OPERATING COMPANIES

The current EOR programmes of the operating companies were reviwed in the light of the results generated herein as described in Table 7. A good consistency between the OPCO's EOR programmes and the results of this study was noted, except in the cases of Kotla and Bahi PL-7 candidates.

For Kotla field the company has proposed to handle only miscible CO_2 tests for this field. Based on the prediction of correlations the miscibility will not be achieved at the initial reservoir conditions. Our analysis shows that for this reservoir, condensing gas miscible flood can be realized with enrichment of the field gas with small amounts of LPG.

For Bahi PL-7 field, the OPCO has proposed to conduct only the condensing gas drive tests. Based on the prediction of correlations, significant quantities

Table 10. Using Simon and Graue correlation for predicting solubility, swelling and viscosity of CO_2 – crude oil.

		Bahi PL-7	Dahra-PL7/PL7	Dahra Jofra PL5
Stock – tank oil gravity	Deg API	43.9	38.6	43.7
Oil density at 60° F	gm/cc	0.806	0.831	0.807
Avg. M.Wt of stock –tank oil		160	186	161
Watson k-factor		11.44	11.35	11.14
Initial pressure	psia	1203	1144	974
Temperature	Deg F	150	148	129
CO_2 solubility in STO (from Corr.)	Scf/Stb	716	588	599
Original solution GOR (from PVT)	Scf/Stb	200	149	427
CO_2 solubility in res. fluid	Scf/Stb	516	439	172
FVF of CO_2 saturated res. fluid	(From corr.)	1.27	1.22	1.27
FVF of original res. fluid	(From PVT)	1.109	1.086	1.232
Swelling factor		1.145	1.123	1.031
Initial oil viscosity	cP	1.104	1.254	0.6
Estimated CO_2 sat. oil viscosity	cP	0.4	0.55	

of LPG are required to achieve the miscibility (34% of LBG at the initial conditions and 50% of LPG at the current condition). At the same time, the immiscible CO_2 injection seems to be attractive, especially for this shallow reservoir. Based on Simon and Graue2 s correlation, the reservoir fluid of Bahi PL-7 has the ability to dissolve significant amounts of CO_2 gas (516 scf/stb).

ACKNOWLEDGEMENTS

We thank the National Oil Corporation for its permission and approval to publish this paper. We also thank Dr. Venkaterman for his technical support and advice and Dr. A. Urayet for his valuable comments.

REFERENCES

[1] Sheb M. and Arsheed J. 1987 (March). *Gas Reserves and Requirements for EOR Planning.* Unpublished report, EOR Department, NOC.

[2] EOR Department,1987. CO_2 *Reserves Evaluation, Phase Part I,* unpublished report, NOC March 1987.

[3] Technical and Economic Planning Study for EOR in GSPLAJ 1990 (March). *Preliminary EOR Simulation of EOR Candidate Reservoirs,* Unpublished report, EOR Department, NOC (March 1990).

[4] IPEC Consultant, 1987, December. *Technical and Economic Planning Study for EOR in GSPLAJ. Solvent Gas Reserves and Deliverability for EOR Applications.*

[5] IPEC Consultant, 1987, December. *Technical and Economic Planning Study for EOR in GSPLAJ-Onshore CO_2 Reserves and Deliverability (Phase 1)* Unpublished report.

[6] Holm. L. W. and Josendal, V.A, 1974 (December). Mechanisms of oil displacement by carbon dioxide. JPT, 1427 – 38.

[7] Yellig, W. F. and Metcalf, R.S., 1980 (January). Determination and prediction of CO_2 minimum miscibility pressures. *JPT,* 160-68.

[8] Johnson, J.P. and Pollin, J.S, 1981. Measurement and correlation of CO_2 miscibility pressures, paper SPE presented at the 1981 SPE/DOE enhanced oil recovery symposium, Tulsa, April 5-8.

[9] Mungan. N., 1981 (January-March). Carbon dioxide flooding-fundamentals. *J. Cdn. FJ. Pet Tech.* 87-92.

[10] Cronquist C., 1978. Carbon dioxide dynamic miscibility with light reservoir oils. Paper presented at the 1978 US Doe annual symposium, Tulsa, August 28-30.

[11] Lee, J. I., 1979 (march). *Effectiveness of Carbon Dioxide Displacement Under Miscible and Immiscible Conditions.* Research report RR-40, Petroleum Recovery Inst, Calgary (March 1979).

[12] Alston, R.B., Kokolis, G.P. and Hames, C.F., 1985. CO_2 minimum miscibility pressure.

[13] Benham, A.L., Dowden, W.E. and Kunzman, W.J.1960. Miscible Fluid displacement-prediction of miscibility. *Trans, AIME,* **219**, 229 –37.

[14] Glaso, O., 1985 (December). Generalised minimum miscibility pressure correlation. *SPEJ,* 927-34.

[15] Eakin, B.E., and Mitch, F.J. 1988. Measurement and correlation of miscibility pressure of reservoir oil. Paper presented at the 1988 *SPE Annual Symposium*, Houston, TX, 2-5 October.

[16] Glaso, O., 1990 (February. Miscible displacement: recovery tests with nitrogen. SPE. *Reservoir Engineering*, 61-68.

[17] Firoozabadi and Aziz, 1986 (November. Analysis and correlation of nitrogen and lean gas miscibility pressure. SPE. *Reservoir Engineering* 575-582.

[18] Simon, R. and Graue, D.J. 1965 (January). Generalized correlation for predicting solubility, swelling and viscosity behaviour of CO_2 crude oil systems. *JPT*, 102-106.

Petroleum Res. J. Vol. 14 (2002): P. 13–22, 6 Figs.

Innovative Formation Damage Sample Evaluation Techniques0

I.S.C. Spark, N. Fleming, M.T. Byrne and I.T.M. Patey*

تقنية مبتكرة لتقييم تضرر عينة التكوين الصخري

سبارك ون. فليمينج وم. ت. براين وت. م. باتي

لقد تم استعمال التقدم في اختبارات الغمد عند الضرورة المكمنية التي تجري على عينات موائع المكمن وأخرى لبية في محاكاة العمليات القاعية مثل الحقن بمياه البحر واستخدام طينة الحفر أو كبس المواد الكيميائية، للتعرف على أي ضرر يحدث للتكوين الصخري (فرانسز وآخرون 1995).

وقد تم في حالات متعددة استعمال طريقة النفاذية الراجعة للتعرف على متى حدوث تضرر التكوين الصخري ولكن هذه الطريقة لا يمكن التعرف بواسطتها على الميكانيكية الفعلية مثل حجم الترسب، مانع المستحلب البوليمر، عزو المواد الصلبة وكبح البوليمير الحيوي / خلية، وإنتاج كبريتيد الهيدروجين. ولكي يتم التعرف على هذه الميكانيكيات والحصول على تفسير مفصل لبيانات النفاذية الراجعة يجب إجراء بعض الإختبارات التحليلية الإضافية التي تشمل التصوير الشعاعي بمساعدة الحاسوب C.A.T، رقائق المقطع الصخري، المسح بواسطة المجهر الالكتروني لعينات جافة وأخرى مائعة عند درجات حرارة منخفضة ودراسة تكاثر الميكروبات.

يمكن إجراء هذه التحاليل قبل وبعد الإختبارات، للمقارنة من أجل التعرف على ميكانيكية الضرر. لقد تم مناقشة تقنيات متعددة وكيفية استعمالها لتفسير بيانات النفاذية الراجعة بالتفعيل في هذه الورقة.

Abstract: *Advanced laboratory reservoir conditions flood tests, performed on live reservoir fluids and core materials, have been used to simulate downhole operations such as seawater injection, drilling mud application and chemical squeezes to identify any associated formation damage mechanisms (Francis et al, 1995).*

In many cases return permeabilities are used to identify when formation damage has occurred, but in itself will not identify the actual mechanism such as scale precipitation, emulsion polymer blocks, solids invasion, bio-polymer/cell blockage and H_2S production. In order to identify these mechanisms and to fully interpret the return permeability data, it is necessary to undertake additional analytical techniques, which include C.A.T. scanning, petrographic thin sections, dry and cryogenic S.E.M. and microbial growth studies.

These analyses can by performed before and after tests for comparison, to identify the damage mechanisms. The various techniques and how they are used to fully interpret the return permeability data are discussed in this paper.

INTRODUCTION

The use of laboratory reservoir conditions flood tests to predict possible downhole formation damage mechanisms, has advanced considerably over the past few years with the development of hastelloy alloy. This alloy does not readily corrode to even aggressive fluids such as HF. As a result, hastelloy

* National Oil Corporation, Tripoli, Libya.

is used for laboratory flood test rigs and downhole production tubing where corrosion resistance is required, as discussed by Petersen and Bluem (1989) and Asphanhani *et al.* (1991). In addition to the advances in flood test rig design and metullargy, analytical techniques such as dry and cryogenic S.E.M., thin sections, microbial analysis and C.A.T. scanning have allowed the identification of formation damage mechanisms in laboratory core flood tests to fully interpret the return permeability data obtained. Once the formation damage mechanisms are identified using these techniques, it is possible to identify the best preventative/remedial treatments to use downhole to minimize the problems and to pre-screen these treatments in the laboratory using core flood tests, prior to their use in the well. In order to perform effective laboratory formation damage flood tests, to simulate the situation downhole, it is absolutely essential to use carefully selected cores to represent the major injection/production intervals. It is also important to use cores, field muds, crude oil and downhole chemicals from wellsite, so that the laboratory flood tests closely match these materials downhole, with all the chemical additives present. By utilising these materials and by mimicking the relevant temperature, pressure, mud hydrostatic pressure and chemical application temperature and pressure, the laboratory flood tests will closely match any possible formation damage mechanisms which may occur in the well. Through analysing the core before the flood test is performed (untreated samples) and after (treated samples), it is possible by utilising C.A.T. scans (computer aided tomography), thin sections, dry and cryo S.E.M. (scanning electron microscopy) and microbial analysis to determine, the formation damage mechanisms and relate these to the return permeability and fluid loss volumetric data (King and Adegbesan, 1997) and Francis (1997).

COMPUTER AIDED TOMOGRAPHY ANALYSIS

The analytical technique of computer aided tomography has been used for many years to determine, by non-destructive X-ray scans, formation damage mechanisms such as mud solids invasion (Krilov, 1991).

This technique is used primarily to identify from whole cores the best plugging orientation and sites, to ensure that any sedimentary laminations run parallel to the length of the plugs. A simple planar X-ray scan is used to show the position of any circular AXIAL slice (½ cm thick) (Fig. 1a) and is not used for interpretation purposes.

The AXIAL slice (Fig. 1b) is used to show any vertical fractures, burrows and depth of drilling mud solids invasion, so that these can be avoided when taking the plugs, unless they are representative of the entire reservoir section and would thus be included.

The two longitudinal X-ray slices (Figs. 1c and 1d), taken at 90° to each other, run vertically down the whole core length. These slices are used to identify sedimentary laminations, pebbles and cemented patches so that the plugging tool can be oriented to ensure that any laminations run parallel to the length of the plugs, since fluid flow in the reservoir would be along these laminations. It is also important that permeability barriers to plug fluid flow such as large pebbles, highly cemented regions and clay wisps are avoided as this would not represent the matrix of the reservoir, where fluid flow would occur.

The C.A.T. scan technique is also very useful for determining the best locations to plug unconsolidated cores, as these can be performed with the core still present inside the aluminum core barrel liner, thus avoiding disturbing the unconsolidated core (Figs. 2a, 2b, 2c and 2d).

The section of core in (Fig. 2a) shows that the unconsolidated core is well preserved with no fracturing. The axial slice (Fig. 2b) shows that the annular space between the barrel and core is well preserved (white region) and the drilling mud (black) has not invaded the core to a high degree and thus good plugs can be obtained from this core section.

The section of core immediately below this is highly fractured (Fig. 2c), the annular space is lost and mud solids invades the fractures (Fig. 2d) showing compaction of this region of core has occurred and thus no suitable plugs could be taken from this region of the core.

The C.A.T. scan technique used in this fashion ensures that plugs best represent the reservoir fluid flow paths, contain the relevant sedimentary features, and are <u>not</u> invaded by drilling mud solids prior to the laboratory flood test being performed.

THIN SECTION ANALYSIS

The thin section technique is used to analyse rock samples prior to testing (untreated samples) and again

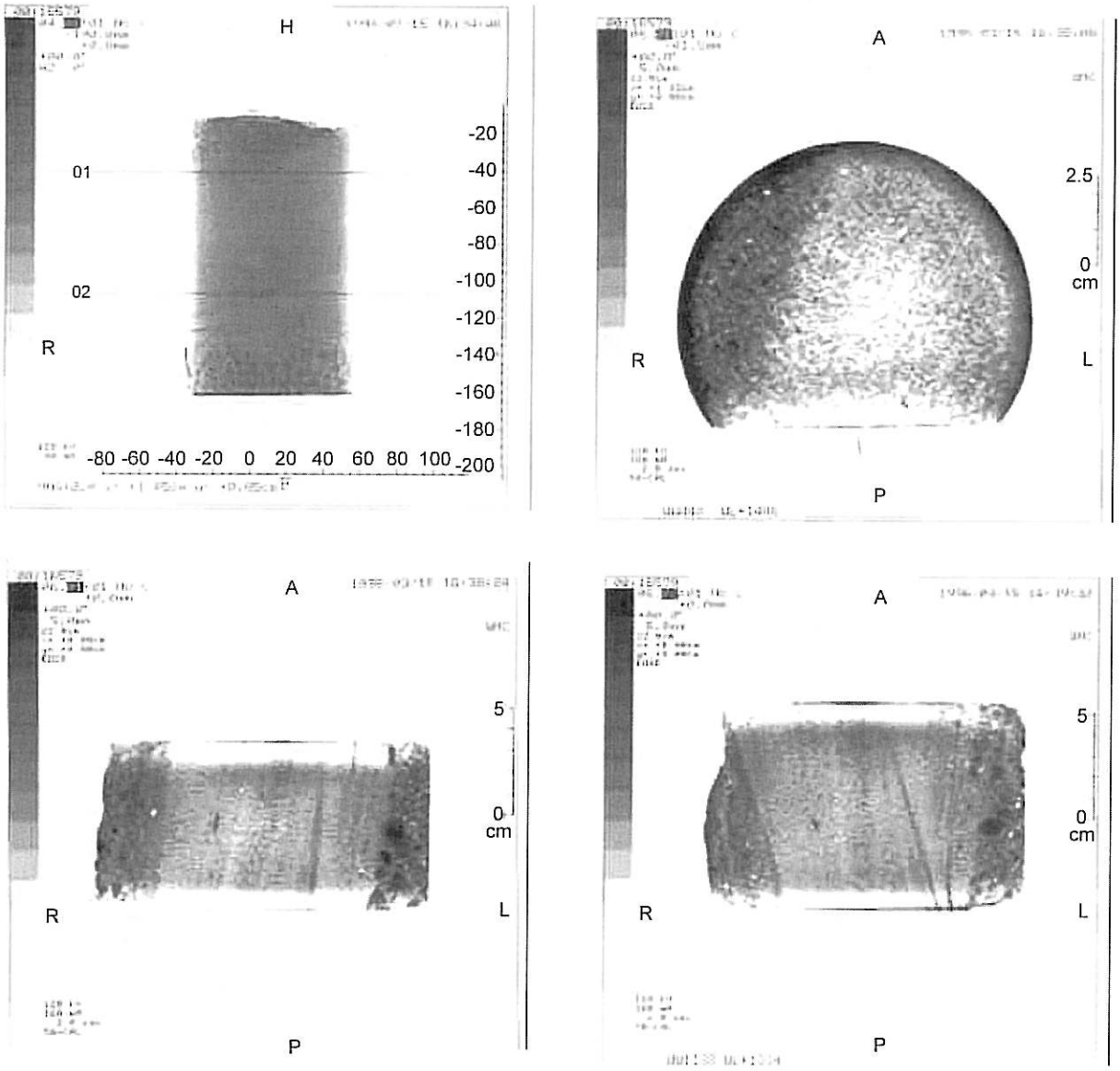


Fig. 1a. Planar X-ray scan shows the position of any axial slices (horizontal lines).
Fig. 1b. This axial slice shows that drilling mud solids have invaded only the outer rim of the core. A bedding surface cross-cuts the axial slices (higher and darker areas).
Fig. 1c. Longitudinal slice showing a conglomerate with rounded pebbles. Central Portion is of a laminated sandstone.
Fig. 1d. Longitudinal slice at 90° to Fig 1c.

after the flood test is performed (treated samples) to determine any solid formation damage mechanism. This technique uses a thin rock slice (30μm thick) which is optically transparent, mounted on a glass slide, to examine the natural distribution of clays and cements in the rock before a flood test and lengthways down a plug at the end of flood test analysis for comparison. The thin sections can identify solid formation damage mechanisms such as drilling mud cake development and degree of invasion (Fig. 3a), acid dissolution of mud during clean-up with associated mud fines migration (Fig. 3b), and acid matrix wormhole dissolution with clay mineral fines migration (Figs. 3c and 3d). These thin sections observe damage mechanisms optically in two dimensions only (30 μm in thickness), whereas dry S.E.M. observes this damage in three dimensions.

DRY S.E.M. ANALYSIS

The dry S.E.M. (scanning electron microscope) analysis is performed on a rock chip prior to flood test analysis (untreated sample) and after flood test

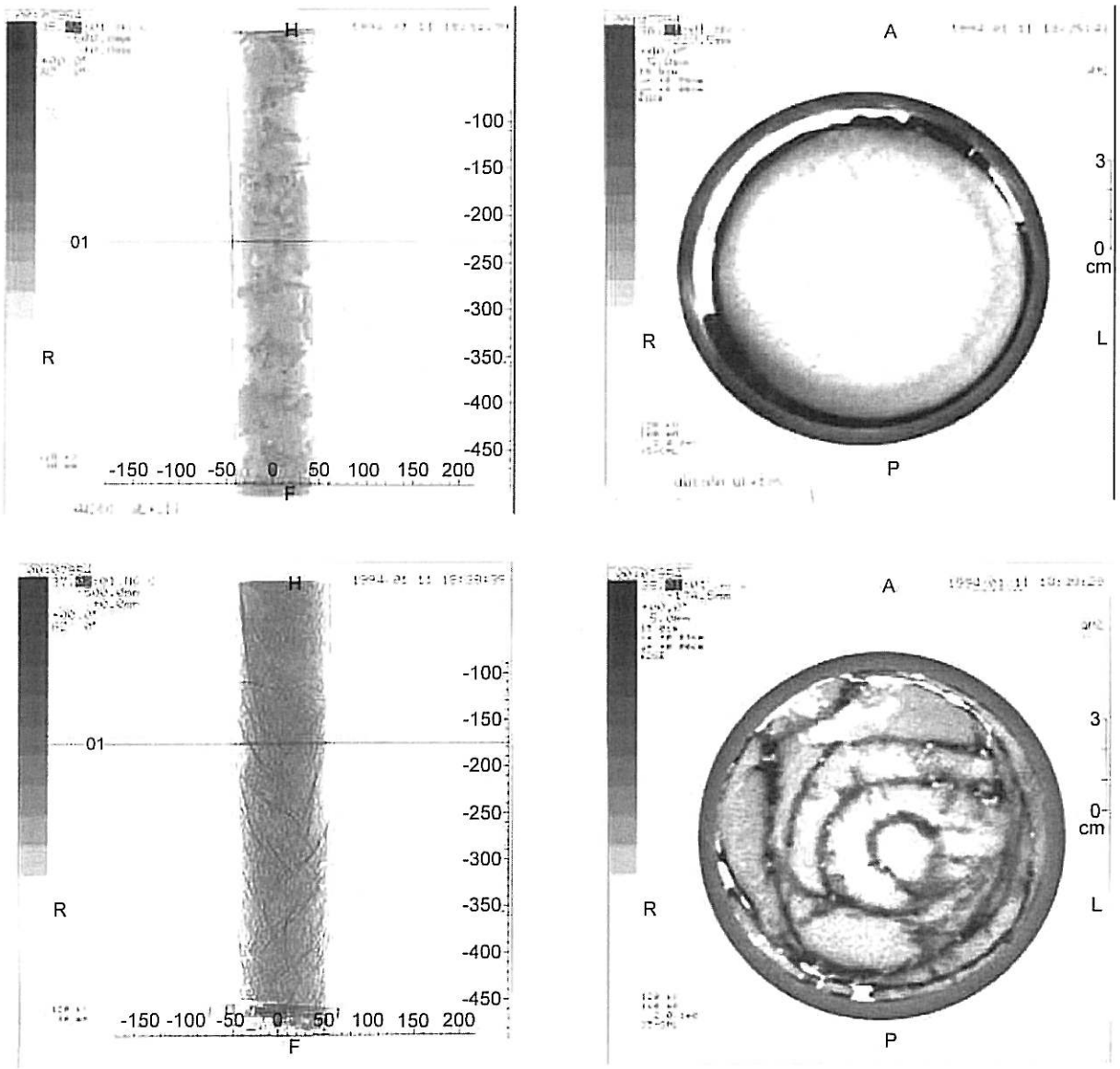


Fig. 2a. Plannar X-ray scan shows the position of the axial slice shown in Fig 2b.
Fig. 2b. The annular space between the barrel and core is well preserved (white region) and the drilling mud (black) has not invaded the core. Good plugs can be obtained from this section of core.
Fig. 2c. Abundant fractures are visible in this section of core.
Fig. 2d. No annular space is visible and mud solids (black) have invaded along fractures. No suitable plugs can be obtained from this section of core.

analysis (treated samples) on selected regions of the plug (injection/production end faces of the plug), to identify solid formation damage mechanisms in three dimensions. Drilling mud cake development and solids invasion (Fig. 4a), sodium formate polymer drilling mud cake and strands blocking and bridging pores (Fig. 4b), and excessive scale inhibitor retention (Fig. 4C) as discussed by Carbone *et al* (1999), can be observed by dry S.E.M. analysis. Incompatibility between injection water and the natural reservoir formation brine can result in scale precipitate formation, such as aragonite (calcium carbonate), which can significantly reduce the permeability of the rock and seriously reduce the injection rate (Fig. 4d). Fluid losses from drilling muds and clean-up chemicals can cause significant collapse of natural pore lining clays, such as platy/hairy illite, causing a stimulation in the near wellbore region if the clay collapses onto the pore walls (Figs. 4e and 4f) or can cause a dramatic reduction in permeability if the clay collapses onto the pore throats.

The dry S.E.M. analysis can therefore be used to identify solid formation damage mechanisms such as scale precipitation, mud solids invasion, clay migration

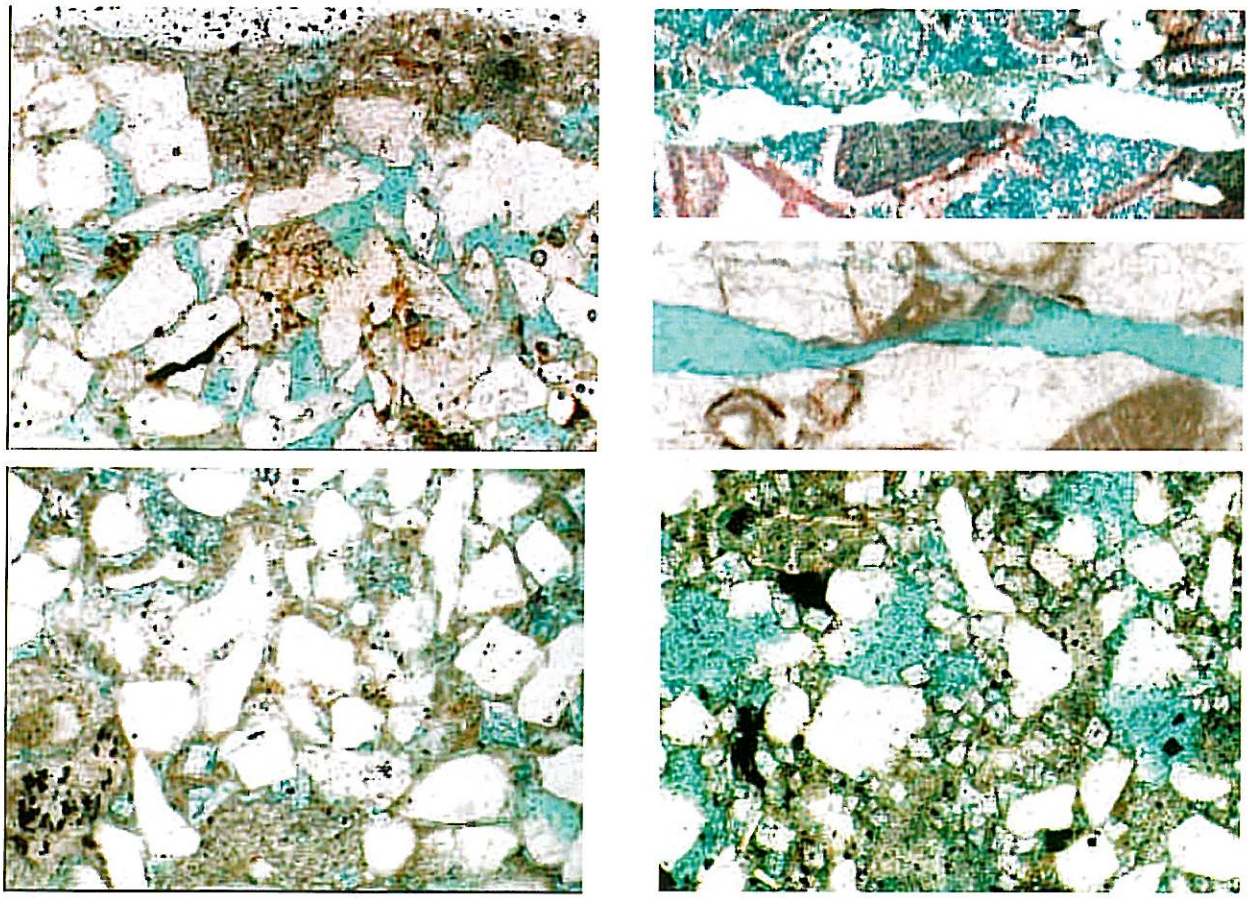


Fig. 3a. Remnants of dolomite weighed mudcake are present on the injection face of the plug. The mud solids fill only those pores exposed at the injection face, with no obvious evidence for mud solids invasion.
Fig. 3b. (Top) Foamed mud has been applied to a naturally fractured sample. Mud solids line and bridge the fracture. (Bottom) Application of acid has caused the removal of the mud, with the solids being smeared along the facture surface.
Fig. 3c. Thin section analysis prior to acid stimulation showed the sample consists of common quartz grains and clay matrix partially replaced by dolomite.
Fig. 3d. After acid stimulation of the sample in Fig 3c dolimite rhombs have been locally dissolved with the formation of wormholes. Acid application has also caused local clay dispersal.

and collapse, and cement dissolution textures in three dimensions.

CRYOGENIC S.E.M. ANALYSIS

The cryogenic S.E.M. (scanning electron microscope) analysis is used to show fluid formation damage mechanisms such as micro-emulsion blocks, water/oil blocks, asphaltene precipitation and polymer blocks, often resulting from fluid losses to the reservoir. These fluid losses can originate from the drilling mud, clean-up/completion chemicals and from chemical squeeze treatments such as scale inhibitors directly into the oil leg of fields. The technique uses fully saturated rock chips taken prior to flood test analysis (untreated samples) and from the saturated plug after completion of the flood test. These saturated rock chips are then cryogenically frozen in liquid nitrogen and placed on a cooled stage (-170°C) in a cryogenic S.E.M. The samples are freshly fractured inside the S.E.M. prior to being analysed. These cryogenic S.E.M. rock chips can be used to show fluid formation damage mechanisms such as drilling mud filtrate retention along channelised flow paths within gas field samples (Figs. 5a and 5b). Water blocks from formate mud fluid losses being retained in a gas field sample (Figs. 5c and 5d), and micro-emulsion formation with KCl brine losses, from a KCl polymer mud system and KCl brine clean-up chemicals (Figs. 5e and 5f) can also be observed.

The cryogenic S.E.M. samples can thus be used to identify any fluid formation damage mechanism providing the liquid phases are immiscible with each other i.e. Oil/water, polymer/water, asphaltene/oil separation.

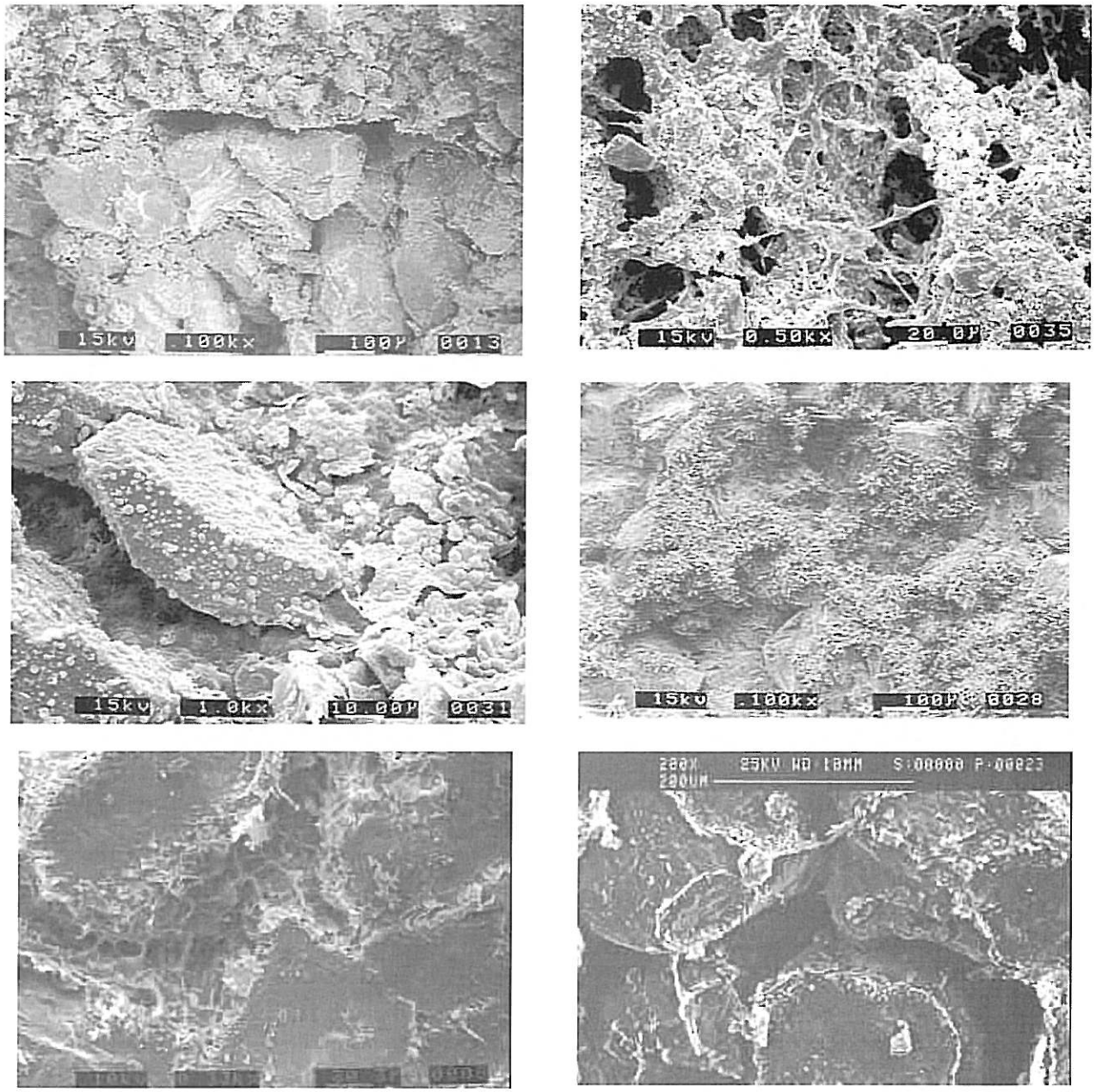
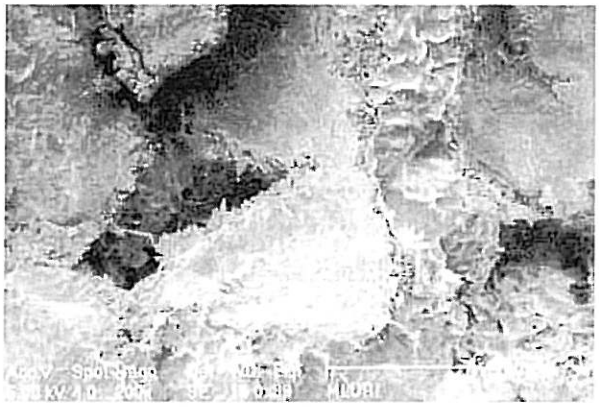
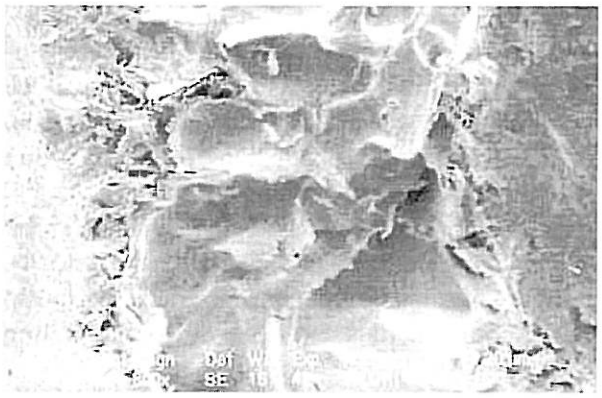


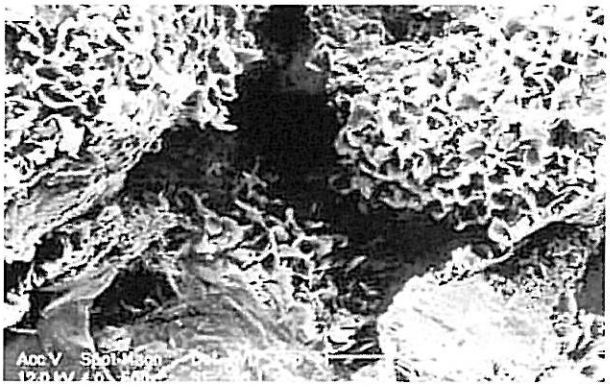
Fig. 4a. A well developed calcite mudcake in excess of 300µm has formed on the injection face. Evidence for mud solids penetration to approximately 400µm.
Fig. 4b. A view looking down on to the injection plug face. Strands of solium formate polymer based drilling mud coat grains and locally block pores.
Fig. 4c. Scale inhibitor formed as a thin film (1µm thick), now partially desiccated and globules on quartz grains, lowering rock permeability.
Fig. 4d. An aragonite scale has formed locally on quartz grains and partially blocks the pores.
Fig. 4e. Pore lining and pore bridging, illitic clay is present (x200).
Fig. 4f. After testing, mud and clean-up chemical filtrate losses have caused the collapse of pore lining, illite clay significantly increasing the permeability (x200).

MICROBIAL FORMATION DAMAGE

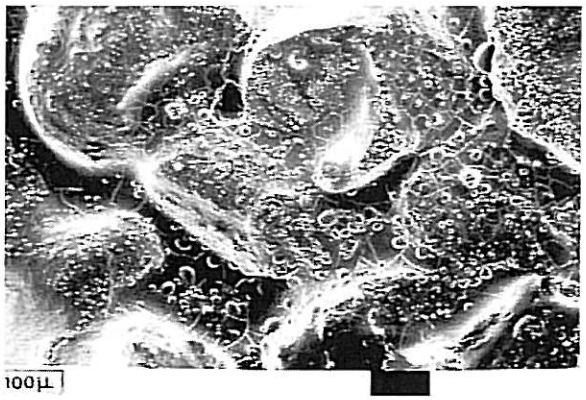
The effect of microbes on oilfield reservoirs in terms of indigenous bacteria (present in field prior to any drilling) and introduced bacteria from drilling muds (Ezzat, 1997) and other well operation chemicals has been very actively researched in recent years. The major formation damage mechanisms associated with microbial activity within wells and reservoir rocks are biopolymer pore plugging, microbe cell pore blockage, H_2S gas production and insoluble metal sulphide precipitation. The major controls on microbe











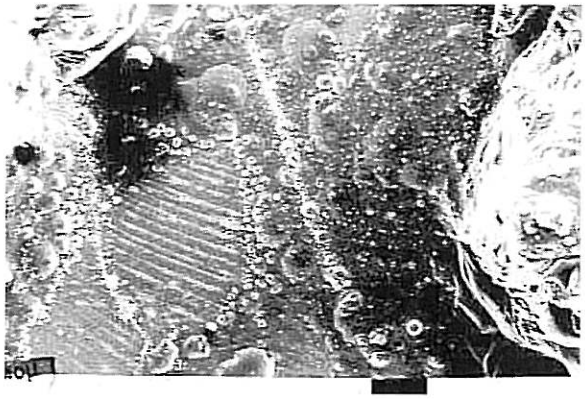


Fig. 5a. Mud filtrate losses pass along a distinct channel within a gas well. Pores adjacent to this channel within a gas well. Pores adjacent to this channel are filled with gas only.
Fig. 5b. Higher magnification view of plate 5a showing that the liquid within the channel fills the large, intergranular pores, but not the micropores between the illitic clay fibres.
Fig. 5c. (Before testing). Plug sample from a gas well in which no liquid was visible within the larger, intergranular pores or the micropores of the pore lining clay.
Fig. 5d. (After testing of sample shown in Fig 5c). Excessive filtrate losses from a mud have been retaine within the sample forming water blocks.
Fig. 5e. (Before testing) Plug sample from an oil well in which oil is the main liquid filling pores, pore lining droplet of formation brine are commonly present.
Fig. 5f. (After testing of sample shown in Fig 5e). Filtrate losses after KCl mud and KCl clean up application resulted in the formation of a microemulsion. Locally coalescence of droplet has formed larger KCl brine droplets.

growth activity are nutrient availability (often fractions of the crude oil e.g. Acetate, butyrate, propionate, hexadecane), a source of phosphate, nitrate, sulphate, sulphur or hydrogen, and probably of most importance the temperature. The SRB (sulphate reducing bacteria) are mainly responsible for the production of H_2S gas and insoluble metal sulphide precipitates in reservoirs. By undertaking microbial analysis of fresh cores (must be well preserved) and drilling muds, and by inoculation into suitable growth media at various temperatures up to the field temperature, it is possible to determine whether H_2S production is

likely to be a problem from either the indigenous and/or introduced bacteria (Wood and Spark, 1999). Once the thermal gradients of the field have been assessed to the water injection profiles, it is possible to model the bacterial populations to temperature and thus predict where H_2S production, polymer plugging, insoluble metal sulphide precipitation and microbial cell plugging are likely to occur within the field. The presence of sulphate reducing bacteria in live drilling muds, core materials and reservoir formation brine from new oil fields is discussed in detail by McGovern-Traa, C. *et al* (1997). Dry and cryogenic S.E.M. techniques when applied to microbial samples can be used to determine bio-polymer/cell plugging (Fig. 6a and 6b), water based drilling mud microbial degradation with the precipitation of iron sulphide (black colour), complete breakdown of mud properties and liberation of H_2S gas (Fig. 6c), and the size, distribution and morphologies of the different cell types (Figs. 6d, 6e and 6f).

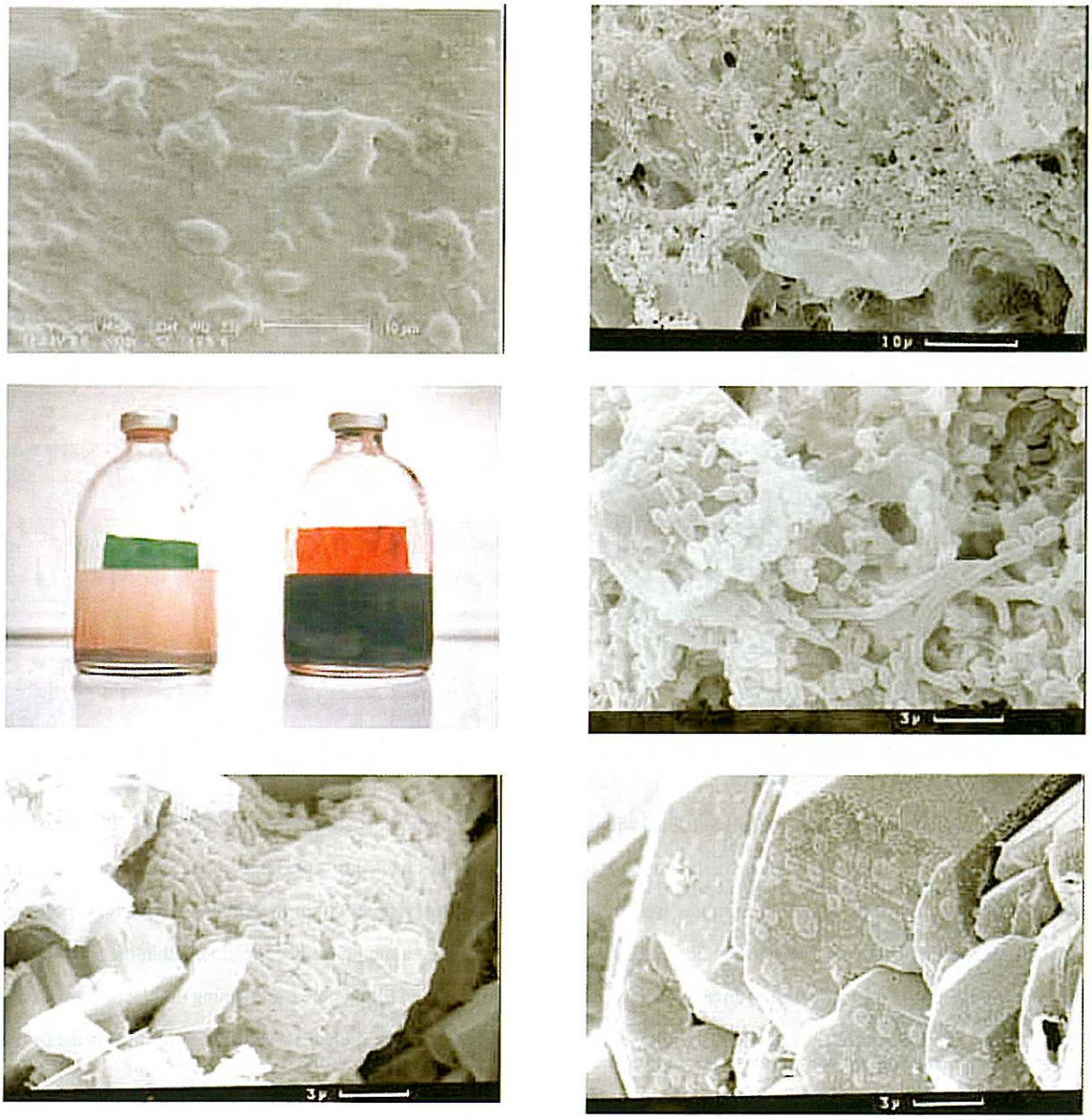


Fig. 6a. Cryogenic S.E.M. showing the occurrence of biopolymer in formation brine.
Fig. 6b. Dry S.E.M. showing the occurrence of biopolymer coating framework grains and partially to completely blocking pores.
Fig. 6c. (Left) Live WBW inoculated into growth media at 30C (0 time). (Right) Same mud after 48 hours incubation shows FeS precipitation and H_2S gas production at 400ppm. The mud has been completely broken down due to microbes (SRB).
Fig. 6d. Elongate, rod shaped and ovoid bacteria within a chalk sample.
Fig. 6e. Ovoid cells forming locally in pores as aggregated beehive colonies.
Fig. 6f. Circular aggregates of tiny coccoid (nanobacteria?) individually up to 0.025µm in size.

CONCLUSIONS

By careful utilisation of CAT scanning, thin section petrography, dry and cryogenic S.E.M. analysis and microbial testing it is possible by combining all these techniques, to fully determine the formation damage mechanisms, which can then explain return permeability and filtrate loss data gained from reservoir conditions flood tests.

It is essential to ensure that all materials used in the reservoir conditions flood tests and the pressure/ temperature conditions are relevant to the field and wells in question, if accurate determination of the formation damage mechanisms is to be made using the analytical techniques described above.

After the formation damage mechanisms have been identified, it is then possible to suggest the most suitable remedial and/or preventative measures to be taken to minimise any formation damage in the reservoir.

It is then possible to pre-screen chemicals in the laboratory using reservoir conditions flood tests such as drilling muds, clean-up/completion chemicals, squeeze chemicals and injection water prior to their use in the well to avoid anything which may cause significant formation damage.

ACKNOWLEDGEMENTS

The authors would like to thank Chemille James for typing the manuscript, Jonathan Wood for the S.E.M. photographs, Bruce Duncan and Adrian Jenkins for the laboratory analysis. A very special thanks is given to Steve Anthony and Corex (UK) Ltd for support in the publication of this paper.

REFERENCES

Asphahani A.I., Prouheze J.C., and Petersen G.J., 1991. Corrosion-Resistant alloys for Hot, Deep, Sour Wells: Properties and Experience, *SPE* **19184**, SPE Production Engineering (November).

Carbone C.L., Fleming N., Spark, I.S.C., and Patey I., 1999. Scale management through laboratory analysis and wellbore monitoring surveys, *SPE* **54733**, SPE European Formation Damage Conference, The Hague, 31st May-1st June.

Ezzat A.M., Rosser H.R., and Al Hummani A.A., 1997. Control of microbiological activity in bio-polymer based drilling muds, *SPE* **39285**, SPE/ADC Middle East Drilling Technology Conference, Bahrain, 23rd-25th November.

Francis P.A., Eigner M.R.P., Patey I.T.M. and Spark I.S.C., (1995) Visualisation of drilling-induced formation damage mechanisms using reservoir conditions core flood testing, *SPE* **30088**, SPE European Formation Damage Conference, The Hague, 15th-16th May

Francis, P., 1997. Dominating effects controlling the extent of drilling-induced formation damage, *SPE* **38182**, SPE European Formation Damage Conference, The Hague, 2nd-3rd June.

King R.W. and Adegbesan K.O., 1997. Resolution of the principal formation damage mechanisms causing iInjectivity impairment in the pembina cardium reservoir, *SPE* **38870**, SPE Annual Technical Conference and Exhibition, San Antonio, 5th-8th October.

Krilov Z., Steiner I., Goricnik B. and Wojtanowicz, A. 1991. Quantitative determination of solids invasion and formation damage using CAT scan and barite suspensions, *SPE* **23102**, Offshore European Conference, Aberdeen, Scotland, 3rd-6th September

Marshall D.S., Gray R. and Byrne M. 1999. Return permeability a detailed comparative study, *SPE* **54763**, SPE European Formation Damage Conference, The Hague, 31st May-1st June.

McGovern-Traa C., Leu J.Y., Hamilton W.A., Spark, I.S.C. and Patey, I.T.M., 1997. Petroleum geology of the Irish Sea and adjacent areas, *Geol. Soc.* Special Publication No. **124**, from Meadows N.S., Trueblood S.P., Hardman M., and Cowan G, (editors), p229-236.

Petersen C.W. and Bluem M.F., 1989. Requirements for corrosion- resistant alloy (CRA) production Tubing, *SPE* **19727**, 64th Annual Technical Conference and Exhibition of the SPE, San Antonio, Texas, October 8th-11th.

Wood J.M., and Spark I.S.C., 1999. Observed variations in hydrocarbon reservoir bacterial populations with temperature: A first step in modelling the bacterial populations of hydrocarbon reservoirs, *SPE* **54766**, SPE European Formation Damage Conference, The Hague, 31st May-1st June.

Petroleum Res. J. Vol. 14 (2002): P. 23–36, 24 Figs.

Review of Raguba Oil Field Miscibility Project

Ali H. Al-Khafaji*

مراجعة مشروع الإمتزاجية لحقل الراقوبة النفطي

علي الخفاجي

أحد أهداف مشروع الإمتزاجية لحقل الراقوبة النفطي دراسة الحد الأدنى لتركيب الإمتزاجية باستخدام خلائط مشتقة من غاز البترول المسيل والغاز الجاف. هدف آخر يتمثل في تعيين الحد الأدنى لضغط الإمتزاجية لزيت المكمن مع غاز ثاني أكسيد الكربون.

تم إنجاز تحضير عينتين من زيت المكمن (بضغطي نقطة غليان 1800 و2030 رطل للبوصة المربعة مطلق) وتحاليل الضغط والحجم والحرارة واستناداً على بيانات الضغط والحجم والحرارة، وخلائط غاز البترول المسيل/الغاز الجاف، وخواص ثاني أكسيد الكربون تم ضبط (معايير) معادلة الحالة بصفة مبدئية لتتلائم مع بيانات الضغط والحجم والحرارة. وقد جرى إثرها تطبيق معادلة الحالة للتنبؤ بالحد الأدنى لتركيب الامتزاجية والحد الأدنى لضغط الإمتزاجية.

وتعد هذه النتائج ذات قيمة لتصميم اختبارات الأنبوبة الرفيعة. وتم تعيين الحد الأدنى لتركيب الإمتزاجية لمذيبات غاز البترول المسيل / الغاز الجاف المشتقة مع عينتي زيت المكمن المشار إليها فيما سبق، تجريبياً باستخدام تقنية الإزاحة بالأنبوبة الرفيعة. تم تطبيق هذه التقنية أيضاً لتعيين الحد الأدنى لضغط الامتزاجية لثاني أكسيد الكربون مع عينة زيت بضغط 2030، استخدمت علاقات مسترجعات الزيت التراكمية مقابل الحجم المسامي للغاز المحقون لإيجاد مسترجع الزيت عند إختراق ثاني أكسيد الكربون.

كما جرى القيام باختبارات الانتفاخ لعينتي زيت المكمن المذكورتين بإضافة خلائط من مذيبات غاز البترول المسيل / الغاز الجاف المشتقة عند الحد الأدنى لتركيب الامتزاجية لهما – 40% و35% غاز بترول مسيل، كما تم استخدام ثاني أكسيد الكربون بنقاوة 99.19% لانتفاخ زيت المكمن عند ضغط 2035.

Abstract: *Study of Minimum Miscibility Composition (MMC) using mixtures of synthesized Liquefied Petroleum Gas (LPG) and Dry Gas (DG) is one of the objectives for Raguba oil field miscibility project. The other essential objective is to determine the Minimum Miscibility Pressure (MMP) of the reservoir oil with CO_2. Preparation of two reservoir oil samples (bubble point pressures (P_b) =1800 psia and 2030 psia) and PVT analyses are accomplished. Based on the PVT data and the LPG/DG mixtures and CO_2 properties, Equation of State (EOS) parameters were preliminary tuned to match the PVT experimental data. Thereafter, the EOS was applied to predict both MMC and MMP. These findings are valuable to design slim tube and swelling experiments. Then, MMC of synthesized LPG/DG solvents with the above two reservoir oil samples was determined experimentally using slim-tube displacement technique. This technique was also applied to determine the CO_2 MMP with oil sample of P_b = 2030 psia. Cumulative oil*

* Petroleum Research Centre, Tripoli, Libya.

recoveries versus pore volume gas injected relations have been used to find out the respective oil recovery at the CO_2 breakthrough.

Swelling tests were also carried out on these reservoir oils (P_b =1800 psia and 2030 psia) by adding mixtures of synthesized LPG and DG solvents at their MMC - 40% LPG and 35% LPG respectively. Carbon dioxide (CO_2 -99.19% pure) was also used to swell the reservoir oil 2035.

INTRODUCTION

Investigation of miscibility for different solvents and gases with reservoir oil is one of the most important processes to enhance oil recovery. Literatures on theoretical studies[1,2,3,4,5], experimental laboratory investigations[6,7,8,9] and field applications[10,11] of miscibility are available. Miscibility is achieved at certain conditions of pressure and temperature depending on the composition of both the reservoir oil and the injected gases or solvents. There are generally two types of miscible processes, the first contact miscible (FCM), where solvent (LPG) mix directly with reservoir oil in all proportions and their mixtures always remain in a single phase. The second process is the multiple contact miscible (MCM) process (dynamic miscibility processes). In which, gases or solvents are not directly miscible with reservoir oil, but under appropriate conditions of pressure, temperature and oil-gas or oil-solvent compositions, *in-situ* miscibility could be achieved through repeated contacts of the injected material with reservoir oil. The MCM is of three kinds: the vaporising, the condensing and condensing / vaporising miscible processes.

Representative reservoir fluid samples are very essential to obtain an accurate physical and chemical reservoir fluid properties [12,13, 14,15]. Therefore, two reservoir oil samples were prepared by direct recombination of the separator oil and gas obtained from Raguba oil field well No. E40. The bubble point pressures (P_b) of these samples were1800 psia and 2030 psia respectively. Conventional PVT analysis of the recombined oils was described elsewhere [18].

Minimum Miscibility Composition (MMC) determination for synthesized LPG/DG solvents and/ or Minimum Miscibility Pressure (MMP) of carbon dioxide with the above oils are essential for the Raguba enhanced oil recovery project[16,17,20,21,22]. Peng-Robinson cubic equation of state (EOS) modeling was first applied to predict the MMC of LPG/DG solvents with these reservoir oil samples [18,19].The MMP of carbon dioxide CO_2 -99.19% pure with reservoir oil sample P_b = 2030 psia was also predicted by the EOS[23].

Two types of miscibility tests were conducted on reservoir oil samples of the Raguba oil field using slim tube displacement technique [21, 22]. First series tests were devoted for Minimum Miscibility Composition determination for the two reservoir oils. Each oil was displaced repeatedly at a pressure slightly higher than its bubble point pressure by solvents composite of different mole percentage of LPG and DG. The MMC of LPG/DG mixtures with oils having (P_b= 1800 psia and 2030 psia) was found to be equal to 40% LPG and 35% LPG respectively. The oil recovery mechanism for both oils was a condensing drive. Second series tests were conducted to determine the MMP, where the oil of (P_b =2030 psia) was displaced at different pressures using CO_2. The CO_2 MMP with this oil was found equal to 2710 psia. The mechanism of oil recovery was a vaporization drive.

Another objective of the Raguba EOR project is to conduct two types of swelling experiments [21,24]. Firstly, to swell the two oils with the LPG/DG solvent at their MMC and secondly, to swell the reservoir oil of P_b = 2035 psia with CO_2. The swelling tests were carried out in five steps for the LPG/DG solvent and four steps for CO_2. In each step a specific volume of LPG/DG solvent and/or CO_2 was added to the respective oil in a long window PVT cell at a pressure of 5015 psia. At this high pressure, the solvent and/ or the CO_2 was forced to dissolve into the oil and form a new mixture. As a result, the composition and the physical properties of the new mixture will completely differ from the original one. Hence, bubble point pressure, swelling factor, mixture density, and gas oil ratio (GOR) were calculated at each solvent addition.

RESERVOIR OIL SAMPLE PREPARATION

Separator oil and gas were studied and directly recombined in the PVT cell at the current average GOR of 427SCF/STB to obtain a reservoir oil sample of bubble point pressure of 1800 psia at reservoir temperature of 206°F. This procedure was repeated at GOR of 480 SCF/STB to obtain an oil sample of bubble point pressure equal to 2030 psia. A Core LAB long window PVT cell with a heating jacket was used for preparing and testing of the reservoir oil samples.

Complete PVT analyses were carried out on each of the above reservoir oils.

TUNING OF EOS PARAMETERS

In order to assure the accuracy of EOS predictions of miscibility conditions for these oils (P_b = 1800 and P_b = 2035 psia), the EOS parameters must first be tuned to match experimental data. Then more reliable analyses of recovery mechanism and miscibility conditions may be made. Before tuning commencement, C_7/fraction for both oils should be characterized. It was found that two pseudo components of C7+ were adequate to model these oils. The properties of the two pseudo components of C_7+ are: (MW of C_7-C_{13} and C_{14}+) 139 and 302 g/g-mole respectively, Pc= 23.72 and 14.84 Atmosphere and Tc = 707 and 956°K, respectively. Then, tuning of EOS is accomplished using regression option in CMG PROP software. The regression variables are critical pressure and temperature, the volume shifts of methane, hexane and the C_7+ components. Also, the binary interaction coefficient exponent and the molecular weights of the C_7+ components were used as regression variables. These variables were adjusted to match the experimental data for both oils including the bubble point pressures, the constant mass expansion data, the differential liberation data, and the separator flash data. A high weight was given for matching the bubble point pressure data, since matching other experimental data/ depends on having an accurate bubble point pressure. After several different regression runs, a good match with the experimental data was achieved (See figures. 1-6 as an example for oil P_b=1800 psia).

DETERMINATION OF MICIBLLITY CONDITIONS USING EOS

Using the tuned EOS parameters, miscibility conditions and the mechanism of oil recovery can be analysed using pseudo-ternary diagrams as well as pressure-composition and pressure-temperature diagrams. First, the pressure-temperature diagram was generated for each oil (Fig. 7). These diagrams are consistent with the typical diagrams for black oils with the reservoir temperature much lower than the critical temperature. Also, pressure-temperature diagrams for LPG/DG solvents are generated. It appears that these solvents are of a single phase at the injection conditions (1850 psia and 2100 psia and reservoir temperature = 206 °F) as revealed in figure 12. Next, series of pseudo-ternary diagrams were generated for oil P_b =1800 at injection pressure of 1850 psia contacted by various solvents made up by blending LPG with dry gas in different molar ratios (from 30% to 60% LPG). The compositions of these various solvents, LPG and DG are presented in Table 1. Figure 8 shows the ternary diagram for this oil contacted by solvent of *55%* LPG. From this diagram, evidently miscibility is achieved when the solvent composition is around 55% LPG or greater. The pressure-composition diagrams with different solvents are shown (Fig. 9) From this figure, it is evident that until the LPG/DG ratio is *50%* the principal mechanism of recovery will be via vaporising mechanism. However, at higher LPG/DG ratios, the mechanism becomes principally a condensing mechanism. Thus, miscibility is achieved with LPG solvent of 55 % or greater by a multiple-contact conde6sing mechanism, where the liquid phase becomes enriched with intermediate compounds (C_2-

Table 1. Solvents composition of the blended LPG/DG samples used in slim tube experiments.

Comp.	Dry Gas	0.15* LPG	0.20 LPG	0.25 LPG	0.30 LPG	0.35 LPG	0.40 LPG	0.45 LPG	0.55 LPG	LPG
	Mole%	Mole %	Mole %	Mole %	Mole %	Mole %	Mole %	Mole %	Mole %	Mole %
N_2	1.35	1.15	1.08	1.02	0.95	0.88	0.82	0.75	0.61	
C_1	86.42	73.46	69.14	64.81	60.49	56.17	51.85	47.53	38.89	
C_2	8.35	7.47	7.18	6.88	6.59	6.29	6.00	5.71	5.12	2.47
C_3	2.83	6.85	8.20	9.54	10.88	12.22	13.56	14.90	17.58	29.65
IC_4	0.39	3.79	4.92	6.05	7.18	8.31	9.44	10.57	12.84	23.03
IC_4	0.65	7.28	9.49	11.70	13.91	16.12	18.33	20.54	24.96	44.85

*Mixture of solvent contains 15% LPG + 85% DG

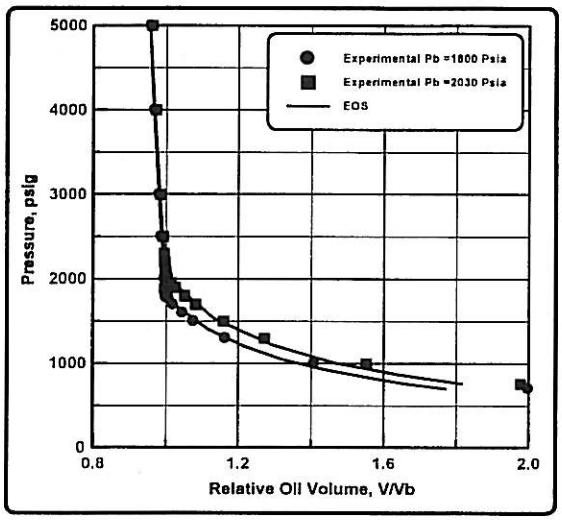


Fig. 1 EOS match, relative oil volume *vs* pressure, P_b = 1800 and 2030 psia, Raguba oil field, well No. E40.

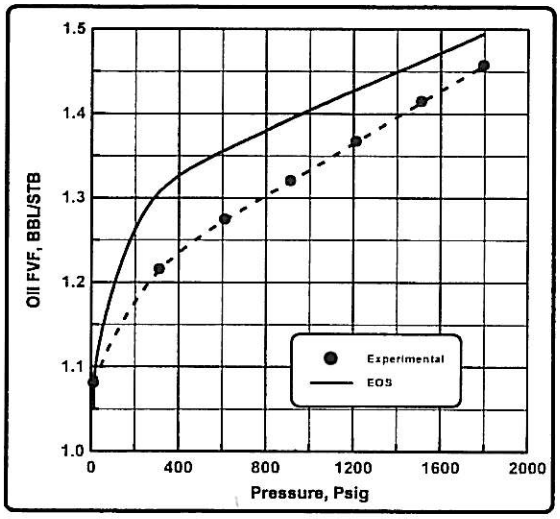


Fig. 2. EOS match, oil FVF *vs* Pressure, P_b = 1800 psia, Raguba oil field, well No. E40.

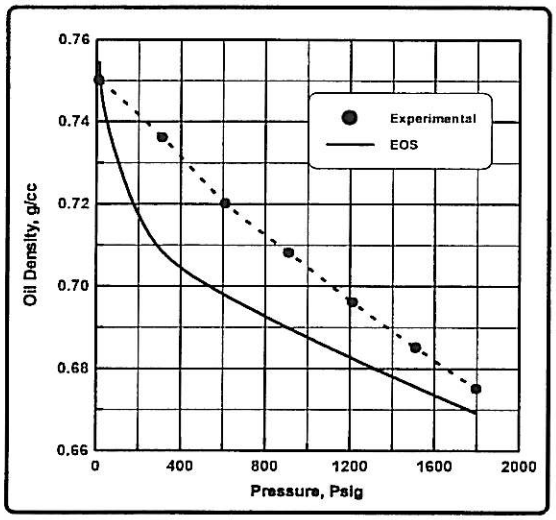


Fig. 3. EOS match, oil density *vs* pressure, P_b = 1800 psia, Raguba oil field, well No. E40.

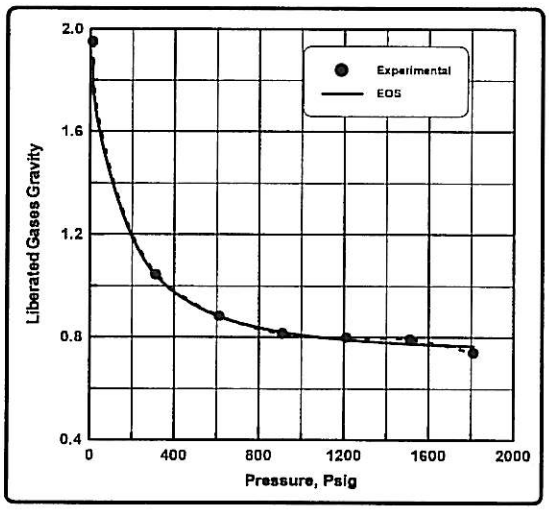


Fig. 4. EOS match, liberated gases gravity *vs* pressure, P_b = 2030 psia, Raguba oil field, well No. E40.

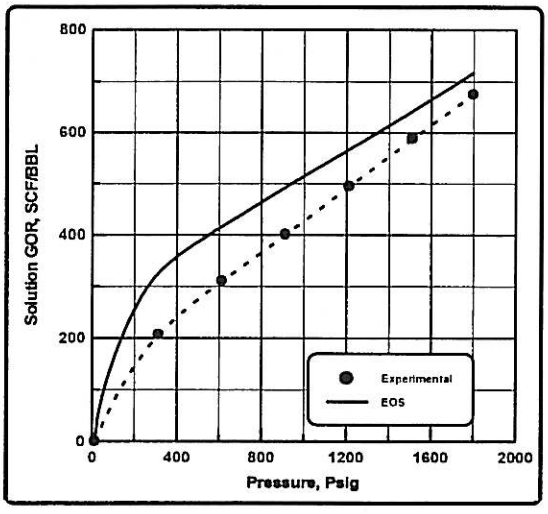


Fig. 5. EOS match, solution GOR *vs* pressure, P_b = 1800 psia, Raguba oil field, well No. E40.

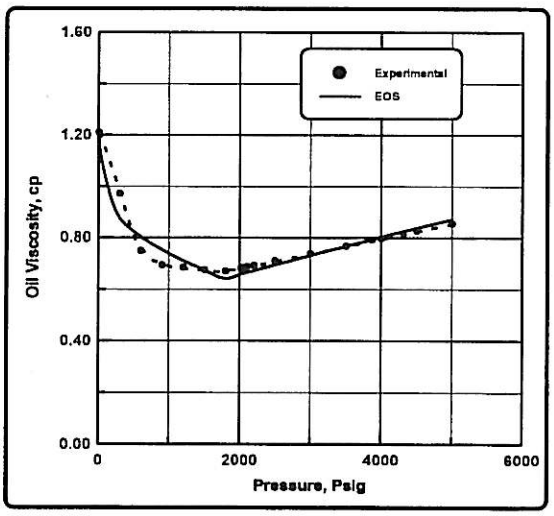


Fig. 6. EOS match, oil viscosity *vs* pressure, P_b = 1800 psia, Raguba oil field, well No. E40.

C_6) to the point that it becomes miscible with the injected solvent.

In the same manner, the MMC of LPG/DG solvent with oil P_b=2030 psia at pressure of 2100 psia found to be equal to 50 % and greater as shown in figure 10. Also, it appears that up to 40% LPG in the solvent, the principal mechanism of recovery is a multiple vaporizing mechanism but for more LPG in the solvent the mechanism becomes primarily a multiple condensing mechanism.

Ternary diagrams[16,17] for oil P_b =1800 psia contacted with CO_2 at several different pressures were generated to determine the miscibility pressure for this oil with CO_2. The ternary diagram for pressures of 1850, 3000, and 4400 psia is shown (Fig. 11). For all these pressures no miscibility was achieved at pressure less than 4400 psia and the mechanism of recovery seemed to be a condensing/ vaporising mechanism. However, the results do not seem correct because CO_2 should be able to achieve miscibility with most black oils at pressures lower than 3000 psia. Therefore, the MMP of CO_2 with this oil was calculated using Glaso[20] correlation for pure CO_2 and found to be equal 2572 psia. Similar results were achieved for oil P_b2030 contacted with CO_2 at several different pressures, 2100, 3000 and 4400 psia. Also, the MMP of CO_2 with this oil was calculated using Glaso[20] correlation for pure CO_2 and found=2669 psia. Accordingly, the results obtained by EOS may be misleading because the EOS was tuned only with black-oil data and not data for oil mixed with CO_2 that is not available yet.

EXPERIMENTAL WORK

Synthesizing of LPG and Dry Gas

Sirte Oil Company (SOC) has specified the composition of two basic mixtures, a Dry Gas (DG) mixture and Liquefied Petroleum Gas (LPG) mixture as shown in Table 1. The two basic mixtures have to be synthesized from pure hydrocarbon components. Addition of individual component was carried out using synthesis of gas mixtures, *e.g.*, compounds like methane, ethane, etc. in the required proportion in one container. This can be done either by volumetric, or by gravimetric method. The gravimetric method was preferred because of the relatively small masses of gas components, which had to be combined. Accordingly, both mixtures were synthesized by weight compositional balance. Therefore, a precision weight transducer (Type Z6H) and an electronic readout (Type Hottinger Baldwin DK38 digital) was used. Sufficient amounts of LPG and DG mixtures needed for all slim tube experiments were prepared following this method.

LPG/DG Solvent Preparation

Sufficient amounts of solvents made up by blending LPG with DG in molar ratios of LPG/DG: 55/45, 45/ 55, 35/65, 25/75 and *15/85* were prepared and used in the slim tube displacement tests for the reservoir oil of P_b=1800 psia. Also, solvents with mole percents of LPG/DG: 40/60, 35/65, 30/70, 20/80 and 15/85 were prepared and used to displace the reservoir oil of P_b2030 psia.

Determination of MMC And MMP Experimentally

The slim tube technique for oil displacement has been used as the dynamic means of miscibility [2,3,8,10]. Miscibility apparatus was used for oil displacement by either mixtures of LPG/DG solvent to find the MMC or CO_2 to find the MMP.

Miscibility apparatus

The CORLAB Inc. miscibility apparatus was used in this investigation (Fig. 13) It consists of a pressure control system to monitor the inlet and the outlet pressures of the slim tube, a temperature control system includes an air bath and has a control panel to yield a constant temperature, a fluid flow control system comprising of a motorized mercury pump has a minimum rate in the range of 6-9 cm^3/h, a density meter to measure the produced fluid density at reservoir temperature and test displacement pressure. It is also connected to a fluid separator at which the recovered hydrocarbon and liberated gas were separated at atmospheric conditions. A coiled slim tube (stainless steel) with 40 ft long and 0.18 in. ID packed with 80/120 mesh Ottawa sands was used. Porosity and permeability of the slim tube column are 40.5% and 9.56 Darcys respectively.

Slim tube displacement test

The slim tube system and the solvent cylinder were cleaned, dried and evacuated. The required solvent volume was injected into the solvent cylinder and pressurized using the Ruska motorized pump. The

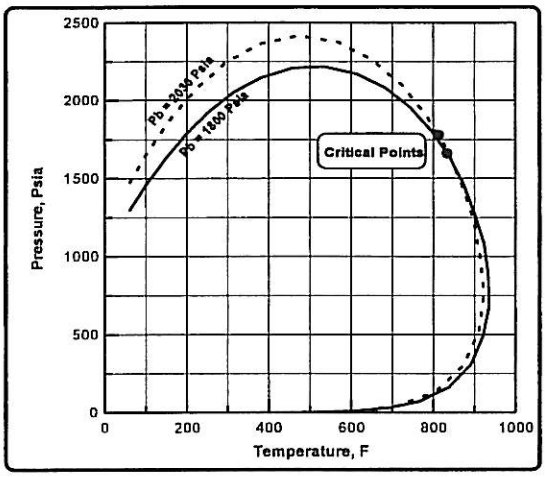


Fig. 7. EOS generated, pressure – temperature diagram, P_b = 1800 and 2030 psia, Raguba oil field, well No. E40.

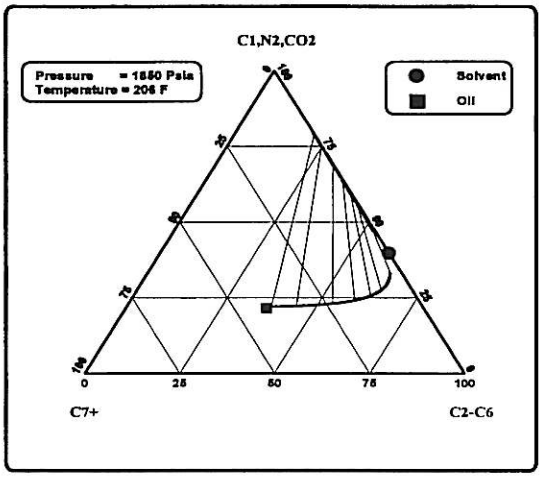


Fig. 8. Ternary diagram for solvent LPG/dry gas ratio 55/45, reservoir oil of P_b = 1800 psia at 206 °F.

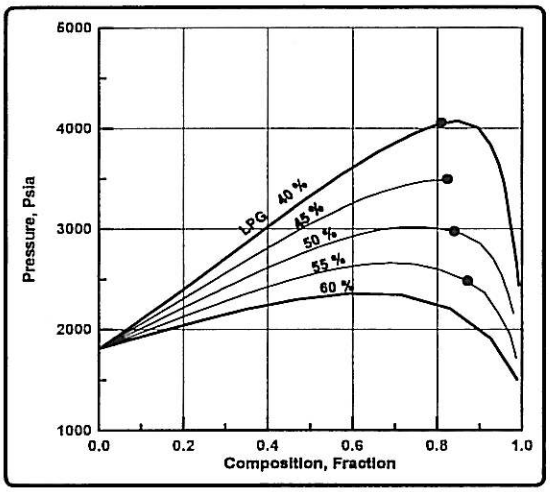


Fig. 9. EOS generated, pressure – composition diagram for oil 1800R and 5 mixture of LPG and dry gas, Raguba oil field, well No. E40.

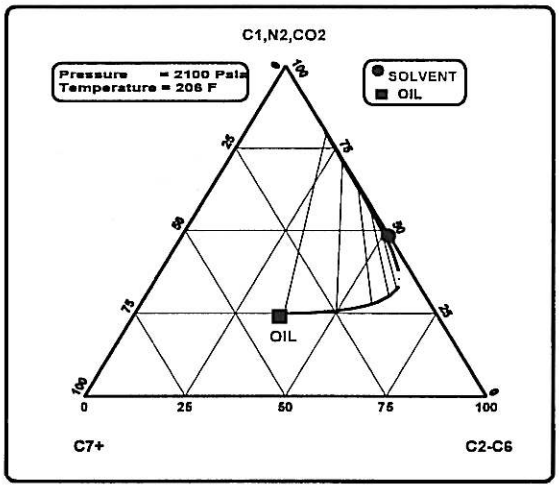


Fig. 10. Ternary diagram for solvent LPG/DG ratio 50/50 reservoir oil of P_b = 2030 psia at 206 °F, Raguba oil field, well No. E40.

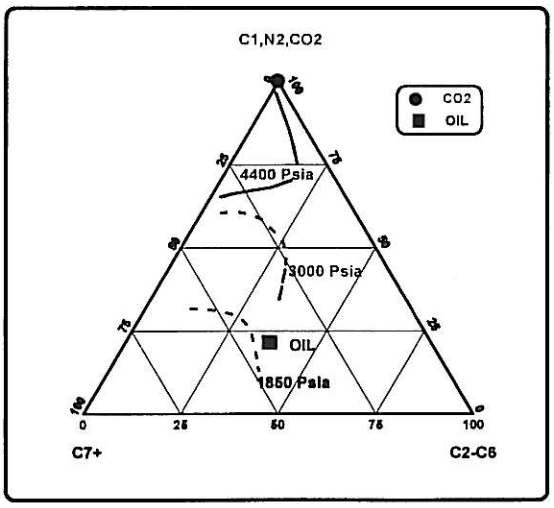


Fig. 11. Ternary diagram for Co_2 and reservoir oil of P_b = 1800 psia at 206 °F, Raguba oil field, well No. E40.

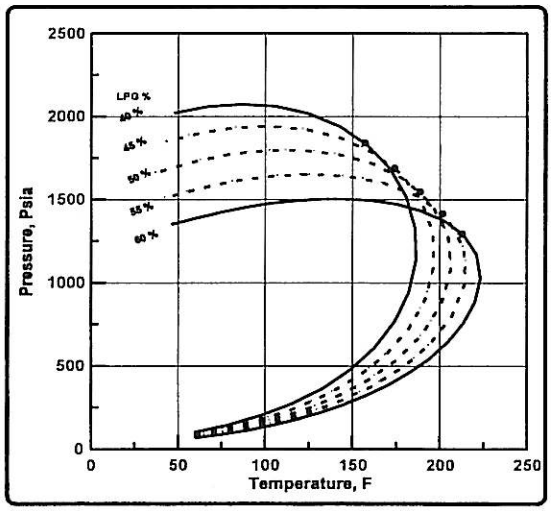


Fig. 12. EOS generated, pressure – temperature diagram for different mixture of LPG and DG, Raguba oil field, well No. E40.

slim tube and the downstream part of the system were filled first with toluene at pressure equal to the injection pressure. Then, a volume of the reservoir oil about 1.2-1.5 of the system volume was injected to displace the toluene. A slim tube displacement test was started after heating and stabilizing the reservoir temperature at 206°F.

A-Solvent injection

The solvent in the solvent cylinder was injected into the slim tube by a motorized pump to displace the reservoir oil at the required injection pressure and at constant flow rate. The produced gas and oil were sampled at regular intervals of 60 minutes.

B-Blow down

When solvent volume of about 1-1.2 of the system volume was injected, the inlet valve of slim tube was closed and the blow down was started. The downstream pressure was slowly lowered at the backpressure regulator to the atmospheric pressure and the recovered oil weight and gas volume were measured.

C-Toluene wash

At the end of the blow down, a sufficient amount of toluene was injected into the slim tube and the recovered oil and toluene was collected in a flask pre weighted. The flask and the contained fluids were weighted. Toluene in the flask was evaporated using Buchi Rotavapor type RE- 121 and the flask was re-weighed. Then the weight of the remaining oil in the flask was calculated.

Swelling Experiments

LPG/DG solvent preparation

Based on the slim tube experiments, the minimum miscibility compositions of LPG/DG needed for oil samples of P_b=1800 psia and 2035 psia were found 40/60 and *35/65* molar ratios respectively. Therefore, sufficient solvent volumes were prepared by blending LPG and DG at the nominated molar ratios. Compositions of these mixtures were determined by chromatography and listed as shown in Table 2. The composition of both reservoir oils was also presented in Table 2.

Swelling tests

Three swelling experiments were carried out to investigate the effect of LPG/DG solvent mixture and/or CO_2 injection into the reservoir oils of bubble point pressure of 1800 psia and 2035 psia. A (COREXPORT) long window PVT cell apparatus was used for the oil swelling experiments. Volumes of LPG/DG solvent mixtures of a molar ratio of 40/60 were calculated at solvent: oil molar ratios of 15, 30, 50, 70, and 85 percents and were added to the oil sample of bubble point pressure of 1800 psia in a PVT cell in five steps. This procedure was replicated for the oil sample of bubble point pressure of 2035 psia using LPG/DG solvent of a molar ratio *35/65*. CO_2 was added into a new oil sample of bubble point pressure of 2035 psia in the PVT cell at CO_2 /oil molar ratios of *15,* 30, 50, and 70 percents in four steps following the same procedure.

In each addition of LPG/DG solvent or CO_2 into the corresponding oil, a constant composition expansion study was performed on the new mixture. All PVT data were smoothed using the dimensionless compressibility Y-Function method. Liquid and gas volumes at pressures below the bubble point pressure were calculated from the Cathometer reading taken at the gas-oil interface for the mixture in the PVT

Table 2. Compositional analysis of injection solvents in swelling tests, Raguba oil field, well No. E40.

Component	Solvent for oil P_b=1800 psia (40% LPG + 60% DG)	Solvent for oil P_b=2035 psia (35% LPG + 65% DG)
	Mole %	Mole %
N_2	1.49	1.70
CO_2	0.02	0.00
C_1	53.06	57.79
C_2	6.14	6.59
C_3	12.91	12.03
IC_4	8.93	7.46
NC_4	17.21	14.27
IC5	0.03	0.03
NC5	0.02	0.03
IC6	0.03	0.04
NC6	0.03	003
C7+	0.13	0.03
Total	100.00	100.00

cell. Swelling factor, mixture density, and gas oil ratio were also calculated at each solvent addition. Solvent: oil molar ratio was re-calculated based on the actual solvent moles added into the reservoir oil.

RESULTS AND DISCUSSIONS

LPG/DG Solvents MMC Determination with Oils of P_b =1800 and 2030 psia

From the preliminary tuning of the equation of state (EOS) carried out on the reservoir oil of P_b = 1800 psia[2,6] solvent MMC was predicted at *55/45* of LPG/DG mole percentage. The first slim tube displacement test was then started at the above predicted solvent composition. This run in turn shows that the reservoir oil was completely miscible with the displacing solvent at the test conditions (injection pressure is 1850 psia at reservoir temperature equal to 206°F).

Miscibility of LPG/DG mixture solvent with reservoir oil is defined in this investigation as: the composition of the solvent in which *95%* or more of the oil saturating the slim tube system is recovered when solvent volume of about 1.2 of the pore volume is injected. Accordingly, LPG/DG compositions of *55/45* and *45/55* molar ratio solvents were found miscible in displacing the reservoir oil since the cumulative oil recovery was higher than *95%*. The other three compositions, LPG/DG: *35/65, 25/75* and 15/85 molar ratio solvents were immiscible as shown in figure 14. LPG/DG solvent mixture of a molar ratio 40/60 was found as the MMC. This ratio was obtained from the intercept of the straight lines of the miscible and the immiscible regions as represented (Fig. 14). Obviously the EOS for this oil overestimated the minimum miscibility composition.

Another five slim tube displacement experiments were conducted on reservoir oil of P_b=2030 psia. Various solvents made up by blending LPG with DG in molar ratios (40/60, *35/65,* 30/70, 20/80 and 15/85) were used. Based on the preliminary tuning of the equation of state (EOS) curried out on this oil, the MMC was predicted at a solvent of *50/50* of LPG/DG mole percentage. Because the EOS was overestimated the MMC as indicated in reservoir oil of P_b=1800 psia, a molar ratio 40/60 was judged to start the slim tube displacement series tests. At this molar ratio, the solvent was completely miscible with the displaced oil. The injection pressure on these five series experiments was constant and equal to 2100 psia. The intercept of the two straight lines in figure 15 shows that a minimum miscibility composition of 35% LPG and 65% DG was required to achieve miscibility with reservoir oil P_b =2030 psia. Overestimating of the MMC by EOS for this oil was also verified.

Recovery mechanism for both oils was found to be a multiple contact condensing drive mechanism in which hydrocarbon intermediate compounds (C_2-C_6) in the solvent condense into the reservoir oil until a sufficient quantity of this solvent exists at the displacement front to cause miscibility with the oil. An oil recovery more than 100% was observed in the slim tube displacement tests when the solvent was miscible with the oil, probably because of the predominant condensing drive mechanism.

MMP Determination for Oil of P_b = 2030 psia

To fmd the minimum miscibility pressure (MIMP) of CO_2 (99.18% pure) with reservoir oil of bubble point pressure 2030 psia, five CO_2 injection pressures: 3515, 3015, *2515,* 2315 and 2115 psia were conducted for oil displacement in the same slim tube described before.

Cumulative oil recovery versus pore volume gas injected relations were used to find the respective oil recovery at the CO_2 breakthrough. Minimum miscibility pressure of CO_2 with reservoir oil is defined as the pressure at which 80% or more of oil saturating the slim tube system is recovered at CO_2 breakthrough. The MMP of CO_2 with this oil was predicted to be 2710 psia at reservoir temperature-206°F as illustrated in figure 16.

The mechanism of oil recovery was a vaporizing drive at which CO_2 vaporizes hydrocarbon compounds (C_2-C_{30}) from the reservoir oil until a sufficient quantity of these hydrocarbons exists at the displacement front to cause miscibility with the oil. Cumulative oil recovery was found to be less than 100% when the CO_2 was miscible, because of the predominant vaporizing drive mechanism. The MIMP of CO_2 with this oil was calculateusingGlaso[23] correlation for pure CO_2 and was found to be equal to 2667 psia, which is in good agreement with the experimental results.

SWELLING OF RESERVOIR OILS P_b =1800 PSIA AND P_b =2035 PSIA WITH LPG/DG SOLVENTS

On the basis of the slim tube displacement experiment, the 40% LPG plus 60% DG hydrocarbon solvent was found to be miscible with oil of P_b =

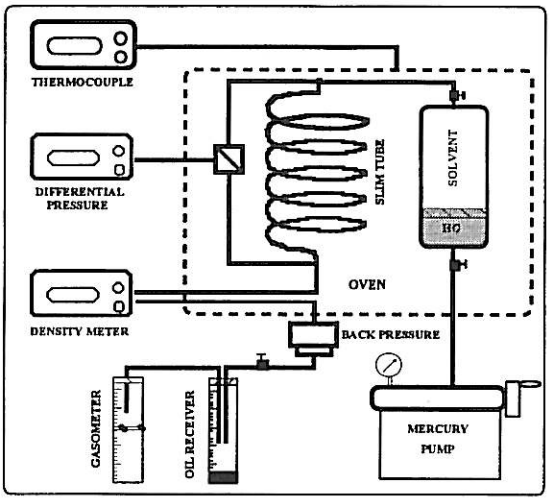


Fig. 13. Schematic diagram of slim tube apparatus.

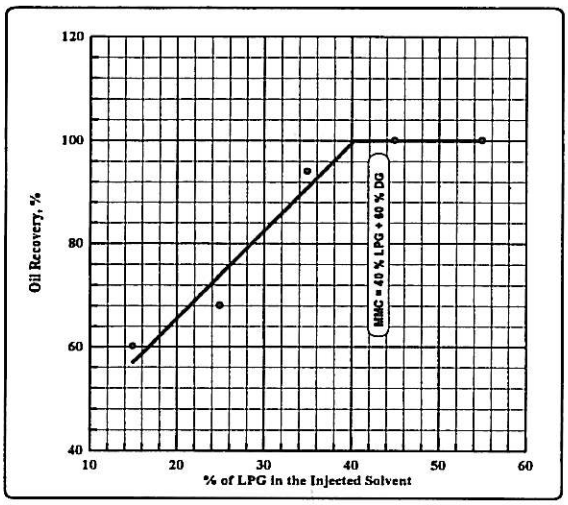


Fig. 14. Oil recovery as a function of % LPG in the injected solvent, reservoir oil (P_b 1800 psia), Raguba oil field, well No. E40.

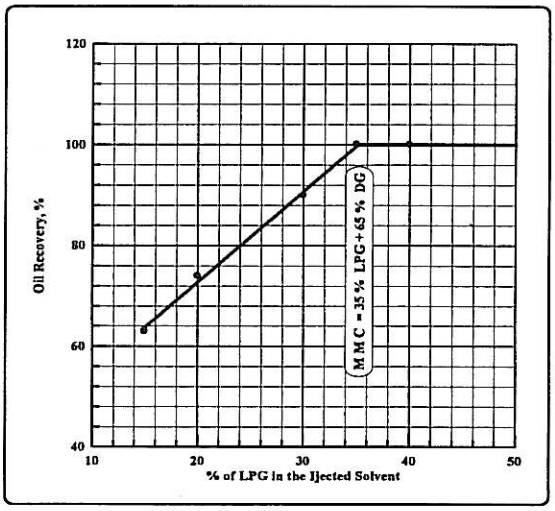


Fig. 15. Oil recovery *vs* pressure for reservoir oil (P_b 2030 psia) with CO_2, Raguba oil field, well No. E40.

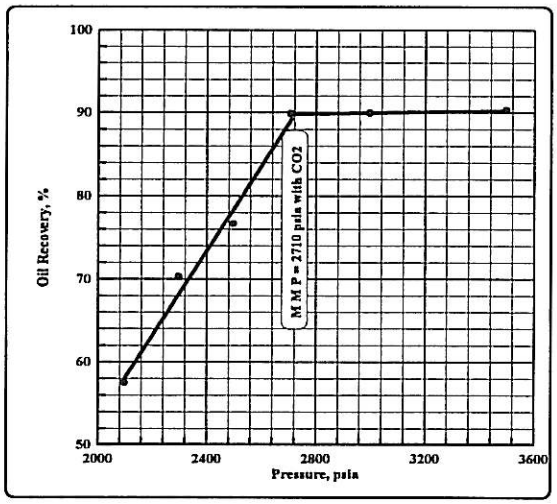


Fig. 16. Oil recovery *vs* pressure for reservoir oil (P_b 2030 psia) with CO_2, Raguba oil field, well No. E40.

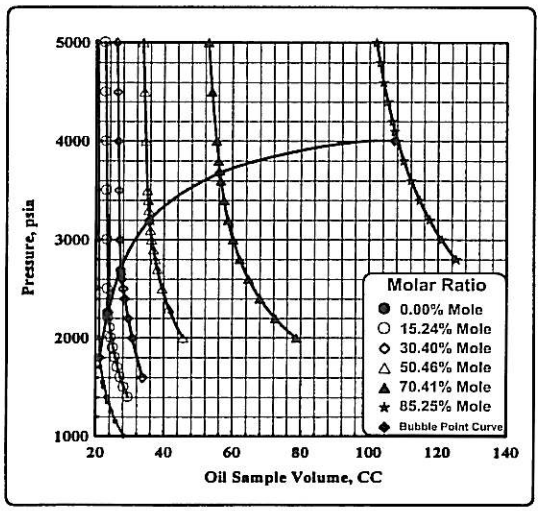


Fig. 17. Pressure – volume relations obtained from swelling of reservoir oil 1800R with 40% LPG +60% DG solvent at different LPG – oil molar ratio.

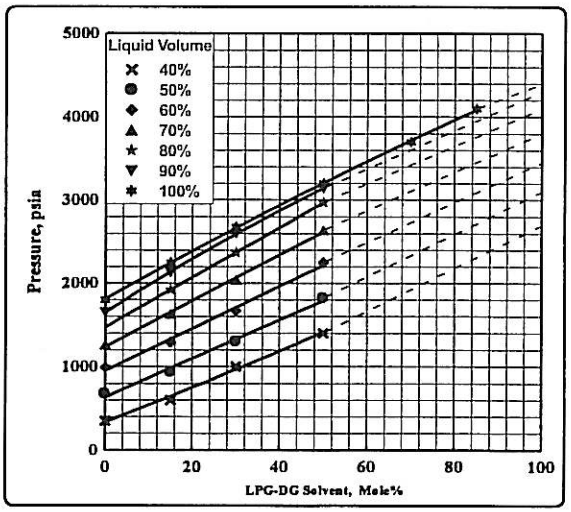


Fig. 18. Swelling test, quality lines, P_b = 1800 psia with 40% LPG +60% DG solvent at different LPG/DG – oil molar ratio.

1800 psia at reservoir temperature 206°F. Table 3 shows the summary of hydrocarbon swelling tests carried out on the reservoir oil sample of P_b =1800 psia.

The above oil was swelled by adding LPG/DG solvent mixture of a molar ratio 40/60 in five steps. Pre-calculated solvent volume for each addition was done according to solvent: oil molar percents of *15, 30, 50,* 70, and 85 as shown in Table 3. Pressure versus oil sample volume is plotted in figure 17. Pressure-composition (P-X) diagram represents quality lines as liquid percents in the swollen oil are shown in figure 18. Swelling factor and mixture density at the bubble point were calculated and illustrated (Figs. 23 and 24) as a function of the solvent mole percent added to the oil sample.

Table 3. Summary of hydrocarbon swelling test at 206 "F for reservoir oil sampl of P_b = 180 psia, Raguba oil field, well no. E40 .

Fluid	LPG/DG mole %	Saturation pressure psia	Swelling factor	Mixture density g/cc
Resvoir oil	0.000	1800	1.000	0.6749
Mixture # 1	15.24	2263	1.115	0.6468
Mixture # 2	30.40	2702	1.288	0.6107
Mixture # 3	50.46	3195	1.682	0.5556
Mixure # 4	70.41	3676	2.652	0.4816
Mixture # 5	85.24	4006	5.072	0.4194

Peg-Robinson equation of state (EOS) is applied to model the swelling experimental data for oil of P_b = 1800 psia, using the Computer Modelling Group (CMG PROP) software. Table 4 presents a comparison of the experimental data with EOS predicted values for saturation pressure and swelling factor for oil sample of P_b =1800 psia. Swelling factor values predicted by EOS match very well with the data experimentally obtained for five additions of LPG/DG mixtures as represented in figure 23. Predicted saturation pressures using EOS modelling are in a good match with the experimental data when LFG/DG mole is 50% and lower. At a higher molar percent, the predicted saturation pressures are under estimated.

LPG/DG solvent mixture of a molar ratio 35/65 was found as the minimum miscibility composition (MMC) with oil P_b = 2035 psia at reservoir injection conditions (2100 psia and 206°F). The compositional analysis of the reservoir oil and the injected hydrocarbon solvent *(35%* LPG+65% DG) were listed in Table 2. Therefore, this solvent was applied to swell reservoir oil at five steps. LPG/DG solvent mixture at solvent: oil mole percentages of 15, 30, 50, 70 and 85 were used. Table 5 shows the summary of hydrocarbon swelling tests carried out on the reservoir oil sample of P_b =2035 psia. Pressure versus oil sample volumes were plotted (Fig. 19). Pressure-composition (P-X) diagram represents quality lines as liquid percents in the swollen oil were shown (Fig. 20). Swelling factor and mixture oil density obtained from these tests as a function of the solvent/mole percent are plotted (Figs. 23 and 24).

SWELLING OF RESERVOIR OIL P_b = 2035 PSIA WITH CO_2

Carbon dioxide CO_2 (99.19% purity) was applied to swell the reservoir oil of bubble point pressure 2035 psia at reservoir temperature of 206 °F. Volume of CO_2 added to the reservob-oil was calculated at the CO_2: oil molar ratios of 15, 30, 50 and 70. Pressure versus oil volume is plotted in figure 21. Pressure-composition (P-X) diagram represents quality lines as liquid percents in the swollen oil were shown (Fig. 22). Swelling factor and mixture oil density as a function of added solvent: oil mole percent are plotted (Figs.

Table 4. Comparison of experimental data of hydrocarbon swelling test with EOS predicted values, reservoir oil sample of Pb = 1800 psia, at 206 "F, Ragua oil field, well no. E40.

Fluid	LPG/DG mole %	Saturation pressure psia	Predicted saturation pressure psia	Swelling factor	Mixture density g/cc
Resvoir oil	0.000	1800	1801	1.000	1.000
Mixture # 1	15.24	2263	2206	1.115	1.115
Mixture # 2	30.40	2702	2624	1.288	1.283
Mixture # 3	50.46	3195	3154	1.682	1.672
Mixture # 4	70.41	3676	3462	2.652	2.639
Mixture # 5	85.24	4006	3197	5.072	5.347

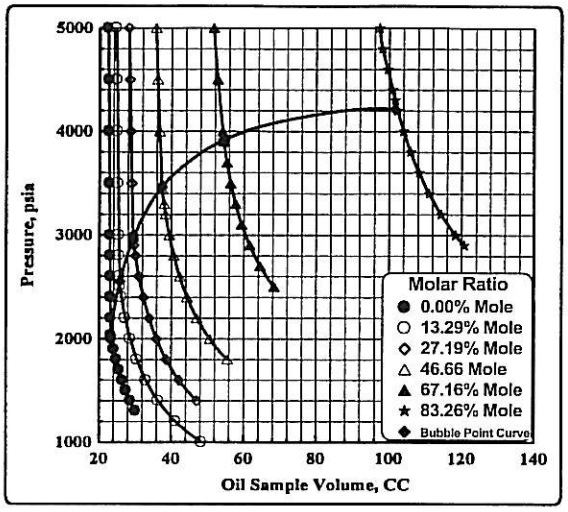


Fig. 19. Pressure – volume relations obtained from swelling of reservoir oil 2035R with 35% LPG+65%DG solvent at different LPG/DG – oil molar ratio.

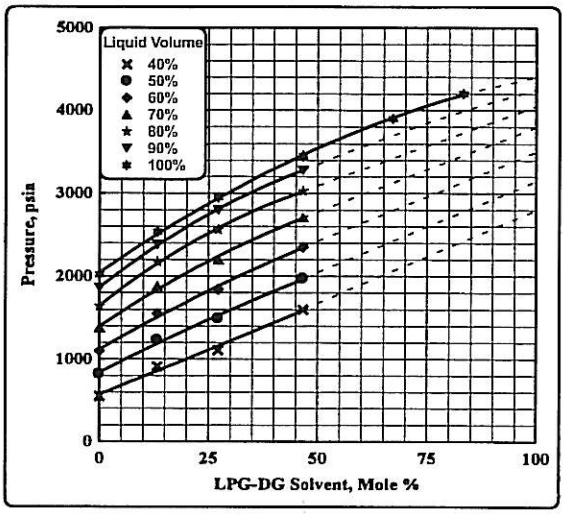


Fig. 20. Swelling test, quality lines, P_b2030 pia with 35% LPG+65% DG solvents at different LPG/DG oil molar ratio.

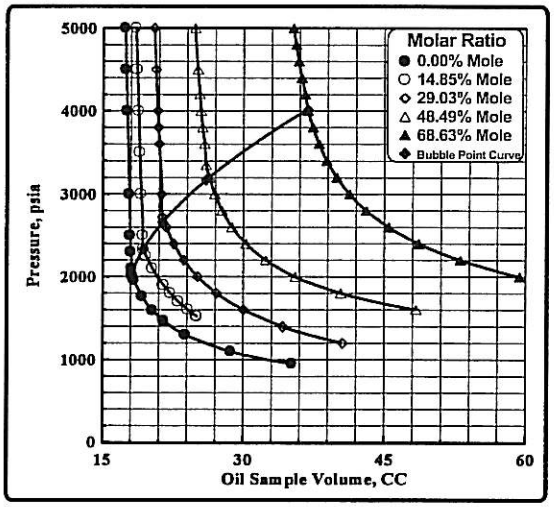


Fig. 21. Pressure – volume relations obtained from swelling of reservoir oil 2035R with CO_2 at different CO_2 oil molar ratio.

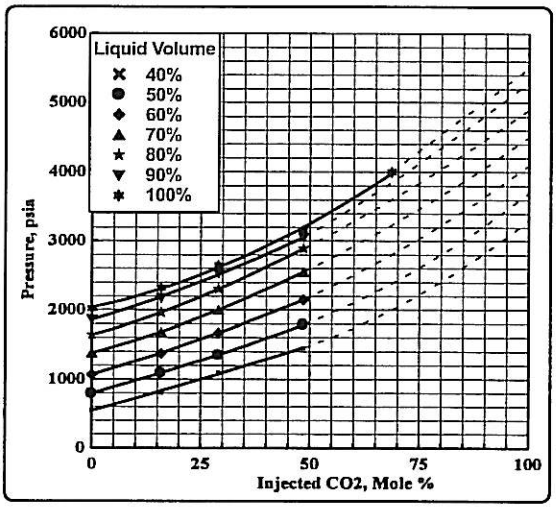


Fig. 22. Swelling test, quality lines, P_b = 2030 psia ith CO_2 at different CO_2 oil molar ratio.

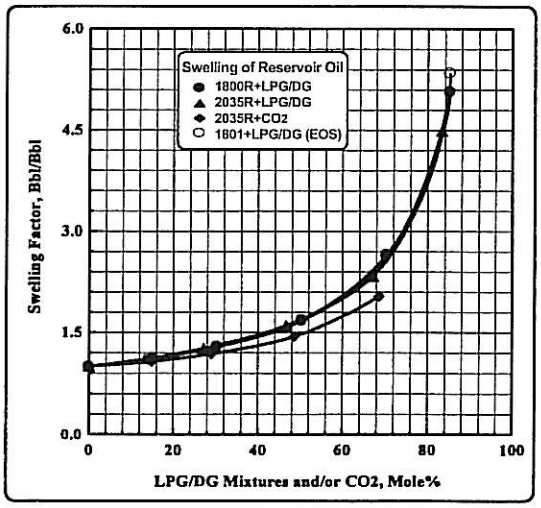


Fig. 23. Swelling factor for reservoir oils after injection of LPG/DG and / or CO_2 at 206 °F.

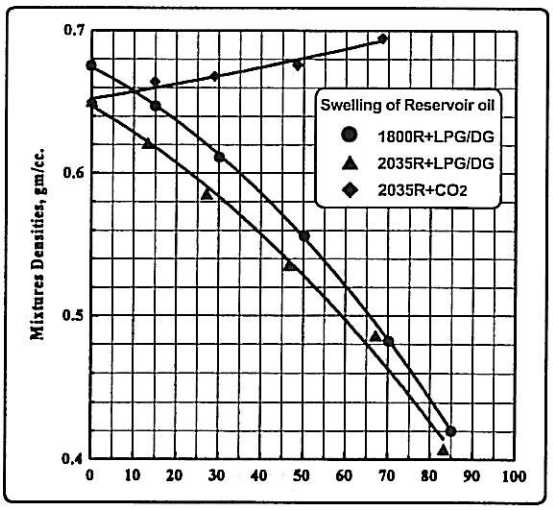


Fig. 24. Mixture densities for reservoir oils after injections of LPG/DG and / or CO_2 at 206 °F.

Table 5. Summary of hydrocarbon swelling test at 206 °F for reservoir oil sample of P_b = 2035 psia, Ragua oil field, well no. E40.

Fluid	LPG/DG mole %	Saturation pressure psia	Swelling factor	Mixture density g/cc
Resvoir oil	0.000	2035	1.000	0.6502
Mixture # 1	13.29	2551	1.106	0.6209
Mixture # 2	27.19	2965	1.262	0.5853
Mixture # 3	46.65	3465	1.601	0.5355
Mixture # 4	67.15	3915	2.333	0.4861
Mixture # 5	83.26	4215	4.489	0.4071

Table 6. Summary of carbon dioxide swelling test at 206 °F for reservoir oil sample of P_b = 2035 psia, Ragua oil field, well no. E40.

Fluid	LPG/DG mole %	Saturation pressure psia	Swelling factor	Mixture density g/cc
Resvoir oil	0.000	2035	1.000	0.6500
Mixture # 1	14.90	2336	1.068	0.6641
Mixture # 2	29.00	2657	1.181	0.6681
Mixture # 3	48.50	3172	1.436	0.6760
Mixture # 4	68.50	4015	2.036	0.6947

23 - 24). The summary of CO_2 swelling results carried out on the reservoir oil sample of P_b = 2035 psia are shows in Table 6.

Swelling factors for both oils are almost identical when LPG/DG solvent is used for swelling. However, swelling factor for oil P_b = 2035 psia using CO_2 appears to become lower compared to that obtained with LPG/DG solvent when the molar percent is increased as shown in figure 23.

Swollen mixtures density for both oils of pressure 1800 psia and 2035 psia decreases when the added molar ratio of LPG/DG solvent is increased. While swollen mixture's density for oil of P_b pressure 2035 psia increases as the molar ratio of CO_2 added is increased as illustrated in figure 24. Accordingly, sweep efficiency for the displaced oil by CO_2 expected to have an advantage compared to that with LPG/DG solvent when the miscibility conditions are satisfied.

CONCLUSIONS

1. Solvent mixture of a molar ratio LPG/DG 40/60 was found as the MMC with oil of P_b= 1800 psia, at the injection pressure of 1855 psia at 206°F. Obviously the minimum miscibility composition value was over estimated by the EOS for this oil (LPG/DG: 55/45).
2. Solvent mixture of a molar ratio LPG/DG: 35/65 was found as the MMC at injection pressure of 2100 psia for reservoir oil P_b=2030 psia at 206°F. The minimum miscibility composition was also overestimated by the EOS for this oil (LPG/DG: 50/50). However, more work should be performed in order to understand the actual reasons for these phenomena for both oils.
3. The oil recovery mechanism for both oils (P_b =1800 psia and 2030 psia) was found to be a multiple contact condensing drive mechanism when displaced by LPG/DG solvent at miscibility conditions.
4. The MMP of CO_2 for reservoir oil of bubble point pressure of 2030 psia was experimentally determined to be 2710 psia at reservoir temperature of 206°F. The mechanism of oil recovery was a vaporizing drive. MMP of CO_2 was also calculated using Glaso[12] correlation for pure CO_2 for comparison and was found to be equal to 2667 psia, which shows good agreement with the experimental results.
5. Swelling factor values predicted by EOS match very well with the data experimentally obtained for five additions of LPG/DG mixtures into oil reservoir P_b = 1800psia.

6. Predicted saturation pressures using EOS modelling are in a good match with the experimental data when the molar percent of LPG/DG is *50%* and lower. At a higher molar percent, the predicted saturation pressures are under estimated.
7. Swollen mixture density for both oils of P_b pressure 1800 psia and 2035 psia decreases when the added molar percent of the LPG/DG solvent is increased.
8. The swollen mixtures density for the oil of P_b pressure 2035 psia increases as the molar percent of the CO_2 added is increased. Therefore, sweep efficiency for the displaced oil by CO_2 expected to have an advantage compared to that with LPG/DG solvent when the miscibility conditions are satisfied.

ACKNOWLEDGEMENT

Thanks are expressed to the management of Sirte Oil Company for entrusting the Petroleum Research Centre to conduct this project. Thanks are also extended to the management of the Petroleum Research Centre and Reservoir Fluid Section for their support; and to the EOR Group for their contribution in the experimental work.

REFERENCES

[I] Al-Khafaji, A.H., Al-Dulaimy, S.N. and Al-Doury, M.M., 1989. Correlation for minimum miscibility pressure, hydrocarbon gas-oil systems,. *JPR* , **8**, 1, 15-23.

[2] Luks, K.D., Turek, E.A. and Baker, L.E., 1987. Caldiilation of minimum miscibility pressure. *SPERE*, (November) 501-506.

[3] Glaso, O., 1980 (May). Generalised pressure-yolume-temperature correlations,.*J. Pet. Tech.*

[4] Short course prepared and presented by Hycal Research Laboratories Ltd., 1990. Design, Interpretation and Use of Experimental Laboratory Data for Miscible Flood Processes, Second Edition 1990.

[5] Benham, A.L., Dowden, W.E. and Kunzman, W.J., 1960. Miscible fluid displacement prediction of miscibility, *Trans., AIME* **219** 229-237.

[6] Thomas, F.B., Bennlon, D.B., Bennlon, D.W., Recent development in laboratory data sets for determination of miscibility limits," Paper CIM/ AOSTRA 91-4, Prsented at the CIM/ AOSTRA Technical Conference in Banff, (April 2 1-24) 1-24.

[7] Brigham, W.E., Reed, P.W. and Dew, J.N., 1961. Experiments on mixing during miscible displacement in porous media, *Soc. Pet. Tech. J., Trans., AIME*, **222**.

[8] Nutakki, R., Hamoodi, A.N., Li, Y.K., and Nghieiii,L.X., 1991 (October). Experimental analysis, modelling, and interpretation of recovery mechanisms in enriched-gas pprocesses,. Paper *SPE* 22634 presented at the 66th annual technical conference and exhibition of the Society of Petroleum Engineering held in Dallas, TX.

[9] Orr, F.M., Jr., Sijva, M.K., Lien, C.L. and Pelletier, M.T., 1982 (April). Laboratory experiments to evaluate field prospects for CO_2 flooding, *J. Pet. Tech.* 889-898.

[10] Des Brisay, C.L., Gray, J.W. and Spivak, A., 1975 (August). Miscible flood performance of the Intisar (D) field, Libyan Arab Republic, *J. Pet. Tech.* 935-943.

[11] Frazier, G.D. and Todd, M.R., 1982 (April). Alvord (3000-ft Strawn) LPG-design and performance evaluation, paper SPE/DOE 10692, presented at the SPE/DOE third joint symposium on enhanced oil recovery of the Society of Petroleum Engineering held in Tulsa Ok.

[12] Standing, M.B., 1977. *Volumetric and Phase Behaviour of Oil Field Hydrocarb Systems's.* Reinhold Publishing Corporation, New York.

[13] Al-Khafaji, A.H., 1995. *Standardisation. of PVT Studies-Experimental and Analyses. Internal Rept.,* Petroleum Research Centre, Tripoli, Libya.

[14] Whitson, C.h.,1992. *Advanced PVT and Fluid Characterisation,*. HOT Engineering GbH, Leoben, Austria.

[15] Raynald, M., 1968. Etudes PVT des fluides de gisements d'hydrocarbures. *Institut Francais du Pétrole.*

[16] Alston, R.B., Kokolis, G..P. and James, C.F. CO_2 minimum miscibility pressure: a correlation for impure CO_2 streams and live oil systems, *Soc. Pet. Tech. J.* 268-274.

[17] Holum, L. W. and Josendal, V.A. 1982 (Feb.). Effect oil composition on miscible-type displacement by carbon dioxide. *Sec. Pet. Tech.* J. 87-98.

[18] Enhance Oil Recovery Project, 1996. *Raguba Oil Field, Phase-1 PVT Studies, Phase-2 Equation of State Modeling.* Unpublished Rept. Prepared by Petroleum Reserarch Centre for Sirte Oil Company, Tripoli, Libya.

[19] Al-Khafaji, A.H., Alswieh, M., Abuzbeda, S.T. and Alabani, S.O. 1996 (Jan.). Equation of state application to predict MMC and MMP for Raguba oil field, Libya. Petroleum Research Journal **8** 1997.

[20] علي حبيب الخفاجي، بشار حسن الرئيس: "استخلاص البترول المدعم في الوطن العربي إلى أين؟" (دور التقنيات الحديثة في زيادة الاحتياطي البترولي) منظمة الأقطار العربية المصدرة للبترول (أوبك)، دمشق، سورية، للفترة 28–30 9/9/1990.

[21] Enhance Oil Recovery Project 1996. *Raguba Oil Field, Phase-3: Miscibility Studies; and Phase-4: Swelling Studies.* Unpulished Rept. Prepared by Petroleum Research Centre for Sirte Oil Company, Tripoli, Libya.

[22] Al-Khafaji, A.H. Abuzbeda, S.T., and Dahab, M.F., 1999. Slim – tube technique for miscibility conditions of Raguba oil field, Libya, The 6th International Mining, Petroleum and Metallurgical Engineering Conference (20-24 February 1999) Giza, Egypt.

[23] Glaso, O. Generalised minimum miscibility pressure correlation. *Soc.Pet. Eng. J.* 927-934.

[24] Al-Khafaji, A.H., Dahab, M.F., Alabani, S.O., and Alswieh, M., 1997 (November). Swelling of Raguba reservoir oil using LPG/DG mixtures and carbon dioxide. The 5th Mediterranean Petroleum Conference and Exhibition, Tripoli, Libya.

Petroleum Res. J. Vol. 14 (2002): P. 37–44, 10 Figs.

A Case History of Attic Oil Recovery of a Unique Multi-layered Bottom Water-drive Carbonate Reservoir

AM. Reda, C. Wong, M. Gharsalla and A. Majdoub*

إستخراج نفط لمكمن علوي جيري لحالة فريدة تتم بواسطة الدفع بالمياه عند القاع

رضا عبد المولى، و س. و نغ، و م. غرس الله و أ. المجدوب

تصف هذه الورقة دراسة محاكاة بعقد الإمتياز 103د في حقل الجيزة بليبيا، الذي يتكون المكمن فيه من صخور جيرية متعددة الطبقات غير إعتيادية ليكون ذا ميزة فريدة حيث يتم الدفع النفطي فيه بواسطة المياه عند قاعه بفعل تسرب كثيراً من المياه من نطاق تغليف بئر حقل المكمن أسفله وليس بواسطة اكتساح المياه الجوفية.

سلطت الظروف المحيطة بفقدان ماء المكمن، وما ترتب على ذلك تحديد لحالة الإنتاج العادية عند إيقاف الحقن، الضوء على وجود طبقة فريدة مجواة وسط التكوين ذات مسامية فريدة تصل إلى 4.5 دارسي. كما أدى مكان وتأكيد وجود طبقة ذات مسامية عالية إلى التعرف على تجمع هائل من الزيت.

هدفت هذه الدراسة إلى تحديد كمية وقوة الخزان الجوفي المائي ومعرفة الزيت المحصور والمتسرب وبحث إستراتيجية للإنتاج الأمثل. كل ذلك تم إنجازه بعد حل لغز تسرب المياه المبكر والذي يشمل الموقع والحجم والشكل وهل تأثير ذلك على نظام الدفع بالمياه طبيعياً.

Abstract: *This paper describes a simulation study of 103D El-Giza, an unusual multi-layered bottom water-drive carbonate reservoir in Libya that features a unique pre-mature water-out, caused not by aquifer invasion but by a massive casing leak of injection water from an underlying reservoir. The circumstances surrounding the reservoir's water-out and subsequent revival to normal production when injection was halted, sheds the light on the existence and extent of a unique 4.5-darcy high permeability vuggy layer in the middle of the formation. The location and confirmation of this dominating high permeability layer led to the identification of a significant attic oil accumulation.*

* Zueitina Oil Company, Tripoli, Libya

The objectives of the study were to quantify the strength of the aquifer, identify trapped and bypassed oil and investigate a strategy to optimize their recovery. These were accomplished after solving the puzzle of the early water-leakage, including its location, volume and profile and sorting out its impact on the natural water-drive system.

GEOLOGY

The reservoir is a symmetrical, dome-shaped structural trap with a shallow relief of 140 feet and a relatively uniform net pay of 50 feet (Fig. 1), overlying a massive bottom aquifer of thickness of 1300 feet. The oil zone is predominantly good quality, fossil-rich calcarenite carbonates. Contrastingly, the quiver is exclusively fine-grained tight calcilutite. Despite similar porosity (Fig. 2) showing across the oil zone, the reservoir is actually layered, as evidenced in the dramatic differences in its resistivity indicators. Based

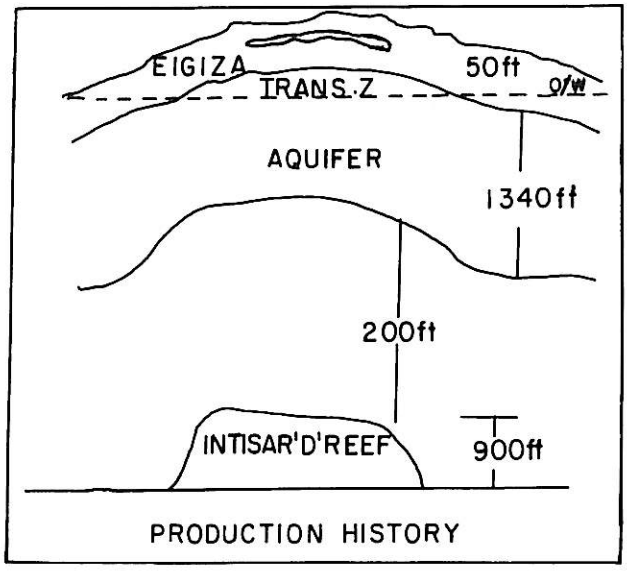


Fig. 1. Schematic structure of El-Giza.

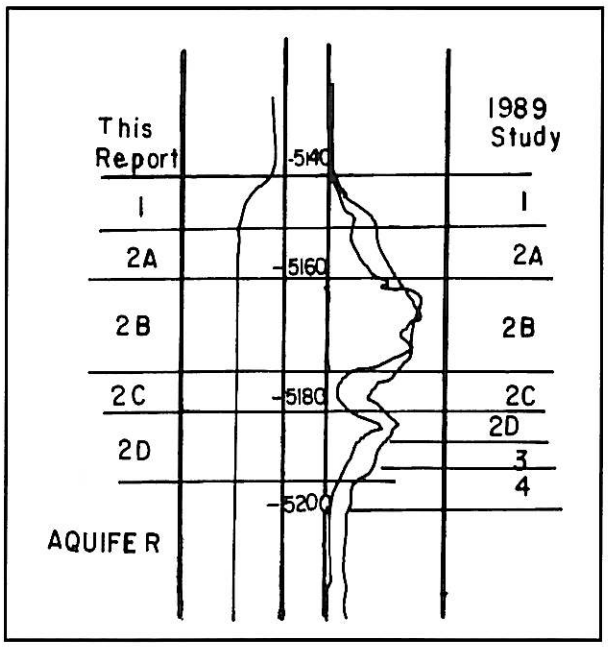


Fig. 2. Layer definitions.

on core permeability and resistivity logs, the thin oil zone can be broken down into five layers (1, 2A, 2B, 2C and 2D). All these layers, with the exception of 2B, and including the tight 2C, can be readily correlated across the field. From core analysis, the bulk of the productive intervals, *i.e.* 2A, 2B and 2D, have permeability in a range of 50 to 150 md, the tight layers, 1 and 2C, 5 md and 10 md, respectively, and the bottom aquifer, a mere two md.

However, this permeability only represents the rock quality of the matrix. Build-up tests show that five of the eight wells have overall permeability exceeding 700 md and as much as 150 md. This test-derived permeability indicates that a secondary porosity system exists. Since no open fractures have been identified in the core, the secondary porosity is most likely vuggy. Core study has, indeed, identified a large amount of mouldic vugs. Numulites and operculinoids are of size up to 20 mm in diameter. The location and area extent of these vugs become the first major puzzle of this study, which need to be resolved before simulation of the production history can proceed.

PRODUCTION HISTORY

The production history itself presents another major puzzle. The entire reservoir actually watered out in 1980, after a 7-year production and an oil recovery of only 8 MMSTB (nine per cent of original oil in place (OOIP) of 84 MMSTB) as shown in the water cut history in figure 3. It is interesting to note that this global water-out was not caused by natural aquifer invasion. Instead, it was caused by the leaking of injected fresh water, intended for another reservoir, the 'D reef', some 3300 ft below. This was confirmed by the low salinity water production and the unusual rise of the reservoir pressure (Fig. 4) prior to

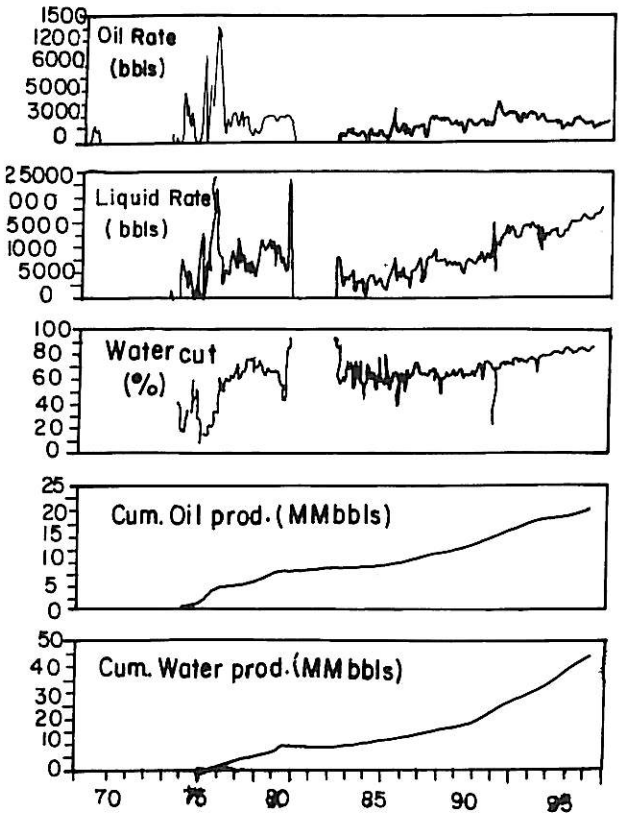


Fig. 3. Production history.

commencement of full-scale production in 1974. It was more amazing that when the 'D reef' water injection was terminated in 1982 and the El-Giza was returned to production, the reservoir has been able to produce normally ever since. It is important to note that during this second phase production period; (1) the produced-water salinity became gradually more saline and finally returned to the formation water salinity of 128,000 ppm by the later 1980s and (2) the reservoir pressure went on a major slide, losing more than 500 psi until stabilizing in 1994. The salinity development showed that a large amount of injected fresh water was stored when production was temporarily suspended in 1980 and was back-produced in the period of 1983-1990. This further confirms that the secondary porosity in El-Giza is of a vuggy nature rather than fracture, since fracture has little pore volume and would not serve as the capacitance required to retain the large amount of invaded fresh water. Two major conclusions can be drawn from the pressure and production history: (1) a thief zone of vugs in the reservoir was flooded by the invading fresh water during the early period of production (1974-1980) and this thief zone was resaturated with oil when fresh water invasion stopped and the flooded fresh water back-produced and (2) the bottom aquifer, despite its massive size, is not active, *i.e.* unable to maintain pressure for the given withdrawal rates of the 1980s.

THE ATTIC OIL RECOVERY PROJECT

Based on the understanding of the reservoir's geology and performances, a 2-phases, 3D simulation study was conducted using ECLIPSE. This simulation exercise had the objectives of: (1) confirming reservoir characterization, (2) history-matching the fresh water-leak period of 1974-1980 and the bottom water-drive period of 1982-1997, (3) identifying the remaining oil distribution in reservoir, (4) quantifying the strength of the bottom water-drive and (5) predicting the merits of increasing the reservoir withdrawal rate by switching from gas-lift to electrical submersible pump (ESP) production.

When the numerical model was satisfactorily history-matched, it was not surprising to find that most of the remaining oil was located as a blanket at the top two layers, i.e. 1 and 2A. In the prediction phase, the base case, *i.e.* the status-quo gas-lift operation, only achieved an overall oil recovery of 36.3%. At the end of the base case prediction (2025), it was astonishing to find that some 32.6% of the reservoir's OOIP of 84.3 MMSTB or 96.8% of the OOIP of the

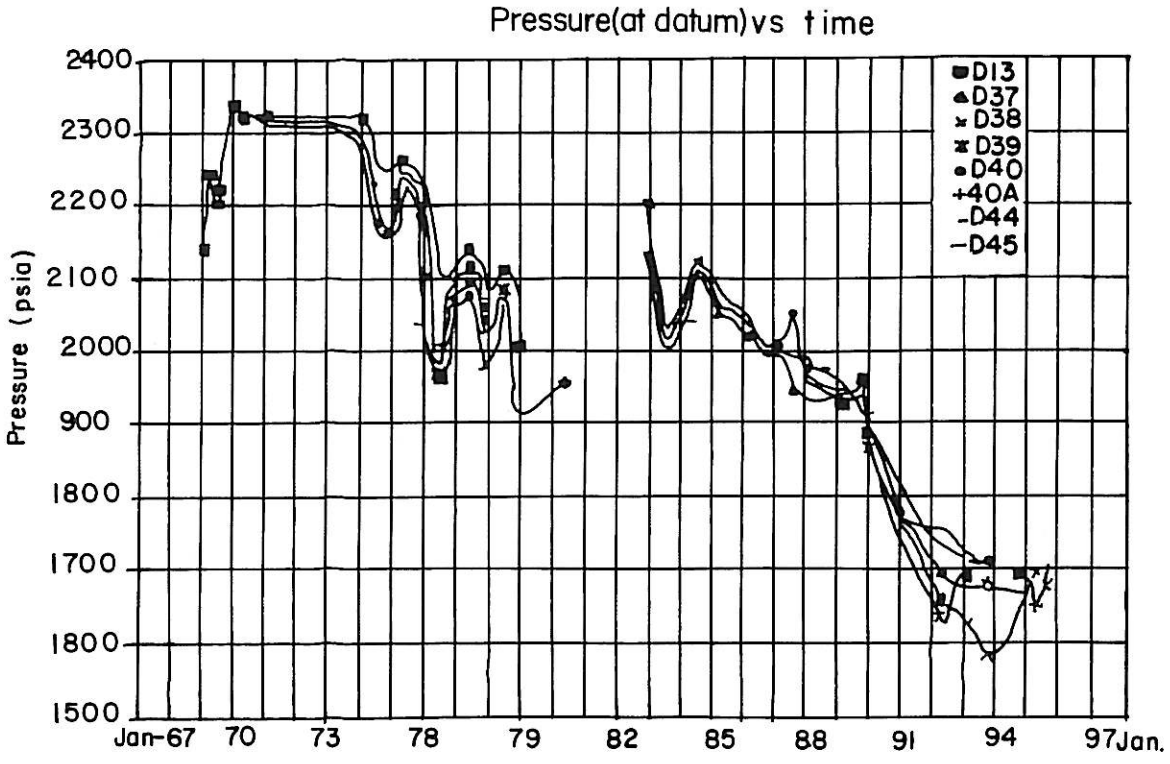


Fig. 4. El-Giza pressure history.

top two layers, 1 and 2 A remained at the reservoir's attic. It was more astonishing to find that the reservoir's overall recovery could be increased by 6.2% of the OOIP to 42.5% by switching to ESP operation.

The incremental recovery in the ESP case was found to be a result of the ESPs' ability in more than doubling the reservoir's withdrawal rate. This increased withdrawal caused the reservoir pressure to drop rapidly in the vuggy (high permeability) 2B layer, thereby pulling oil down from the thinner attic (layers 1 and 2A) across the field like a blanket (Fig. 5a,b).

It should be explained that the ability of ESPs in doubling the withdrawal rates in El-Giza is due to the production bottleneck caused by the gas-lift operation itself. Under gas-lift, small drawdowns (as little as 150 psi) and high wellhead pressures (as much as 650 psig) are the norm. These bottlenecks are caused by excessive pressure loss in the well bores due to the impulsive nature of the fluid stream and by the surface facility under-design in handling the third phase flow of such an emulsive fluid. ESPs eliminate the third phase flow and, therefore, most of these bottlenecks, thus following a much bigger drawdown to bring the bottom hole flowing pressure down to the productive 600 psig. The El-Giza oil is a 29 degrees API crude, having a low saturation pressure of 410 psia.

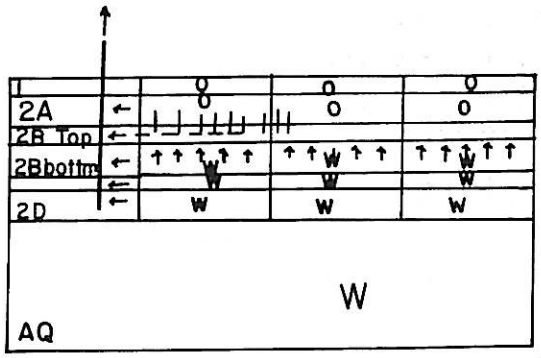


Fig. 5a. Fluid movement under gas-lift.

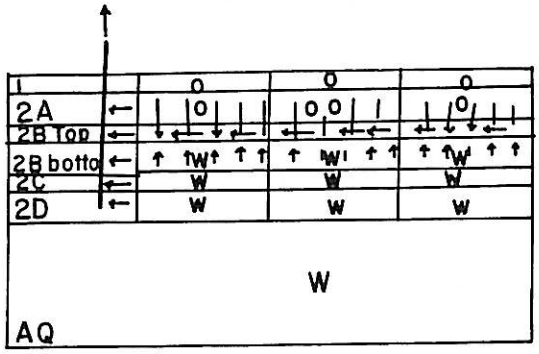


Fig. 5b. Fluid movement under ESPs.

Under ESP operation, simulation showed that the benefit was not limited to recovering more oil from the attic. Production was also projected to more than double immediately from the current 2100 STB/D to 4700 STB/D.

These production and recovery (Fig. 6) projections yield a highly, economically prolific project, with incremental NPVs (at 10%) of 52 MM$ at $29/Bbl, or 27 MM$ at $10/Bbl, with a payout time of less than 6 months.

Since the completion of the study, an ESP has been implemented on a pilot well, D13 and the simulation model's prediction of ESPs ability of doubling the oil production rate has been confirmed. Test results have shown this well's production increased from 300 STB/D to 790 STB/D at water cuts even lower than those under gas-lift. The production engineer's fear of the higher withdrawal rate drawing in more water and accelerating the water-out of these already high water cuts wells is now overcome. The project is now waiting for the extension of the power highline and the field-wide installation of ESPs.

CONVENTIONAL ANALYSIS AND SIMULATION

The benefits of this project, in terms of production, recovery and economics, are small in Libyan standards and are by no means unique. The uniqueness of this project, in fact, lies in the puzzles and the approaches in solving these puzzles. In the modeling exercise, it was equivalent to simulating a water flood history without the knowledge of the injector locations, the amount of injection as well as the injection profile. Although the location of the

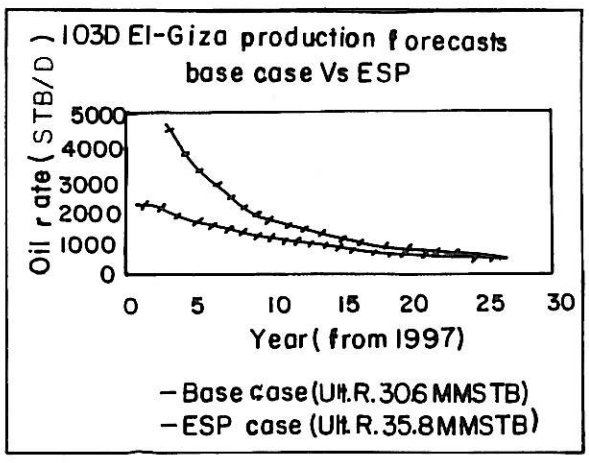


Fig. 6. 103D El-Giza production forecasts.

vuggy thief zone at the top of layer 2B is rather obvious as demonstrated in the resistivity logs, the areal extent and its connectivity are not known. In addition, the total pore volume of the thief zone, which dictates the pace of the water-out in the fresh water invasion period as well as the water cuts development in the fresh water back-produced period, has to be estimated correctly, bearing in mind that the major objective of the simulation is to quantify the strength of the aquifer's natural water drive. This requires first filtering out the influence of the fresh water invasion, more importantly in the later period (1982-1990), when aquifer water gradually replaced fresh water that was left behind in the reservoir. The analysis that led to the proper initialization of the numerical model are summarized as follows:

(1) **Fresh Water Leak Volume**. The history shows that the reservoir pressure was in equilibrium (at 2200 psia) when production was reactivated in 1982. The total amount of fresh water invasion was easily estimated from material balance at 18.5 MMRB or approximately 20% of the total hydrocarbon pore volume.

(2) **Fresh Water Leak Location**. There were 16 water injectors in the 'D reef' project. Temperature logs were run on some suspected injectors but failed to identify the culprit. Intuition suggests that the leaking of such a large amount of water will require a direct passage to the vuggy zone. This intuition limited the search only to the high structure area where the vuggy zone existed. This reduced the suspected injectors to seven. The analysis of the historical pressure trends and early salinity patterns had further reduced the suspect to two injectors in the east, D38 and D24. The pressure history has clearly demonstrated that the producer in the east, D13, has a consistently higher-pressure trend than all other wells throughout the entire water leak period. The lowest salinity of D13 confirms that the D38 well was the nearest well to the source of the water leak. A visit to the injection record of these two injectors finally identified D24 as the source of the water leak. The other injector, D38 has a small injection volume and cannot account for the leak. Using D24's injection profile and the historical pressure trends of the producers, a hypothetical injection profile was created to serve as initial injection input for the pseudo injector at the D24 location.

(3) **Thief Zone Location**. A vuggy zone has little surface area to trap irreducible water. The abnormally low water saturation environment of a vuggy zone, therefore, can easily be identified from the resistivity logs. Using resistivity logs, the thief zone was identified to be at the top of the 2B zone and in only the high structure area, covering 6 of the 8 El-Giza producers (Fig.7). This area coverage is consistent with the wells' high build-up permeability distribution.

(4) **Thief Zone Permeability**. A flow meter survey was conducted at D40a. This survey (Fig. 8) showed 85% of the flow coming from a 10-ft. interval at the top of the 2B zone. Using the well's overall build-up permeability of 1250 md, the permeability of this 10 feet vuggy zone was estimated at approximately 4500 md.

(5) **Reservoir Characterization**. Using the vuggy zone permeability of 4500 md, the overall build-up permeability of the wells and the matrix core permeability as a guideline, the individual zones were characterized for all 45 wells that penetrated the reservoir. The resistivity logs were heavily used in correlating the reservoir properties for the 38 wells that did not have a build-up test. A log-core match and the reservoir characterization of the individual layers of the D1 well are shown in figure 9.

(6) **Aquifer Influence**. The bottom aquifer is situated in an exclusively fine-grained calcilutite

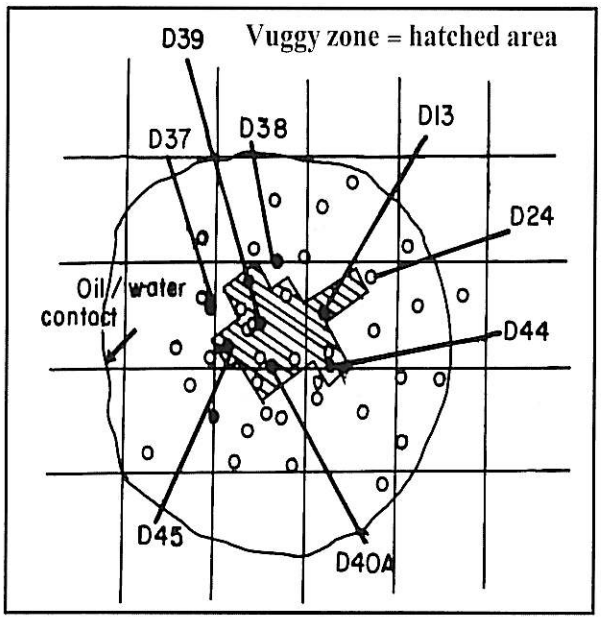


Fig. 7. El-Giza vuggy zone area extent.

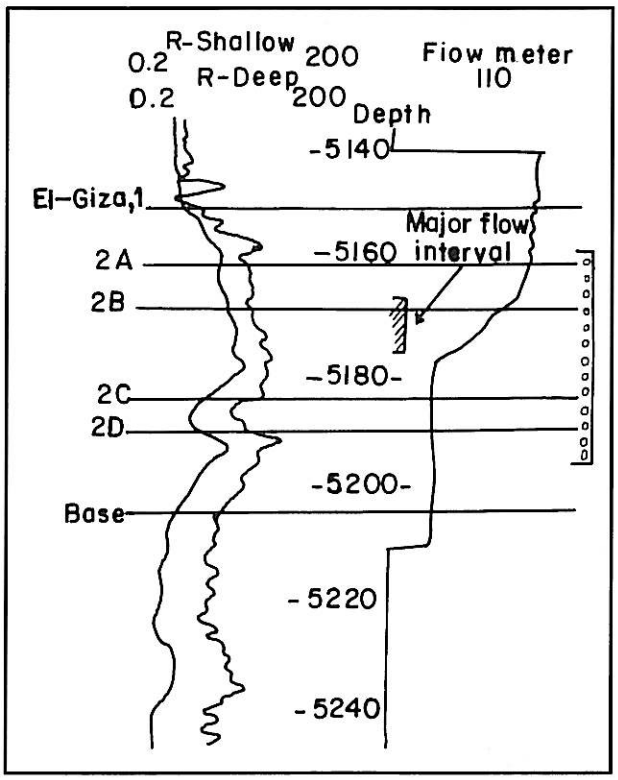


Fig. 8 D40A flow meter.

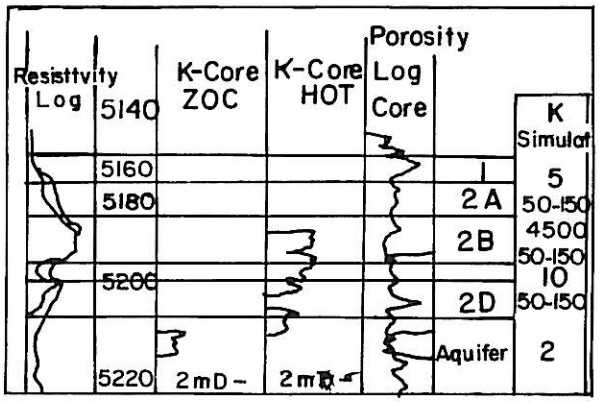


Fig. 9 DOI log core correlation.

carbonate. The core-measured permeability of 2 md was used to characterize the entire aquifer, with the exception of the southern area of D40.

Using the core-measured 2-md to represent the aquifer rock is consistent with the DST result of the aquifer at the D1 well. The reason the southern area was initially given a slightly higher permeability is due to the observation that this area is the only area that registered a water/oil contact movement. A TDT survey was conducted in the early 1980s on 10 wells, covering the entire reservoir.

The above analysis has provided a reasonably good understanding of the reservoir and enabled an adequate initial characterization of the reservoir for simulation. As it turned out, the only major effort spent in the history match was adjustment in the thickness and areal distribution of the vuggy zone as well as the injection profile. The results of the reservoir's history match is shown in figure 10 and the individual well history match in Table 1.

Table 1: Summary of history match results. (at April 1, 1996)

Well	Cum. oil (MMSTB)		Cum. water (MMBbl)		Water cut (%)	
	Model	Actual	Model	Actual	Model	Actual
D13	3.73	3.76	9.06	7.43	82.2	85.1
D37	2.23	2.23	4.04	3.44	83.1	75.3
D38	1.58	1.58	1.45	1.42	65.6	65.3
D39	4.36	4.40	11.28	8.02	82.7	66.2
D40	1.39	1.38	1.57	2.51	–	–
D40a	0.34	0.34	3.44	5.42	93.1	96.9
D44	2.94	2.94	7.09	6.47	90.2	89.7
D45	2.78	2.78	2.89	4.19	60.3	68.3
Field	19.36	19.41	40.83	38.90	84.4	83.9

CONCLUSION

This attic oil recovery project is a successful improved-oil-recovery project, but is not extraordinary in terms of scale, numbers or economics. However, it is a classical example of good reservoir engineering work. In conclusion, three major issues can be highlighted from this project as follows:

1- Secondary porosity frequently exists in a marine carbonate environment, particularly in Libya and the nature, location and areal extent of the secondary porosity have to be understood and expedited prior to a successful simulation.

2- The behaviour of water influx, which dictates the production and recovery of a water drive reservoir, is not only a function of the size of the aquifer, but more importantly, the nature of the aquifer rock itself.

3- This study utilized all available reservoir engineering tools, i.e. production history, pressure history, core, logs, build-up tests, DSTs, TDTs, salinity, material balance, core floods, PVT and inflow-outflow performances *etc.* A good analysis of the data is the key to this project's success. Simulation only serves to confirm concepts and quantify numbers.

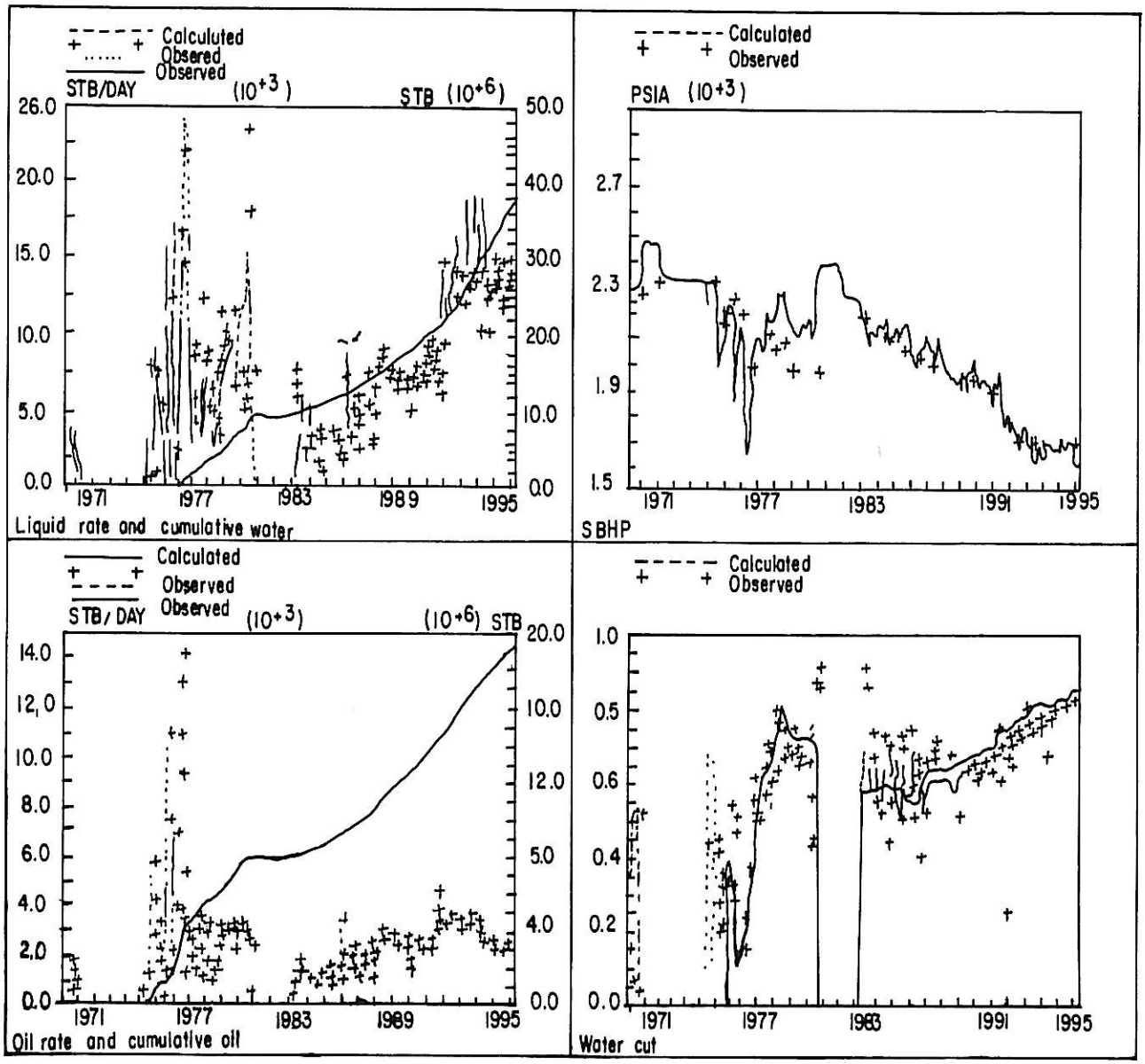


Fig. 10. Total field history match.

ACKNOWLEDGEMENT

The authors wish to express their appreciation to the management of the Zueitina Oil Company for the permission to publish this paper and to Mr. C. Struyk for his contribution in the petrophysical analysis of this project.

REFERENCES CONSULTED

[1] Engineering Dept., Occidental of Libya Inc. 1969. *El-Giza Development 103D Structure.*

[2] Vadjama, U.N. 1977. *103D El-Giza Status report.*

[3] Vargas, T. and Sharafeddin, A., 1988. *Formation Evaluation of El-Giza Reservoir, NC 103D.*

[4] HOT Engineering, 1990. *103 D El-Giza Reservoir Study.*

[5] PHH, 1979. *103 D Reef Simulation Study.*

Petroleum Res. J. Vol. 14 (2002): P. 45–58, 12 Figs.

Water Shut Off Field Experiences to Improve Hydrocarbons Recovery in Depleted Reservoirs

G. Burrafato,* E. Pitoni, G. Vietina and L. Mauri**

خبرات حقلية في مجال إيقاف المياه لتحسين إنتاجية النفط في مكامن مستنفذة

ج. بورافاتو، و إ. بيتوني، و ج. فيتيني و ل. موري

تستخدم الهلاميات في العالم للتحكم في إنتاج الماء في آبار الغاز والزيت لغرض تحسين إنتاجية النفط وزيادة كفاءة الدفع خلال عمليات حقن المياه لسد الطبقات ذات النفاذية العالية، أو للمحافظة على إنتاجية الآبار وذلك بالتقليل من معدل إنتاج المياه. تكمن النقطة الحساسة في معرفة ميكانيكية إنتاج المياه. وقد يكون من المهم، بعد هذه الخطوة، الأخذ في الإعتبار عن إمكانية تطبيق المزيد من الأنظمة الميكانيكية المعتمد عليها قبل التركيز على الأنظمة الكيماوية، أما بالنسبة لطريقة الأنظمة الكيماوية فهناك نقطتين أخرتين حساستين يجب أن تؤخذا في الإعتبار.

- إختيار النظام الكيماوي.
- الوضع السليم للمائع المعالج.

تعتمد الفائدة الجمة التي يمكن الحصول عليها على معرفة وضعية الحقل و/أو البئر إضافة إلى التشخيص الجيد للمشكلة. أما بالنسبة لإيقاف المياه الكيماوية فإن دعم النشاطات المعملية مهم جداً لإختيار أو تأكيد النظام المناسب وصياغته من أجل زيادة معدل نجاح العلاج نفسه.

إن مراجعة مشاكل المياه وتقنيات وضع الهلاميات إلى بدائل وطرق غير إعتيادية للإزاحة باستخدام هلاميات ومبلمرات. وتم تطبيق هذه التقنيات من أجل ستكمال إنتاج النفط من مكامن غاز طينية مستنفذة.

تم تطوير هذه التقنية الجديدة للتقليل من المصاريف ولجعلها أكثر إجتذاباً. هذا بالإضافة إلى تصميم تطبيقات معدل النفاذية النسبية لمعالجة الإكتمال الأكثر تعقيداً.

تم في هذه الورقة تقديم نبذة مختصرة للنشاطات المعملية الخاصة باختيار البوليمرات والهلاميات المناسبة وكذلك بيانات المعالجة الحقلية ونتائج العلاج بالهلاميات ومن تطبيقات معدل النفاذية النسبية.

هذه التطبيقات تم دراستها للتقليل من تكاليف معالجة الحفر وزيادة إحتياطيات هامشية من مكامن مستنفذة ومتعددة الطبقات، وبالرغم من أن العديد من النقاط المذكورة تتعامل مع آبار الغاز إلا أن تطبيقاتها على آبار الزيت يبقى ممكناً.

Abstract: *Gels are used world-wide to control water production in oil and gas wells in order to improve hydrocarbons recovery, to increase sweep efficiency during water injection by plugging high permeability layers, or to keep wells producing by reducing water production rate.*

The critical issue is the correct identification

* SPE.
** ENI-Agip E&P Division.

of water production mechanism. After this step it is important to consider whether the more reliable mechanical systems can be applied before focusing on chemical systems.

For the chemical system approach there are two more critical points to consider:

- *the selection of the chemical system;*
- *the correct placement of the treatment fluid.*

The maximum benefit that can be achieved depends on the knowledge of the status of the field and orlthe well and on a good problem diagnosis.

For chemical Water Shut Off (WSO), the support of laboratory activity is very important to select or verify the right system and formulation in order to increase the rate of success of the treatment itself.

A review of water problems and gel placement techniques has led to a study of alternative and unusual displacement methods using gels and polymers. These techniques have been applied in order to complete the hydrocarbons recovery in shaly gas depleted reservoirs.

A new bullheading technique had been developed to reduce costs and to make WSO more attractive. Moreover, Relative Permeability Modifier (RPM) applications had been designed to treat more difficult completions (dual completion, short strings, selective strings, gravel pack' completions) and thin multi-layered reservoirs.

In this paper a brief summary of laboratory activities for a correct polymers and gels selection is reported as well as field treatment data and results from bullheading gel treatment and from RPMP application.

These applications had been studied to, reduce treatment costs by rigless operations, produce marginal reservs from depleted and multi-layered reservoirs.

Many of the issues deal with gas wells applications, but they can be easily applied to oil wells.

INTRODUCTION

Water production is, very often, a big concern during the lifetime of oil and gas wells. The increase of water cut leads, sometimes very rapidly, to a dramatic increase in operating costs, resulting in uneconomical production, with the final result of premature well abandonment and loss of reserves.

WSO techniques have been developed to control problems related to water production.

The main topics that can be addressed are:

- recovery of residual reserves not conventionally producible;
- reduction of water disposal costs;
- reduction/removal of water production related problems (scale, souring, water treatment plant costs).

All these topics cause costs that reduce the economic exploitation of reserves, especially in the last part of the life of a field. As a matter of fact, the high work over costs, mainly in offshore fields and the increasing disposal costs do not allow the whole recovery of the available producible hydrocarbons.

In this context, WSO technologies have been introduced to control water production using mainly rigless operations maximizing the hydrocarbon recovery.

WSO technologies available at the moment on the market, consist of mechanical and chemical systems.

Treatments of such situations using polymer gels have been experienced during the past 15-20 years and the polyacrylamide/Cr(III)-complex technology has been recognized to be the most successful chemical technique'. However, placement of these field proven gels is very often the most difficult aspect to be addressed.

Therefore, any well candidate to WSO treatments must fall in specific categories to be treated with gels with a good chance of success. The knowledge of the correct water production mechanism, the presence of reliable separation (shale) between layers producing water and gas or oil, the certitude and possibility to place correctly (in the water producing layer) the gelling solution are only a few of the many attributes that a well must satisfy to be a "good candidate". For the "mature" gel technology, rules for chemical selection and methodologies for correct placement are, generally, well defined resulting nowadays in high success rates. In some situations, in case of a particular formation characteristics or in presence of very complex completion configurations, treatments using gels are not feasible and the "relatively new" technology that simply uses RPM polymers can be invoked and, if possible, applied.

Finally, the economics of the entire process must be re-evaluated in order to achieve a true success in the field.

The selection of candidates is made considering the following criteria:

- definition of motivations of WSO treatment;
- identification of the water production problem;
- screening of the treatable problems;
- identification of the workable solutions (mechanical or chemical);
- evaluation of results achievable;
- treatment costs.

The definition of "good candidate" is not rigid and schematic because it depends on technical feasibility, objective of treatments, regional constrains and economical evaluation which can vary during the lifetime of the field or the wells to be treated.

Often the standard techniques cannot be easily applied because of the presence of unconventional well completions or well situations.

The main concerns, that is a large part of the Italian scenario, are the following:

- sand control completions and/or screens that preclude the possibility to divert a gel/gelant system by installing inflatable packer;
- conventional wells where sand production induces the creation of cavities behind casing, precluding the use of inflatable packers.
- in single completions, usually installed in marginal fields, if tubing ID are small (in case of unloading problems in wells where once formation water starts to be produced),again, inflatable packers cannot be installed because of the to large IDcsg/ODtbg ratio.
- reservoirs are composed by different layers and each layer is usually divided into sublayers, each of them having its own aquifer. Therefore most of the wells have multiple completions in 7" casing with small tubing ID, being
- 2 2/8" tubing OD the most common. Inflatable packers cannot be run through 2 3/8" OD tubing and set against a 17" OD casing because it cannot expand that much;
- the same perforated interval can open a few sublayers to production at the same time and, in this case, it is quite impossible to recognize which sublayer is responsible for water production and, therefore, zonal isolation cannot be applied even if a suitable mechanical system could be applied to divert a gelant;
- the selective completion is difficult to treat because it is not possible to do any kind of conventional diversion for gelant system;
- dual injection without inflatable packers cannot be applied because no sensors exist which can be run through this, so small tubing ID, especially when radiotracers, cannot be used, as well as in Italy.

Moreover, reservoir simulators are not always available and only water production mechanisms due to some well bore problems could be quickly investigated. However, this analysis is very rarely accepted and performed because it too expensive, usually more expensive than the treatment itself.

The usual lack of knowledge relevant to water production mechanisms in Italian gas wells, the complexity of the reservoir lithology and bottom hole conditions, which cannot allow the use of inflatable packers, make standard gel treatments something not applicable in most of the wells. On the other hand, a solution to the problems caused by produced water had to be found in order to produce all the reserves in place.

Bullheading seemed to be the only attractive placement technique for these gas wells.

After an extensive lab activity, a very efficient and very cheap RPM polymer was selected for a field test. In 1989, gas well CA#I was shut in because of excessive water production, leaving downhole a consistent amount of gas reserves; any attempt to put this well in production was unsuccessful. In order to minimize risks associated with bullheading treatment, this well was selected as the best candidate for treatment with RPM polymers.

However, as well as known by literature and confirmed by lab experiments, the efficiency of RPM polymers adsorbed inside a porous media declines with time, because the polymer can be diluted and transported by formation water still produced after the treatment. Therefore, RPM treatments need to be re-injected in the same well to restore productivity once the polymer injected with a previous treatment has back flowed. Even if less efficient than a "true" RPM, a standard crosslinked gel can act as RPM,,once overdisplaced and saturated with gas (nitrogen). This system, once introduced inside a porous media, cannot be removed by produced water and it is supposed to be very long lasting.

Considering how difficult it is to displace uniformly any liquid phase with gas (nitrogen), a simple method for treating gas wells with gel was selected. However, the treatment, consisting of bullheading a plugging gelant and nitrogen, is very risky. For this reason, the gas well selected for the field test, CO# 9SL, was a very poor candidate: minor gas reserves were still in place and water production mechanism was completely unknown, even if some hypotheses

were done based on production data analysis and something very similar to a water coning was recognized as the most likely.

The two candidates were similar in terms of low bottom hole temperature and pressures; both the wells produced from gas bearing zones composed by poorly consolidated, laminated sands.

CO# 9LS is also characterized by a gravel pack sand control completion.

WATER SHUT-OFF TECHNOLOGIES

The production of excess water in a gas or oil well can be originated by the presence of many different problems that can be located near the well bore or deep into the formation.

Depending on the type of problem and location, mechanical devices or chemical treatmen can be used to control unwanted water influx.

Generally speaking, the simple use of bridge plugs or packers to isolate any water-producing zones has to be preferred to solve problems which can be faced by isolating some part of the well bore; because they are cheaper and have higher rate of success. Mechanical systems include cement plugs, since this product is well known and it is used very often in conjunction with other mechanical tools.

However, if the problem cannot be corrected from inside the well bore, some chemical must be selected and pumped deep enough into the formation to fix the problem. Among chemical treatments, inorganic gels, monomeric gels,polyacrylamide based organic gels or simply polymer solutions can be selected. They are suitable for near well bore or deep treatments and must be injected into the formation at a pressure high enough to invade all the interested zone, but below formation fracturing pressure.

However, if very low permeability zones must be treated, the ability of a gelling solution to be injected without applying too high differential pressure (with the risk to exceed fracturing pressure) becomes a real concern. In these cases the use of systems having low viscosity (~ 1 cP) can guarantee the injection of the fluid deep enough (1-3 meters) to obtain good sealing capacity once the gels are developed. Inorganic silicate based formulations or monomeric ("in-situ" polymerized) systems can be the right answer for such situations.

In the last years, polymer gel systems have been considered an emerging technology that now can be regarded as a completely effective and consolidated tool. Treatments, carried out with chromium crosslinked polymer solutions, are the most widely used and, nowadays, internal know-how permits the use of these types of gels having very good control on injectivity, gelation time, propagation depth into the formation and permeability reduction.

One of the main concerns relevant to polymer-gel technology is the (correct) placement of the treatment: the fluid must be injected in the water producing zone to avoid undesirable damage of the hydrocarbon layers.

Polymer solutions have been used in the past, starting during the 1970's, as water control technology based on the ability of some polymers to reduce selectively water permeability leaving almost intact gas and oil permeability (this kind of systems are reported as Relative Permeability Modifier,(RPM)[2,4]. Many treatments were carried out considering their low cost (generally a low polymer concentration is required) and the minimal risk of damage of oil/gas producing zones. In spite of that, the success rate of these operations has been considered too low, but the majority of failures can be attributed to the lack of knowledge of polymer chemistry and to inappropriate candidate selection.

Considering the Italian situation, RPMs were selected as the most suitable system to correct water problems, but gels were not abandoned since they could have found a field of application if a safe system of placement existed. For instance, it is well known that a RPM can work up to a certain permeability, becoming ineffective above certain values, whereas a gel could work fine in this high permeability formations. However, all the studies were oriented towards bullheading treatments because any other system would have required too many details and analyses logs, survey, pressure build up, and so on) to be selected as a suitable technique to restore wells productivity in marginal fields.

Case Histories

In this section a description of the initial situation and the well production parameters will be reported, for each case.

A general picture of the results obtained during a two-years research activity on the use of RPM in low temperature gas wells together with the optimization of the formulation for the treatment in well CA# 1 and the laboratory tests carried out for the evaluation of a new placement technique for a gelling polymer solution suitable for the well CO#9SL will be discussed.

Finally, for each well, field operation and post-job evaluation data will be reported.

BuIlheading an RPM Polymer. Well CA#1. CA#1 is a gas well, shut down since April 1989, after a ten months production period, because the high water cut caused the well to stop flowing. The last production parameters were Q_g = 22000 Sm^3/d, Q_w = 30 m^3/d and FTHP = 34 kg/cm^2. The well was lifted a few times with gas (nitrogen) but gas productivity was never restored and sand was produced with a tremendous amount of water.

This vertical well was work-overed in 1988 and re-completed with a single 2 3/8" , 1.995" ID, tubing in a/7" casing; an external 9 5/8" casing is olso present at perforation depth, 963-966.5 m/RT, 4 spf, E.H.: 0.35". The following layers were identified by log analysis:

- 2.3 m of gas *zone* (963.5-965.8 m/RT).
- 0.4 m of clay (965.8-966.2 m/RT).
- 1.8 m of gas zone (966.2-968.0 mJRT).

The deepest layer was intended not to be perforated, but the bottom section of perfs entered the lower gas layer by 0.3 m, 1 ft, and the lower layer resulted in being completely depleted and watered out. No surveys were run in this well and the water production mechanism was derived on the basis of logs, geologic interpretation of seismic and production data (diagnostic plots[5]).

Other data relevant to this well are as follows:

- SBHT = 48°C(118°F)
- SBHP = 69.3 kg/cm^2, 0.72 kg/cm^2/10 m (985 psi, 0.31 psi/ft)
- STHP = 64.0 kg/cm^2 (910 psi)
- k_{gas} = l3OmD
- k_{brine} = 44 mD, assumed 30% of k_{gas}
- Frac press: 128 kg/cm^2, 1.32 kg/cm^2/10 m (1820 psi, 0.57 psi/ft).

Owing to the reduced layer thickness, no applicable were found in the market. Cement was not considered a valid option because of the risk of plugging the entire perforated interval, Moreover, a void behind casing was expected because of the above mentioned and reported sand production: any sealing device inside casing would have very likely failed. Dual injection was considered at the beginning of the study, but it was found too expensive and inappropriate for this candidate. Finally, bullheading gelant followed by nitrogen overdisplacement, the already described technique, was not available at the moment this well was considered for a WSO treatment.

In this situation the well appeared to be a possible candidate inside a two-years research activity about the use of polymers as Relative Permeability Modifiers.

The research activity. As discussed earlier, the particular Italian situation pushed strongly the EN1-Agip R and D group to the evaluation of new systems capable to control water production in wells where bullheading is the only possible option for placement.

A literature survey highlighted the use, in many previous applications, of a "trial and error" approach rather than a well defined selection grid of well candidates and chemicals. For this reason one of the main targets was to define a series of rules to correctly choose a "good candidate" and the proper chemical agent". The execution of a field test to verify the results, obtained during the research activity was the final goal.

General results. A series of indications have been obtained from the laboratory activities and are fully reported elsewhere[6-9]. In this contest, the main subjects that have been investigated can be pointed out as:

- polymer-rock interactions;
- formation lithology;
- effects on relative permeability.
- injectivity.

The polymer-rock interactions have been investigated studying the adsorption isotherm and the kinetic of this process for more than 14 commercial polymers which were different in electric charge (cationic, anionic and non-ionic), in chemical nature (biopolymer, synthetic polymers co- and ter-polymers) and in molecular weight (2*105– 2* 10^7 Dalton).

Having already in mind the application on the well CA#l, these tests were carried out on a specific sand coming from an offset well drilled in the same area. The mineralogical content of this material is presented in Table 1.

Table 1. Modal content of sandstones (vol.%).

Quartz	49	Smectite	20
K-feldspar	17	Mixed layers	0
Plagioclase	9	Illite	29
Calcite	21	Kaolinite	21
Dolomite	0	chlorite	30
Shale	4		

The adsorption tests permitted a first screening of the collected polymers that have been classified with regard to their ability to adsorb onto the sand. In this way, polymers with "high affinity" to the rock (adsorption from 1-4 mg of polymer/g of sand) and with "low affinity" (below 1 mg/g) were identified. The majority of cationic and some non ionic polymers in the first category, fall while some non ionic and all the anionic polymers fall in the second one.

The adsorption tests were carried out using diluted polymer solutions, generally 1000, 2000 and 4000 ppm, that have been also characterized from the rheological point of view. The rheological behavior in the range of shear rate (1-1000 s^{-1}) and temperature (25-50 °C) investigated is typical of a lightly non-Newtonian fluid with low viscosities ranging from 2 to 5° CP.

The kinetic response of the adsorption tests quantified in about 24 hours the time needed to reach the "plateau" region in the isotherm adsorption curves. In addition, the "plateau" in the curves "adsorption *vs.* concentration" clearly indicated the optimal concentration of 2000 ppm for the polymer treating solutions.

Following these initial tests, three polymers (two cationic, one weakly anionic: some information are reported in Table 2) were selected to further investigate their performances in core flow tests. Sandpacks, obtained using the reference sand, were treated following the procedure reported [8]. Initial absolute brine permeability of about 250-400 mD have been observed in a first series of samples, while, following a more accurate procedure for samples preparation, values of 60-100 mD have been obtained. In Table 3 some results are reported and the good water permeability reduction is quite evident especially using the two cationic polymers, while the gas permeability is only slightly affected. it is important to point out that these results are in good agreement with the adsorption test that gave, for the cationic, higher affinity to the formation sand. Between the two (roughly) equivalent cationic polymers we choose "CAT-1" because it is readily available on the market and all the subsequent tests were performed using this polymer.

In Table 4 additional data, obtained with the goal of deeply investigating the performance of the chosen polymer, are reported. In this Table, test # 2 and # 3 were performed using a "shear degraded" polymer solution. In fact, it is reasonable to imagine that the polymer can be subjected to a mechanical degradation because of the high shear rate reached during the injection in the porous media, especially in the region around perforation tunnels. So, to verify the effectiveness of the polymer solution after such degradation, the mentioned tests have been carried out using a CAT-1 solution (2000 ppm) previously pumped through a sand pack at an injection rate of about 0.6 m/min. Measurements of "Total Organic Carbon" (TOC) content have shown the same amount of polymer before and after the "shear degradation"; so the observed reduction in viscosity, from about 4 to about 2 cP (at 25 °C), was totally due to the polymer chain degradation. The results reported show the equivalence, in terms of k_{gas}, and k_{brine}, reduction,

Table 2. Polymers used in core tests.

Polymer	Structure	Ionic charge	Molecular weight (Dalton)
HPAM	Hydrolyzed Polyacrylamid (D.H. 1%)	Weakly anionic	5 million
CAT-1	Cationic polyacrylamid	Cationic	1-2 million
CAT-2	Cationic polyacrylamid	Cationic	7-800,000

Table 3. Permeability reductions in core flow tests.

Polymer	Initial absolute k_{brine}MD	Äk/ k_{brine}, %	Äk/k_{gas}, %
CAT – 1	413	86	8
CAT – 1	270	81	25
CAT – 1	24	81	49
HPAM	170	65	30
CAT – 2	58	82	53
CAT – 2	86	77	56

Table 4. Permeability reductions with CAT-1.

Test number	Initial absolute k_{brine}, mD	Before treatment		After treatment		Äk/k_{gas}, %	Äk/k_{brine}, %
		k_{gas}, mD	k_{brine}, mD	k_{gas}, mD	k_{brine}, mD		
1	247	690	198	527	35	24	82
2*	15	70	15	50	2	29	87
3*	474	1200	284	1198	205	0	28

between the "sheared" and "unsheared" solutions, if the initial absolute permeability is lower than 300 mD (test 1 and 2), while for higher values a decrease in the performance can be observed (test 3).

During the laboratory injection tests, using the chosen CAT-1 polymer solution (at 2000 ppm), some anomalies were observed with regard to the decrease in injectivity. In fact, it was evident that the CAT-1 fluid, when it moves inside the porous media, had a viscosity "apparently" much more higher than the viscosity measured by rheometers. During pumping, the observed pressure increase, is in the order of ten fold higher than the expected value determined on the purely effective viscosity difference between brine and polymer solution. This was attributed to the first step in the adsorption process that clearly changes the brine permeability and needs higher ÄP to continue the polymer injection. These effects are shown (Fig. l) , where the profiles "injection pressure *vs.* time" for three different concentrations of CAT-1 are reported. Based on these evidences and on the adsorption data mentioned before, a final concentration of 1500 ppm was chosen for the field application.

Field application. The first step of the programme was tubing cleaning. After killing with 3% KCL brine, a 1¼" OD coiled tubing allowed completion fluid to be circulated for cleaning; acid pills were planned to complete this step considering cleaning quite critical in any injection treatment. After more than three times well bore volume pumped down hole and no fluid returned at surface, it was clear that formation injectivity was extremely high, much higher than expected. In order to reduce injectivity, achieving a circulating condition, the same fluid selected for the treatment was pumped down hole in an effort to reduce water permeability, and therefore injectivity, making circulation finally possible.

20 m^3 *(125* bbl) of CAT-1, 1500 ppm in 3% KC1 brine, were prepared and pumped via CT at 1.4 bpm (+40% injection rate, compared to 3% KC1 base brine; CAT-1 acted as a friction reducer, (Fig. 2) and 0.4 bpm of return were obtained just at the end of pumping. A clean fluid was obtained after 0.92 m^3 (5.8 bbl) of fluid recovered at surface; return line was closed at this point and all the pumped fluid injected.

A huge cavern (estimated volume 8 m^3, 50 bbl) was present behind casing and it was responsible for the very high injectivity encountered.

CT unit was retrieved and *35* m^3 (220 bbl) of CAT-1 were bullheaded trying to maintain a constant injection rate, 0.75 bpm, 119 1/min,, for the last 20 m^3 (125 bbl), (Fig. 3). All the treatment was injected in matrix condition (invasion depth 3.4m) without any evident plugging phenomenon and the small pump available for pumping the treatment at very low rate (2 to *5* 1/mm, 0.01-0.06 bpm) was not used. This pump was installed because a tremendous decrease in injectivity was anticipated, according to lab experiments and results; in fact, in standard situations where no voids are present behind casing, very low injection rates have to be addressed.

The injected treatment was finally overdisplaced to gas (nitrogen) for two reasons:

- to push deeper into the formation the excess of polymer which cannot be adsorbed by the already saturated rock surfaces in the near well bore area;
- to prepare the well for clean up.

6654 Nm^3 (235 kscf) of nitrogen were pumped down hole for a complete overdisplacement (Fig. 4) and the well was shut in for 24 hours to allow the

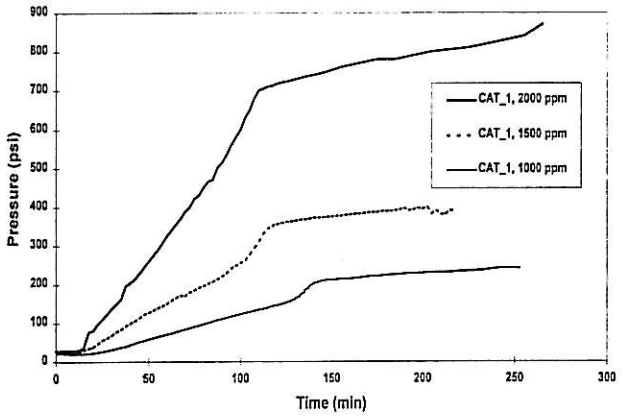


Fig. 1. Injection curves using CAT-1 solutions at different concentrations.

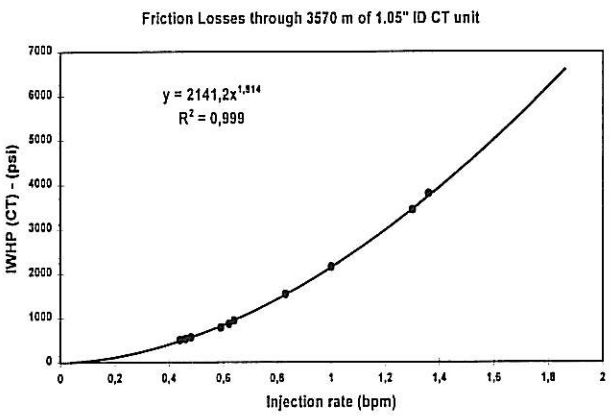


Fig. 2. Friction losses with CAT-1 palymer (well CA # 1).

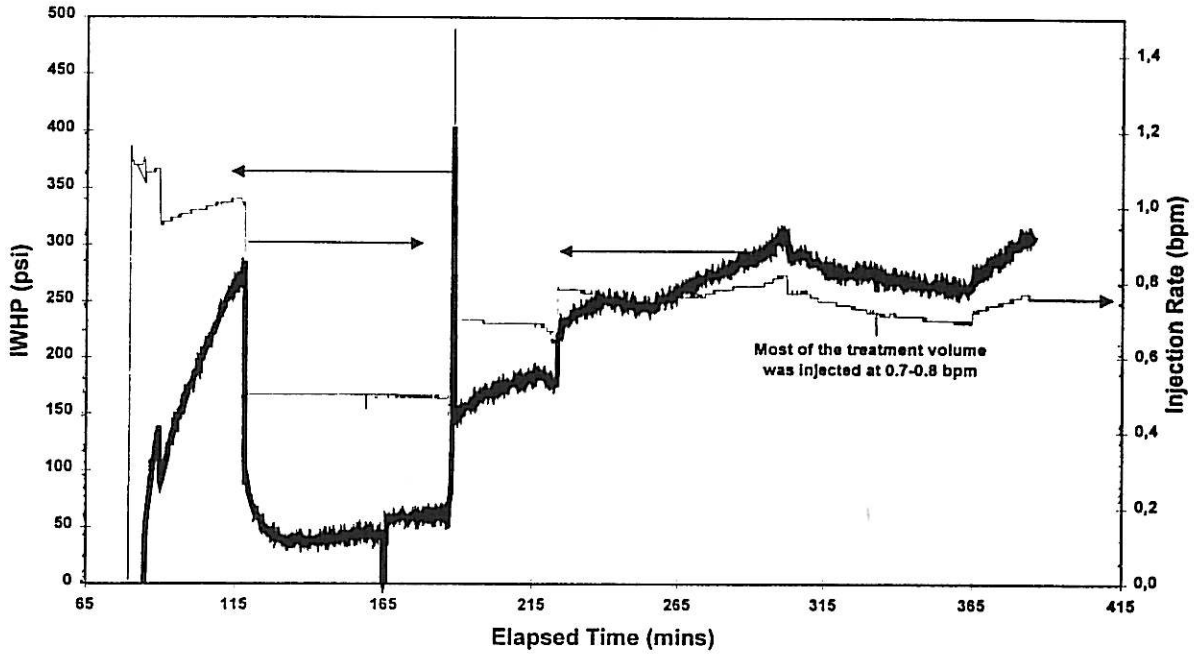


Fig. 3. Bullheading RPM Poleymer treatment (well CA # 1).

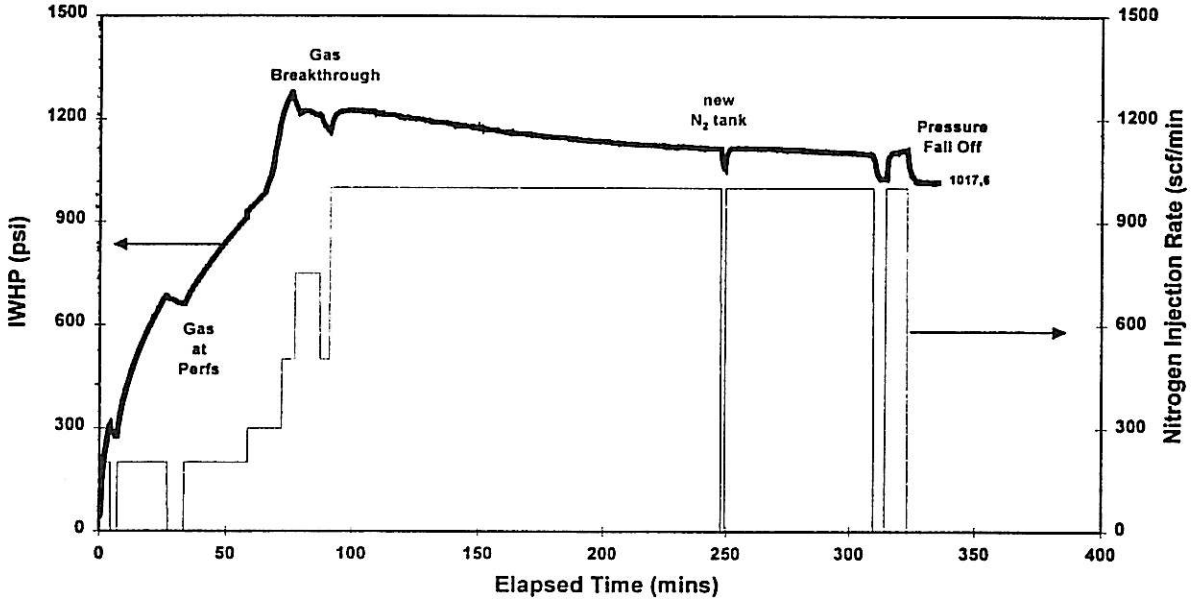


Fig. 4. Overdisplacment of CAT-1 with nitrogen (well CA # 1).

polymer to be almost completely adsored by rock surfaces (invasion depth 4.5 m).

During the beginning of the well clean up (Fig. 5), nitrogen, some hydrocarbons and no water were produced, However,after two weeks, the production stabilized to the following parameters:

Q_g = 31000 Sm^3/d, Q_w = 6 m^3/d and FTHP = 34.7 kg/cm^2.

The production parameter reached even higher values: Q_g = 37000 Sm^3/d, Q_w = 4.5 m^3/d and FTHP=51 kg/cm^2, but the risk to produce sand was very high, therefore it was decided to maintain the well at constant flow rate between 20—25000 Sm^3/d to control sand production and loading problems (Fig. 6).

The increasing water production could be attributed to the release of polymer from formation and to the increasing draw down applied to produce the well at a flow rate higher than 20000 Sm^3/d.

After the treatment, fluids, back-produced from the well, were collected on a regular basis and analyzed. During the clean up phase, the sampling was very frequent, while afterwards the production stabilization, samples were collected every two days.

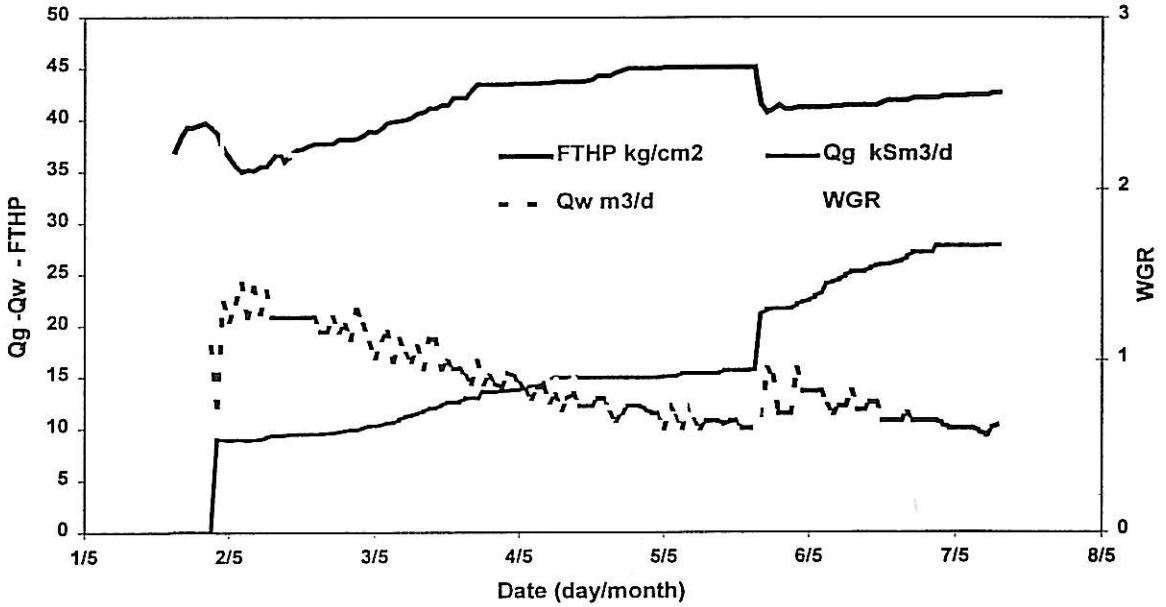


Fig. 5. Production parameters during the clean up phase (well CA # 1).

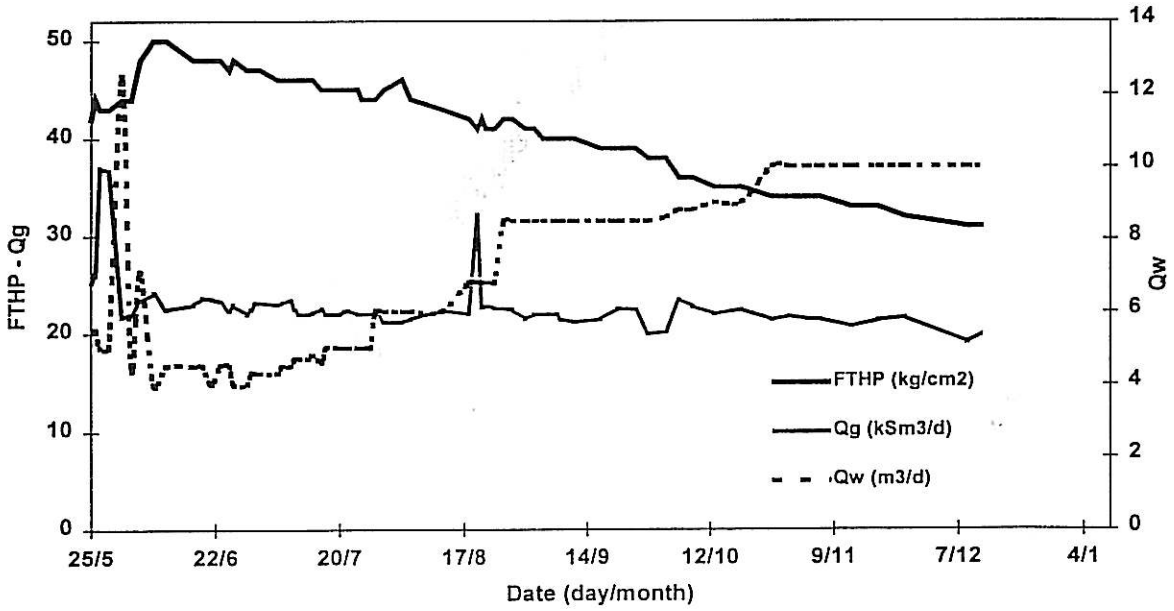


Fig. 6. Production data after the RPM treatment (well CA # 1).

In figure 7 are reported the polymer concentration in the water samples (in terms of ppm of polymer as obtained from TOC analysis) and the amount of CAT-1 still adsorbed onto the formation (considering the total amount of CAT-1 injected, 90 kg) as a function of time.

In the clean up and first production phase, ,the quantity of, polymer released from the formation, was quite high according to the hypothesis that some polymer remained not adsorbed during the shut in period (24 h). After the initial behavior (about 25 days), the polymer produced back stabilized, in terms of absolute concentration, at values of about 50 ppm. On the contrary, in the "adsorbed CAT-1" curve, it is possible to identify a continues decrease in the polymer still present in the well because of the contemporaneous increase in water production (Fig. 6).

Finally, from the economical point of view, it must be noted that the pay-back time for this first treatment has been estimated at two months.

Bullheading a Gelant (PHPA/Cr^{+3} system). Well CO#9SL.

CO#9SL is a vertical well,completed with two 2 3/8" OD, 1.995" ID, strings in 6 5/8" OD, 5.92" ID, casing; minimum restriction: landing nipple 1.875 at

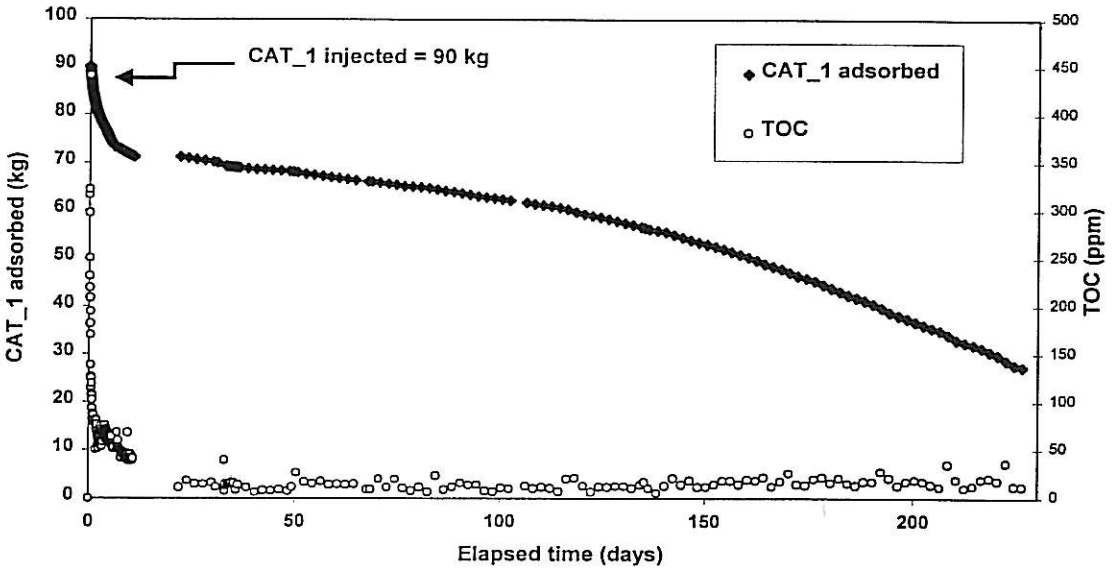


Fig. 7. Polymer adsorption analysis during production days (well CA # 1).

1061 m/RT. The long string was producing dry gas (methane) from two sets of perforations: 1120-1123.5 m/RT and 1127-1136 m/RI. ICGP was installed at the beginning of the life of the well using the high-density technique, very popular at that time, and some damage was expected to be present into the formation due to the polymers (mainly HEC) used to viscosify brines for gravel placement.

The well produced gas for years from this multi-layered zone, which is considered a compartment of a very old, well known Italian gas field located in the North of Italy.

Water started to be produced and gas production continued until the WC was so high the well stopped flowing (last production parameter Q_g = 5000 Sm^3/d, Q_w = 21 m^3/d and FTHP = 20 Kg/cm^2). Every now and then, the well was re-opened and gas started to be produced again, but the water table was too close to perforations and the well died in a few hours. A survey found formation water at 1120.5 m/RT, not above the top of perforations, and, therefore, some pay could be still at high gas saturations, ready to be produced. RST log was not run because of the cost of the log compared to the anticipated, negligible reserves still in place.

From experimental point of view this well was considered a good candidate but it was not a good candidate for any economical reasons because of the very low producible reserves still in place. However, ENI-Agip made the decision to test this novel technology, in view of future applications.

Sometimes it is necessary to inject some fluids, acids for instance, into formations and a complete coverage of the interval is always a big concern, especially in depleted zones and in long exposed intervals. Undoubtedly, gas has always been recognized as the worst displacing fluid which can be used. In fact, in order to displace a fluid, a more viscous fluid has to be used: nitrogen, instead, has a too low viscosity and should be avoided for displacement, unless used in foamed systems.

The treatment technique adopted for this well consisted in:

- injection of a gelant with a long gelling time;
- immediate overdisplacement of the gelant with nitrogen at top of perforations, leaving the whole gel at the bottom;
- shut in for gel development (days to weeks);
- clean up and production.

Some laboratory investigations were carried out using formation sands similar (in terms of permeability and porosity) to the sand to ber treated, without any effort to have a very representative sand; in fact, these tests were run just to assess gel robustness once displaced with nitrogen. Using a standard formulation, 3.5% PHPA + 900 ppm Cr^{+3} with a working time of about 10-15 hours and a gelling time of about 48 hours (a composition mainly formulated considering the very low bottom hole temperature, 37 °C) more that 70% of reduction in water permeability was detected with an increase in gas permeability.

These results were considered positive and the target of the treatment was therefore anticipated as:

- leave the whole gel at the bottom of the completion, trying to plug the IGCP in front of the deepest set of perforations;
- leave just some residuat gel at the top of the completion, allowing any residual gas reserve

to be produced at surface through a system having an encouraging disproportionate permeability behavior.

For treatment design, the following parameters were considered:

- perforations: 1120-1123, 1127-1136 m/RT; 12 spf, E.H.: 0.5"
- SBHT = 37°C (98.6°F)
- SBHT = 103 kg/cm^2, 0.92 kg/cm^2/10 m (1465 psi, 0.40 psi/ft)
- SBHT = 95.8 kg/cm^2 (1363 psi)
- K_{gas} = 300 mD
- K_{gas} = 100 mD, assumed 30% of k_{gas}
- Frac press.: 164 kg/cm^2, 1.46 kg/cm^2/10 m 92335 PSI, 0.64 PSI/FT0.

The only important assumption made while planning the test was that the permeability of the interval was considered constant along perforation. Fortunately, field results confirmed this hypothesis, obtaining excellent productivity for this poor candidate.

At wellsite, a Step Rate Test (SRT) was performed to determine formation fracturing pressure/gradient and , therefore, the pressure limits for the gel injection to e later performed in matrix conditions. Gas (nitrogen) injectivity was also determined in order to have reference points for final evaluations; just a couple of meters of perforations were found free to accept gas, being the lowermost perfs completely watered out.

Gelant, 50 m^3 (314 bbl), was injected at constant flow rate, 0.58 bpm, 92 l/min, in about 9 hours (Fig. 8); the maximum allowable wellhead pressure, 53 Kg/cm^2, 754 psi, was never achieved and the gelant was consequently injected in matrix conditions reaching an invasion depth of about 2 m. The Hall's plot showed a regular trend (Fig. 9), only disturbed

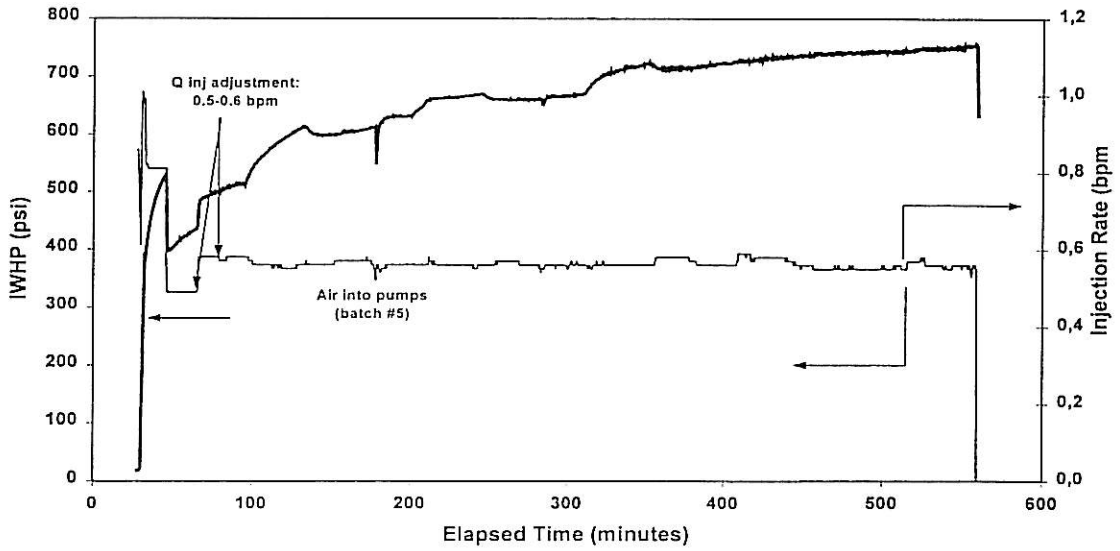


Fig. 8. Gelant injection at constant flow rate (well CO # 9 SL).

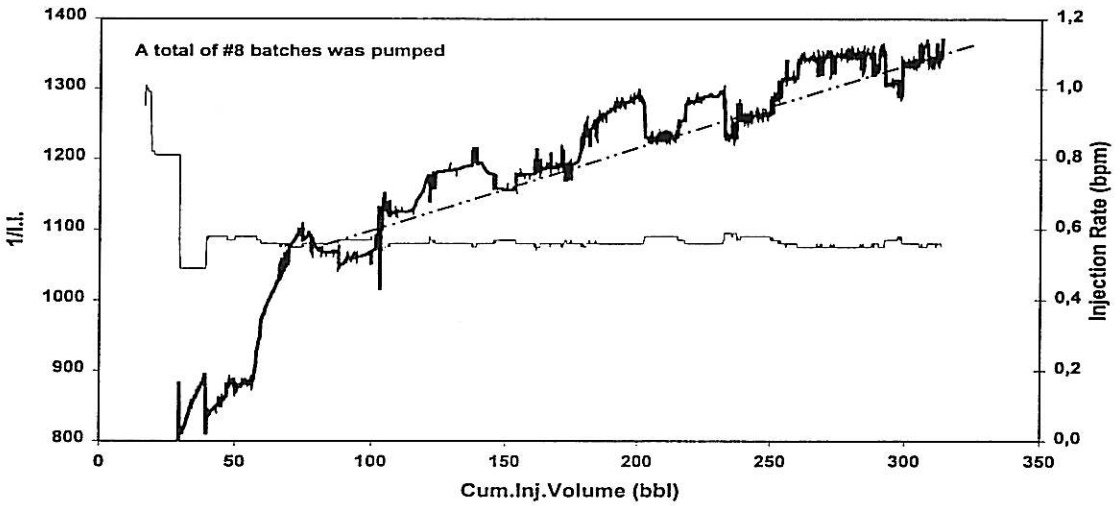


Fig. 9. Hall's plot for the gelant injection phose (well CO # 9).

by some unwanted changes in gel composition caused by the mixing system carried on the field by the service Company.

Gelant was carefully displaced with nitrogen from tubulars avoiding fracturing and, once gas breakthrough was observed through the viscous, not yet gelled, fluid bank around the well bore (Fig. 10), gas was injected at different flow rates trying to determine how much of the initial interval was exposed to flow (Fig. 11). A total of 6229 Sm^2 (220 kscf), of nitrogen was pumped for this stage.

About 1.5 m of pay (top of perforations) were found open to flow and, therefore, the entire zone below was completely invaded by the whole gelant.

The well was shut in for 2 days to allow gel to be formed. When the well was opened it produced spontaneously with the following parameters:

Qg = 17000 Sm^3/d and Qw = 0.2 m^3/d with FTHP = 60 kg/cm^2. After 2 weeks the production stabilized at Qg = 10000 Sm^3/d, Qw = 3 m^3/d.

Owing to the small amount of the reserves the gas production declined continuously down to 5000 Sm^3/d but with a constant WGR (Fig. 12).

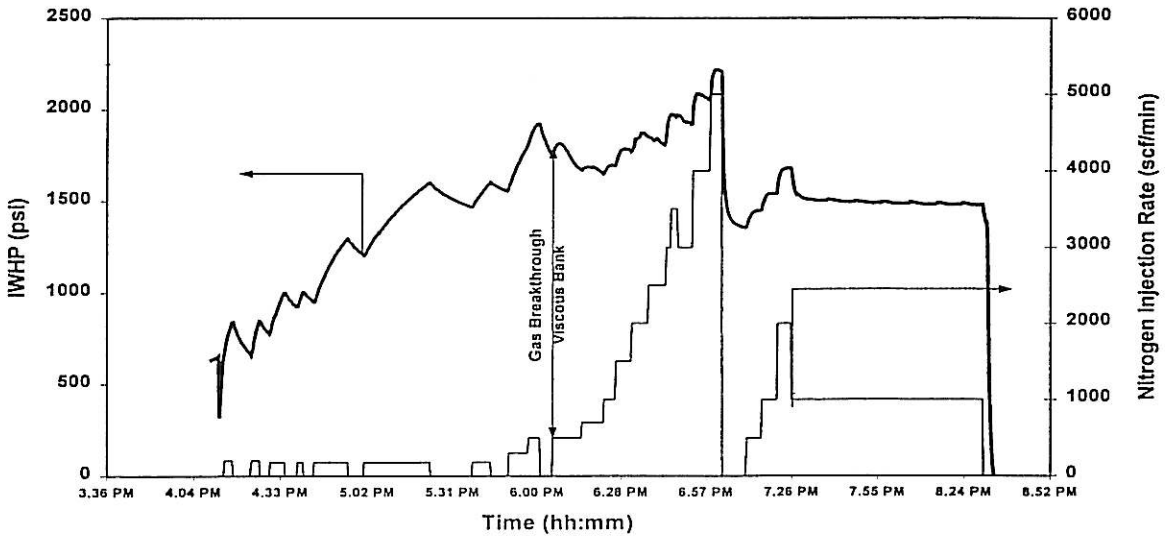


Fig.10. Gelant overdisplacement with nitrogen (well CO # 9 SL).

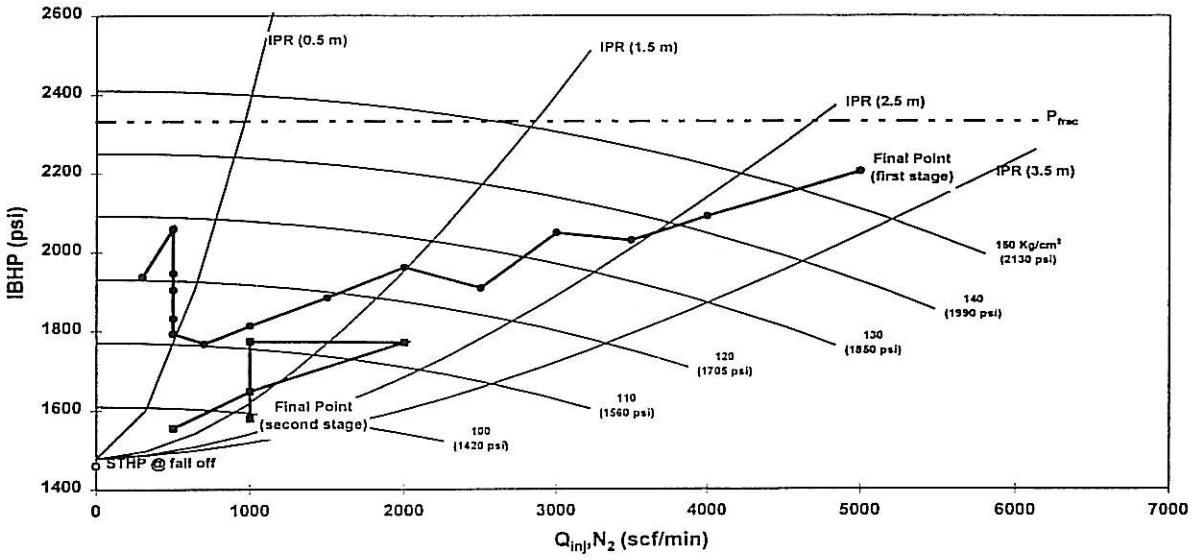


Fig. 11. Monitoring of gelant displacement (well CO # 9 SL).

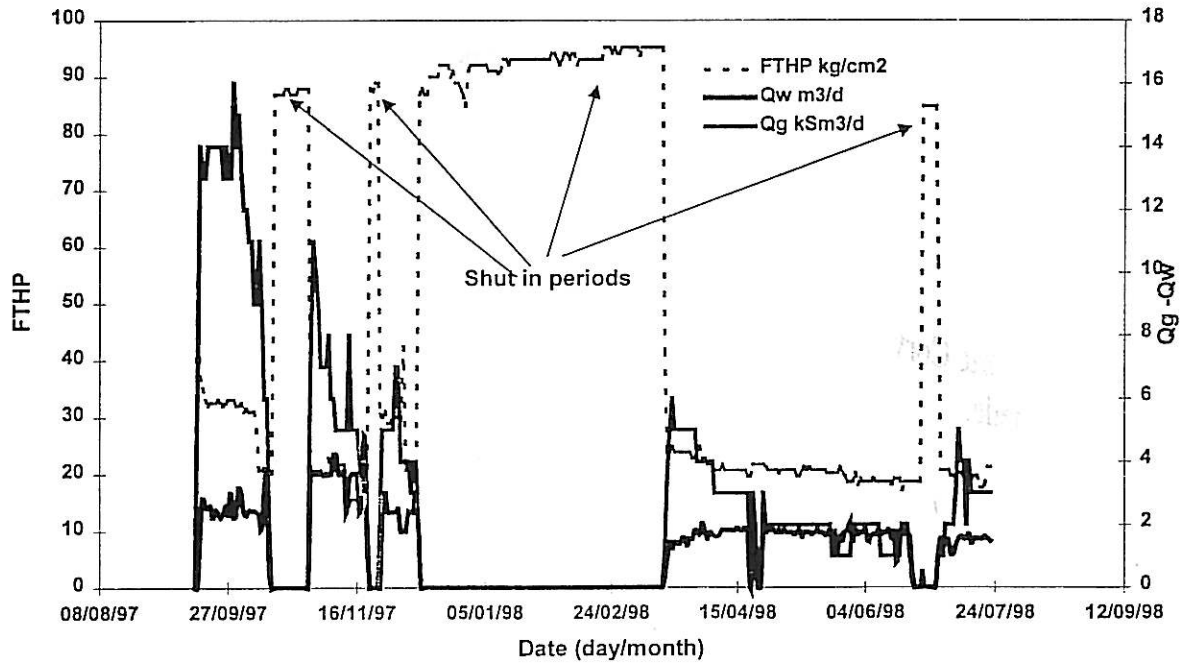


Fig. 12. Production data after treatment (well CO # 9 SL). The well was shut in four times during production.

CONCLUSIONS

The need to produce marginal reserves in depleted reservoirs and to reduce the relevant costs originated by water production and water disposal pushed Eni-Agip Division towards the development of "new methodologies" to make attractive the applications of WSO treatments.

The R&D activities developed during the last years permitted:

- the identification and codification of a series of rules to identify the good candidate and the appropriate chemical for RPM treatments in gas, multilayered and low temperature wells in sand formations;
- the first application of these rules to a field test on well CA#1. This test resulted an economical and technical success. In fact, the well was put again in production with a pay-back time of two months;
- the application of the new bullheading placement technology for a standard gelant solution in well CO#9SL. The confirmations of the possibility to treat in such way this kind of wells can be regarded as a technical success;
- a key of the success is a good candidate selection;
- maximum economic gain can be achieved in oil wells.

Further studies are in progress to exted the knowledge regarding the RPM treatments at higher temperatures and/or in oil wells.

Further applications of the two techniques are already scheduled in others Italian fields.

NOMENCLATURE

WSO	=	water shut off
ID	=	internal diameter, L, in
RPM	=	relative permeability modifier
OD	=	outer diameter, L, in
ICGP	=	inside casing gravel pack
HEC	=	Hydroxy ethyl cellulose
WC	=	water cut
RST	=	reservoir saturation tool
PHPA	=	partially hydrolyzed polyacrylamide
spf	=	shot per foot
SBHT	=	static bottom hole temperature
STHP	=	static bottom hole pressure
STHP	=	static tubing head pressure
k	=	permeability, L^2, mD
TOK	=	total organic carbon
CT	=	coiled tubing
Ppm	=	part per million
Q	=	flow rate
H	=	injectivity index
FTHP	=	flowing tubing head pressure
IWHP	=	injection well head pressure

EH = entrance hole, L, in
SRT = step rate test
WGR = water gas ratio
RT = rotary table

ACKNOWLEDGEMENT

The authors would like to thank ENI-Agip Division for supporting this work and for the permission to publish this paper. Thanks also to SPE that allow to use data included in SPE 54747 (G. Vietina, G. Burrafato, L. Mauri and C. Chiappa) presented in the Hague 31 May-1 June 1999.

Thanks are also due to everyone involved, in lab and in the field, in the activities that contributed to these two successful applications. Special thanks to Luisa Chiappa, Roberto Corvi, Amando Marcotullio and Daniele Mennella.

REFERENCES

[1] Sydansk, R. D., and Southwell, G.P, 1988. More than 12 years of experience with a successful conformance-control polymer gel technology, paper SPE 49315 presented at the 1998 SPE Annual Technical Conference and Exhibition, New Orleans, Sep. 27-30.

[2] White, J.L., Goddard, J.E. and Phillips, H.M., 1973. Use of polymers to control water production in oil wells, JPT (Feb.) 143.

[3] Sparlin, D.D., 1973. An evaluation of polyacrylamides for reducing water production,. *JPT* (Aug.) 906.

[4] Moffitt, P.D.,1993. Long-term production results of polymer treatments in producing wells in western Kansas. *JPT* (Apr.) 356.

[5] Chan, K.S., 1995. Water control diagnostic plots, paper *SPE* 30775 presented at the 1995 SPE annual technical conference and exhibition, Dallas, Oct. 22-25.

[6] Mennella, A., Chiappa, L. and Burrafato, G., 1998. Polymer/rock interactions in polymer treatments for water-cut control, paper *SPE* 39619 presented at the 1998 SPE/DOE Improved Oil Reccovery Symposium, Tulsa, Apr. 19-22.

[7] Mennella, A., Chiappa, L., Bryant, S.L., and Burrafato, G., 1998. Pore-scale mechanism for selective permeability reduction by polymer, paper *SPE* 39634 presented at the 1998 SPE/DOE Improved Oil Recovery Symposium, Tulsa, Apr. 19-22.

[8] Chiappa, L., Mennella, A., Lockhart, T.P., and Burrafato, G., 1998. Polymer adsorption at the brine/rock interface: the role of electrostatic interactions, presented at the 1998 5th International Symposium on Evaluation of Reservoir Wettability and its Effects on Oil Recovery, Trondheim, Jun. 22-24.

[9] Mennella, A., Chiappa, L., Lockhart, T.P., and Burrafato, G., 1999. The development of reliable candidate and chemical selection rules in polymer treatments for water production control, paper SPE 54736 presented at the 1999 SPE European Formation Damage Conference, The Hague, May 31-Jun.1.

SI metric conversion factors

eP x 1.0*	E – 03 = Pa.s
fsi x 6.894	E + 00 = kPa
cf x 2.831	E – 02 = m^3
bbl x 1.589	E – 01 = m^3
in x 2.54*	E + 00 = cm

* Conversion factor is exact.

Petroleum Res. J. Vol. 14 (2002); P. 59–66, 2 Figs.

Miscible Gas Displacement of Facha and Gir Reservoir Oils Using Farrud Reservoir Gas (Ghani Field)

M.F. Dahab and H. A. Belhaj *

الإزاحة بمزج الغاز لمكمني الجير والفاشا باستخدام غاز الفارود المكمني

محمود ذهب والهادي بالحاج

تم تنفيذ برنامج معملي لدراسة جدوى الاسترداد الإضافي بالأزاحة الامتزاجية بغية رؤية إمكانية استخدام غاز (الفارود) كمذيب لزيادة المسترد النفطي لمكمني الفاشا والجير بحقل الغاني.

تضمّن برنامج الدراسة تحاليل الضغط والحجم والحرارة التقليدية واختبارات الانتفاخ للزيت، وكذلك اختبارات الإزاحة باستخدام الأنبوب الرفيع.

وتم استخدام هذه البيانات مع البيانات التحليلية الأخرى للغاز المذاب والزيت المتبقى في حسابات مركبات إنتفاخ الزيت والمسترد النفطي.

وبإضافة غاز الفارود إلى زيت مكمني الفاشا والجير تم إجراء إختبارات الانتفاخ، واحتوت ثماني خلطات تم تحضيرها بنسب 10، 20، 30، 40، 50، 60، 70، و80 جزئي مئوي من غاز الفارود. ومن خلال علاقات الضغط والحجم للخلطات المتحصل عليها بين الغاز المحقون والزيت المكمني عند درجة حرارة المكمن، تم حساب ضغط التشبع للخلطة وقابلية ذوبان الغاز المحقون ومعامل انتفاخ الزيت، وكثافة الخلطات حيث تم استنباط تفاصيل وزن المادة بمركبات اختبارات الانتفاخ بناء على تحاليل مركبات (C_1 إلى C_{30+}) الزيت المكمني مع الغاز المحقون بتوسع.

من أجل تحديد الضغط الأدنى للامتزاجية لغاز الفارود تم تنفيذ ست اختبارات ضغط باستخدام الأنبوب الرفيع لزيت الفاشا المكمني التي يتراوح ضغطها من 1500 إلى 4000 رطل على البوصة المربعة وتم كذلك تنفيذ سبع اختبارات ضغط باستخدام الأنبوب الرفيع لزيت الجير المكمني يتراوح ضغطها من 1000 إلى 4000 رطل على البوصة المربعة. ووجد أن الضغط الأدنى للامتزاجية لزيت الفاشا المكمني 2445 رطل على البوصة المربعة، أما بالنسبة لزيت الجير المكمني فكان 2495 رطل على البوصة المربعة.

إن دراسات الإمتزاجية لكلا المكمنين أظهرت أن الضغط الأدنى للإمتزاجية أعلى بكثير وفوق ضغط المكمنين (1347 رطل على البوصة المربعة للفاشا و1310 رطل على البوصة المربعة للجير). وإن نوع الإمتزاجية التي تم الحصول عليها تتوافق مع نتائج اختبارات الإنتفاخ وتظهر الدفع بتكثيف الغاز.

Abstract: *An enhanced oil recovery laboratory program of miscible displacement has been carried out in order to determine the feasibility of using Farrud hydrocarbon gas as a solvent to increase oil recovery from Facha and Gir reservoirs of Ghani field.*

The study program included conventional PVT analysis, oil-swelling tests, and slim tube displacement tests. These data with dissolved gas and stock-tank oil analytical data were used in compositional, oil swelling and oil recovery calculations.

Swelling tests were performed by adding Farrud hydrocarbon gas to Facha and Gir reservoir oils. Eight mixtures were prepared

* Petroleum Research Centre, Tripoli, Libya, p,o box 6431.

containing 10, 20, 30, 40, 50, 60, 70, and 80-mole percentage of Farrud gas. From P-V relations of injection gas-oil mixtures at reservoir temperature; mixture saturation pressure, injection gas solubility, oil-swelling factor and mixture densities were calculated.

A detailed material balance of swelling test fluid hydrocarbon components were investigated, based on extended (C_1 to C_{30+}) compositional analysis of the reservoir oil and injected gas.

In order to determine Farrud gas minimum miscibility pressure (MMP), slim tube displacement tests at six gas injection pressures ranging from 1500 to 4000 psig were performed on Facha reservoir oil and at seven pressures ranging from 1000 to 4000 psig on Gir reservoir oil.

The MMP for Facha reservoir oil was found 2445 psig and for Gir reservoir oil was found 2495 psig. Miscibility studies revealed that minimum miscibility pressures are extremely high and beyond the reservoir pressure (1347 psig for Facha and 1310 psig for Gir). The type of miscibility development is in agreement with the results of the swelling test indicating a condensing gas drive.

INTRODUCTION

Most of the oil fields of Libya have been producing for the last 25 years with high water cuts and gas oil ratios. Employment of enhanced oil recovery techniques (EOR) to maintain production from these fields at reasonable rates is a crucial matter. The National Oil Corporation (NOC) has adopted miscible gas flooding scheme for increasing oil recovery as the main EOR techniques supported by the availability of huge amounts of natural resources of carbon dioxide (CO_2) and hydrocarbon gases in Libya.

Ghani Field is one of the major oil fields in Libya, and is of a multi-reservoir type. Facha, Gir and Farrud reservoirs are among the main reservoirs in this field.

The availability of Farrud gas in the vicinity of Facha and Gir reservoirs encouraged the operating company (Veba Oil Operations Company) to think seriously of using Farrud gas as a miscible injection gas to increase the recovery from both Facha and Gir reservoirs.

Bottom hole samples from both reservoirs (Facha and Gir) and Farrud surface gas samples were used in this study. The whole experimental program of this study was carried out at the Petroleum Research Centre, Tripoli (PRC).

METHODOLOGY

PVT Analysis

In order to determine original oil PVT properties, a sufficient amount of oil was transferred from a sample cylinder to a high pressure, windowed PVT cell maintained at the reservoir temperature.

Constant composition expansion (CCE) test is made to obtain pressure volume (PV), relationship at reservoir temperature, from which the saturation pressure at reservoir temperature was determined. Having completed the (CCE) test, the separator flash test was conducted. Subsequently, basic PVT properties in terms of formation volume factor (FVF) and produced gas oil ratio were calculated for each of the two oils.

Differential liberation test was performed using an additional amount of reservoir oil at reservoir temperature. From the measured volumetric data and released gas compositional analyses, differential oil formation volume factors (B_{od}), solution gas factor (R_{sd}), gas deviation factor (Z) and gravities were evaluated.

High pressure rolling ball viscometer was evacuated and filled with original reservoir oil. A differential gas liberation process was performed to obtain oil viscosity versus pressure relationship at reservoir temperature. Viscosity values at respective pressure points were calculated from the viscometer calibration data for both oils.

COMPOSITIONAL ANALYSIS

The extended compositional analysis of reservoir oil was obtained by combining the results of separator analysis of solution gas, liberated during single-stage flash separator test. An additional separator test was performed with the separator temperature set at the reservoir temperature. The stock-tank oil was collected after the separator test and associated formation volume factor, gas-oil ratio and stock-tank density data using appropriate mass balance calculations.

ChromPack gas chromatograph (G/C) was used to obtain the analysis of flash gas samples from which

gas molecular weight and density were calculated. Known weight of stock-tank oil was fractionated using Hempel-type distillation column. Four to five fractions in the boiling point ranging from 30 °C to 490 °C were collected. The fractions were weighted and subjected to molecular weight determination by benzene freezing point depression method, and gas chromatographic analysis using fused silica capillary (G/C) technique to obtain weight percent composition of hydrocarbon constituents.

The distillation residue (C_{30+} fraction) was also weighted and then its molecular weight was determined using benzene freezing point depression method. The C_5-C_9 fraction and C_{30} fraction gravimetric and compositional data were combined to calculate respective stock-tank oil analysis. Calculated stock-tank oil composition was then combined using flash gas-oil ratio with the composition of single-stage flash gas to obtain original reservoir oil molecular composition.

SLIM TUBE MISCIBILITY TESTS

Slim tube, filled with toluene, was pressurized to above saturation level. Toluene was then displaced by live oil after two pore volumes were injected. The system was then heated until particular test, *i.e.* reservoir temperature had stabilized. When thermal equilibrium had been established as verified by no fluid production from back-pressure regulator, Farrud hydrocarbon injection at controlled flow rate was started. During the slim tube oil displacement runs, the following experimental data were measured and recorded at time intervals of approximately 60 minutes:

- Time
- Upstream pressure (Farrud HC injection pressure);
- Downstream pressure (back-pressure regulator);
- Amount of mercury injected (pump reading);
- Amount of produced oil (glass receivers);
- Amount of produced gas (gasometer);
- Oven and room temperature, atmospheric pressure.

A run was completed after 1.2 to 1.3 pore volumes (V_{sys}) of Farrud gas (as measured on the volumetric pump) was injected. The upstream valve of the slim tube was then closed and the system pressure was slowly released to the atmospheric pressure. The additional oil produced during this process (blow down oil) was collected and added to the cumulative oil previously produced. The apparatus was then allowed to cool down to room temperature, slim tube assembly removed from the oven and weighed to obtain gravimetric balance data for oil recovery calculations.

Preparation for next run involved injection of toluene into the system to remove all of the remaining oil. Appearance of clean toluene at the down stream end of the system indicated the system being ready for the next run.

Evaluation of data during a slim tube displacement run included the following main steps:

- Cumulative volume of gas injected as measured on the mercury positive displacement pump at room temperature and constant injection pressure were converted to volumes at test temperature by applying pump calibration factors and mercury expansion coefficients according to the following formula:

$$V_{inj} = V_m [\, 1 + B_{Hg} (t - t_r)] \qquad (1)$$

Where

V_{inj} = volume of injected hydrocarbon fluid at reservoir temperature and injection run.

V_m = volume of mercury injected at room temperature and run pressure.

B_{Hg} = coefficient of thermal expansion of Hg at run pressure.

t = reservoir temperature.

t_r = room temperature.

The reservoir condition volumes were converted to pore volume basis:

Farrud HC injected in No. of PV = V_{inj} / PV. (2)

Pore volume used is equal to V_{sys} of slim tube assembly

- Cumulative produced oil recovery was calculated from measured stock-tank oil volumes as a percentage of original oil-in-place (OOIP) using stage separator test.

FVF data:

Oil recovery (%OOIP) = (V_{sto} FVF / PV) * 100 (3)

Where:

Vsto = Cumulative produced stock-tank oil volume (60 °F and 14.7 psia)

FVF = Oil formation volume factor at slim tube test run pressure and reservoir temperature relative to slim tube oil at 60 °F and 14.7 psia.

Total or final recovery after 1.2 PV of Farrud fluid injected was also determined from the gravimetric material balance since the weights of the slim tube containing residual oil after a displacement test were always recorded.

Total oil recovery obtained from the produced oil volumetric data (Eq.3) was higher than the recovery calculated from gravimetric determination of residual oil by using appropriate oil density and FVF data. The difference was more pronounced at higher displacement pressure, which indicates the development of miscibility might be through a condensation process which becomes predominant at lower temperature.

It is characterized by an extraction of medium molecular weight range (C_5-C_{12}) hydrocarbons from injection gas into a dense liquid phase. As a result of this process, a miscible transition zone develops between injected gas and reservoir oil, which efficiently displaces oil.

The other consequence of the process of miscibility development through a condensing drive is an increase of measured produced oil volume (leading to higher than 100%) recovery since part of it was extracted from the injected gas phase. This can be seen from the composition of the produced gas, which contains more light components than Farrud hydrocarbon gas injected. This presumably accounts for the difference in recovery calculated by the volumetric and gravimetric methods used.

RESULTS AND DISCUSSIONS

I - Facha Reservoir

PVT data of Facha reservoir fluid at reservoir temperature of 144 °F is illustrated in Table 1.

During the swelling tests, it was observed that Facha reservoir oil generally tends to emulsify with mercury. Already, after charging the RUSKA 3-window PVT-cell with Facha reservoir oil at 5680 psig (400 kg/cm^2) about 5 mm oil-mercury emulsion formed at the oil-mercury interlayer. During the first five subsequent injections of Farrud gas, the emulsifying tendency increased continuously and finally a column of five cm of emulsion was formed in which the mercury droplets were smaller than 0.1 mm in diameter. During the 5th gas injection (50:50 moles), additionally some asphalt precipitation was observed on the inner surface of the high pressure window PVT-cell. After injection of the 6th gas volume (40:60 mole ratios), severe asphalt precipitation coated the inner wall of the cell window. Simultaneously, the emulsifying tendency increased.

During the PVT cell rocking after 7th gas injection (30:70 mole ratio), more asphalt precipitated and its colour changed to black-grey.

Emulsifying tendency reached maximum and produced 10 cm high emulgated oil-mercury interlayer. During the 8th gas injection at 4970 psig, no difficulties were observed to dissolve this gas volume in the swelled oil. The volume of emulsion remained about the same; however, the asphaltene precipitation was relocated nearly completely from the inner PVT-cell window. It settled as a fine black powder on top of and in the uppermost part of the oil-mercury emulsion. During the constant composition expansion and equilibrium conditions at 1500 psig (105 kg/cm^2), a small shrinkage of the emulsion layer was observed; the amount of precipitated asphalt remained unchanged.

During the course of the subsequent swelling test stages, the oil-mercury emulsion volume decreased only slightly, but did not vanish until the end of the test. After the end of the test, residual oil was bled out from the cell together with finely dispersed precipitated asphalt as well as oil-mercury emulsion. During the cleaning procedure of the 3-window RUSKA PVT-cell, toluene was used to remove residuals from cell window and walls.

The asphalt precipitate remained insoluble also in some aliphatic and aromatic solvents as well as in the mixtures of aromatic and more polar solvents.

The efficiency of Farrud gas to mobilize and displace Facha oil was investigated by measurements of oil produced from slim tube at reservoir temperature of 144 °F and at gas constant injection pressure of 1500, 1850, 2200, 3000 and 4000 psig.

Table 1. PVT data of Facha reservoir fluid at reservoir temperature of 144 °F.

Saturation Pressure (Pb)	235	psia
Flash Formation Volume Factor (B_{of})*	1.1781	bbl/stb
Flash Gas-Oil Ratio (R_f)	207	scf/stb
Differential Formation Volume Factor (B_{od})*	1.1648	bbl/stb
Differential Gas-Oil Ratio (R_d)	161	scf/stb
Thermal Expansion Coefficient at 235 psia	6.63 E -4	cc/cc/°f
Compressibility Coefficient :		
From 1500 to 750 psig	6.50 E -6	cc/cc/psig
From 750 to 235 psig	2.10 E -5	cc/cc/psig
* FVF = oil volume at Pb 144 °F/ stock tank oil at 60 °F		

The oil recovery data are based on volumetric material balance calculations and were checked by gravimetric determination of initial and residual oil in the slim tube.

This resulted in oil recovery in excess of 100% at gas injection higher than MMP when employing flash FVF values to convert produced oil volumes to reservoir oil volumes.

The phenomenon, attributed to the gas condensing mechanism of miscibility development, has no influence on the proper MMP determination. Slim tube runs NO.1 and 2 at 1500 and 1850 psig respectively, show non-miscible displacement features with elongated oil recovery curve and low (71.72 and 82.22%) total oil recovery at 1.2 PV of Farrud gas injected.

The miscible nature of the displacement process is further evidenced by cumulative gas versus produced oil ratio. As shown in Table 2, early gas breakthrough in both cases is also indicative that no appreciable miscible zone formation took place during the runs.

Table 2. Slim tube run pressures with corresponding fraction of pore volume Farrud gas injected at breakthrough (Facha reservoir).

Run pressure, psig	PV of Farrud gas injected at breakthrough
1500	0.77
1800	0.85
2200	0.91
3000	1.00
3500	1.00

Final oil recovery of 92.54% obtained during the slim tube test No. 3 at 2200 psig and corresponding injected gas breakthrough at 0.91 PV are both suggesting near miscible oil displacement conditions. This implies an advanced degree of miscible zone development and corresponding efficiency of oil displacement approaches of first contact miscible process.

The three higher-pressure slim tube runs No. 4, 5 and 6 at 3000, 3500 and 4000 psig are typical for a miscible process characterized with maximum displacement efficiency due to fully developed miscible zone. The measured overall oil recoveries during these runs are in excess of 100% original oil in place.

The explanation of this is related to the mechanism of achieving the dynamic miscibility. The compositional analysis of Farrud injection gas shows increased C_2-C_5 content. When such enriched hydrocarbon gas is injected into reservoir, dynamic miscibility results from the transfer of C_2-C_5 hydrocarbons until a miscible zone develops.

Experimental evidence for enriched gases (or condensing) drive process being operative during slim tube oil displacements in this study is considered to be the following:

- At pressures above MMP, oil recoveries determined using volumetric material balance are larger than 100% of initial oil.
- Additional gravimetric material balance data are consistent with the above volumetric data showing net increase of hydrocarbons material at miscible conditions
- Fluid produced from the slim tube at and after 1 PV of gas injected had light brownish appearance and vaporized quickly at room temperature.

Cumulative Facha oil recovery data at 1.2 PV of Farrud gas injected, (Table 3) were plotted versus corresponding injection pressures, (Fig.1). From this curve, the minimum miscibility pressure (MMP) of Facha oil-Farrud gas system was found to be 2445 psig at reservoir temperature of 144 °F.

Table 3. Slim tube oil recovery at 144°F of Facha reservoir using Farrud hydrocarbon gas.

Gas injection pressure (psig)	Oil recovery at 1.2 PV gas injected (%)
1500	71.72
1850	82.22
2200	92.54
3000	111.66
3500	112.70
4000	112.92

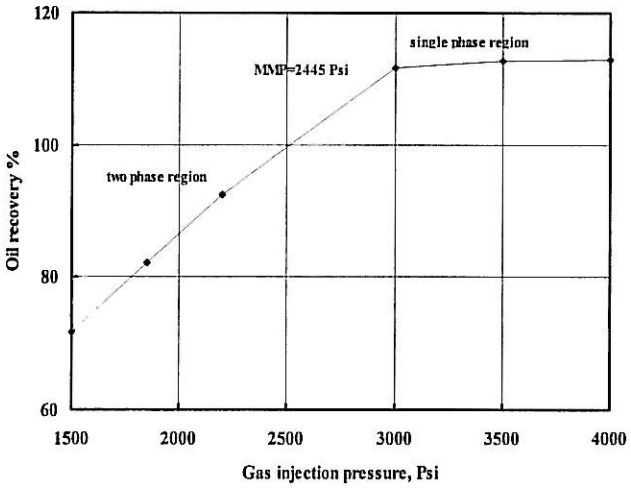


Fig. 1. Prevent oil recovery Vs gas injection pressure (facha reservoir).

II- Gir Reservoir

Conventional PVT experimental study was carried out on Gir reservoir oil at reservoir temperature of 140 °F. Results of such study are illustrated in (Table 4).

The results of the swelling tests revealed the same phenomenon observed with Facha swelling test. That is, Gir reservoir oil tends to emulsify with mercury. After charging the CORELAB long window high pressure PVT-cell, with Gir oil already at 5680 psig, 4 mm of oil-mercury emulsion spontaneously occurred on top of the mercury surface.

During the subsequent Farrud gas injection from injections No. 1 to 6, the volume of emulsion increased continuously up to 40 mm. In this gray emulsion, the diameter of the mercury droplets was far below 0.1 mm. During the 6th gas injection at 4260 psig asphalt precipitation started, covering the inner wall of the cell window with glittering crystal-like particles. By increasing the pressure of the system, the asphalt particles disappeared. When the pressure was decreased, the growth of the asphalt particles reappeared and increased until bubble point pressure was reached.

The Farrud gas injection at the 7th stage (60:40 mole ratio) was performed at 3550 psig. Attempts to dissolve the gas in the swelled oil volume by rocking the cell, increasing or decreasing the pressure, failed. After each rocking of the cell, a gas- like layer (4 cm) remained separately on top of the cell window. At pressures between 5400-5700 psig, this gas or fluid changed its color to a semitransparent fluid exhibiting an intense green fluorescence. Below this uppermost layer, a clearly separated reddish-brown fluid 4 cm high occurred. In this region, some brown asphalt patches occupied the cell window. Below this second layer, again semitransparent and green fluorescent layer (4-5 cm) could be observed, it was followed by a fourth layer colored red-brown but transparent. Finally, to the lowest end of the cell, a layer was found that exhibited a color like crude oil.

Repeated rocking of the PVT cell (including upside down turning) always produced the same sequence of separated, stable and non-miscible layers. Increasing or decreasing the pressure in the cell changed the relative size of the layers or caused disappearance of some. However, the build-up of the immiscible phases could be repeated arbitrarily without change with changing pressure.

Over the following night, a breakdown of electricity occurred in the laboratory causing cooling of the whole equipment down to 95 °F (35 °C). First pressure check at 5660 psig (400 Kg/cm^2) showed that at this pressure a single-phase liquid could be obtained. It was expected that during heating of the test mixture to the reservoir temperature it finally would arrive at the same five immiscible layers, and a gas cap.

However, when reservoir temperature had been attained, a significant change in the system behavior was observed.

The swelled oil was now a single phase liquid. Consequently, the test was continued by conventional PV-relation procedure. Attempts to restore the state of immiscibility by increasing the pressure after arriving below the bubble point pressure failed.

During the measurements of PV-relation, a very different behavior was observed.

At start of the measurement, precipitated asphalt particles in patches and glittering crystals coated the inner wall of the cell window. Through the stepwise pressure reduction, more asphalt precipitated like a yellow-brownish paint on the cell window. At lower pressure, dissolution of the asphalt patches and crystals followed this behavior to globules and fine droplets, which subsequently transformed to a black low viscous immiscible liquid running down the cell window in fine streams.

Commencing the 8th Farrud gas injection (20:80 mole ratio) a similar behavior of the swelled oil was expected as observed in the previous stage, or a complete change into a super-critical fluid. The gas was injected at 3550 psig (250 Kg/cm^2), which is close to the expected bubble point pressure. However, the gas dissolved quickly

Table 4. PVT data of reservoir Gir reservoir fluid at reservoir temperature of 140 °F.

Saturation Pressure (pb)	555	psia
Flash Formation Volume Factor (B_{of})*	1.3487	bbl/stb
Flash Gas-Oil Ratio (R_f)	341	scf/stb
Differential formation Volume Factor (B_{od})*	1.2232	bbl/stb
Differential Gas-Oil ratio (R_d)	306	scf/stb
Thermal Expansion Coefficient at 555 Psia	6.687E-04	cc/cc/°f
Compressibility Coefficient :		
From 1500 to 1000 psig 6.45E-06	cc/cc/psig	
From 1000 to 555 psig 2.13E-06	cc/cc/psig	
*FVF= oil volume at Pb 140 °F/stock tank oil at 60 °F		

in the swelled oil of the seventh stage. The conventional PV-relation was performed but revealed that it became very difficult to accurately define bubble point pressure.

The observations of the behavior of the swelled oil showed considerable changes during pressure decrease. The swelled oil mixture showed differentiation similar to the 7th stage but no gaseous phase occurred in the pressure range between 6000 to 4200 psig. Some different colours and layers partly immiscible were observed, but not clearly distinguishable. The asphaltic matter showed very different behaviour during the stepwise pressure decrease. First asphalt-like matter condensed as a brown paint- on the inner surface of the cell window, changing during further pressure reduction into fine streams of black liquid and droplets running down the cell window. Below the bubble point pressure, the liquid asphalt became a solid mass (3100-2600 psig). Finally, the cell window was completely covered with masses of solid asphalt.

By pressure increase, the behavior could be reversed. Below 2600 psig, after a gas volume of several cubic centimeters had developed, the asphalt diminished from the cell window. It was not dissolved but formed a finely divided black powder which accumulated as a 10 mm thick precipitate on the top of the oil-mercury emulsion. This asphalt precipitation did not change during the subsequent constant composition expansion and release of gas at equilibrium conditions of 1500 psig, as well as during the two injection and releases of 20 mole percent of Farrud gas.

After the complete flash-down of all gas from the swelled oil, more asphalt matter had precipitated, coating not only the cell window but also the inner surface of the metal cell body. At the stage of discharging of the CORELAB PVT-CELL and final cleaning procedure, it was found that the black asphalt was insoluble in all non-polar solvents and mixtures of the solvents.

A total of seven slim tube tests at 1000, 1500, 1700, 2000, 2500, 3000 and 4000 psig and reservoir temperature of 140 °F were conducted using Gir oil and Farrud injection gas in order to evaluate the oil displacement process characteristics and determine minimum miscibility pressure (MMP) for the fluid system investigated .

The main features of the Gir oil slim tube tests in terms of mechanism of dynamic miscibility development and associated experimental oil recovery checks are closely similar to those of Facha oil and are briefly as follows:

- Slim tube tests No.1, 2 and 3 at 1000,1500 and 1700 psig exhibit non miscible gas drive characteristics as documented by measured respective oil recoveries of 58.6, 69.4 and 62.1%. The injected gas breakthrough data, in (Table 5), are consistent with the trend of slow development of the miscibility zone with increasing injection pressure.

Table 5. Slim tube run pressure with corresponding fraction of pore volume Farrud gas injection at breakthrough (Gir reservoir)

Run pressure, psig	P.V. of Farrud gas injected at breakthrough
1000	0.40
1500	0.58
1700	0.68
2000	0.77
2500	0.95
3000	1.0
4000	1.0

- Slim tube run No. 4 at 2000 psig indicates a moderate degree of near-miscibility since both oil recovery and gas breakthrough values have increased in comparison with lower pressure runs.
- The three slim tube runs no. 5 and 6 were miscible processes characterized with 100% of higher oil recoveries and complementary injected gas breakthrough values.

The amount and feature of Gir oil produced during high pressure slim tube displacements furnished evidence for the same conclusions about the type of mechanism responsible for development of multi-contact miscibility as in the case of Facha oil. Condensing gas drive is operative also in the case of Gir oil miscible displacement, which is documented by both gravimetric material balance data and physical appearance of the oil produced at high injection gas pressures.

On the basis of data provided in Table 6, the cumulative Gir oil recovery was plotted versus injection pressure in figure (2) and the value of 2495 psig was

Table 6. Slim tube oil recovery at 140 °F of Gir reservoir using Farrud hydrocarbon gas.

Gas injectionpressure, psig	Oil recovery at 1.2 PV gas injected, %
1000	43.62
1500	65.45
1700	75.13
2000	88.75
2500	108.07
3000	109.50
4000	112.49

determined as MMP for Gir oil-Farrud injection gas system at reservoir temperature of 140 °F.

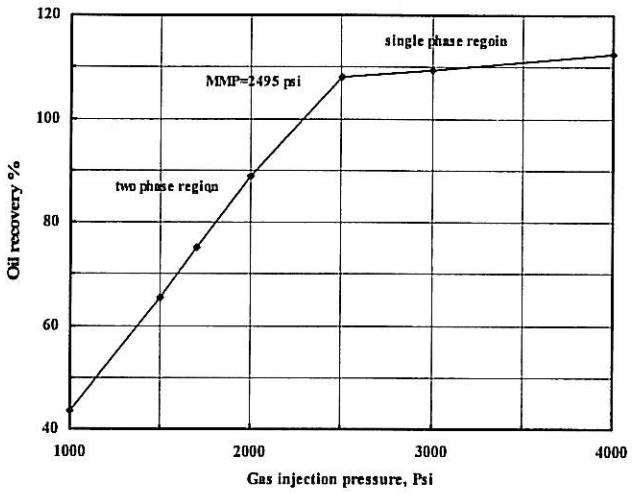


Fig. 2. Prevent oil recovery Vs gas injection pressure (Gir reservoir).

CONCLUSIONS

1. The results of this study revealed that Facha and Gir reservoir oils are both under-saturated oils compared to their reservoir pressures. The released gases from flash and differential vaporization studies exhibit gas compositions highly enriched in heavier hydrocarbons from ethane to pentanes and low methane content.
2. Swelling tests showed that injections of Farrud gas into Facha and Gir reservoir oil already reach reservoir pressure at injection ratios 1:1 to 1:1.5 moles (oil : gas). At the highest injection ratios of 1:4 moles (oil : gas) especially swelled Gir oil exhibit multi-phase behavior at all pressures above the bubble point pressure. The swelling test studies exhibit general behavior of highly gas-enriched reservoir oils.
3. Mass balance checks were performed using densities of all oils and mixtures. The calculated densities from start to end of swelling tests are close to the measured densities of the residual oil after the swelling test procedure. Therefore, the compositional data reported are consistent and show good reliability.
4. Minimum miscibility pressure (MMP) for Facha and Gir reservoir oils using Farrud injection gas have been determined to be 2445 and 2459 psig respectively. These figures are considered extremely high and far beyond the reservoir pressures. The type of miscibility development is in agreement with the results of the swelling test indicating a 'condensing gas drive'.
5. The reservoir oil migration and accumulation history and stratigraphic as well as tectonic events have not been discussed. However, composition of original Farrud gas and gas composition of gas released from swelling tests exhibit similarities pointing to an equilibrium separation process occurring at a certain geological or time of oil accumulation.
6. In general, when it comes to miscibility studies, achieving single-phase state does not always mean that oil-gas miscibility is reached, as gas condensation could be the case. Facha and Gir reservoir oils with Farrud gas injection is a good example of such a case.
7. Also, reaching the minimum miscibility pressure does not always increase the mobility of reservoir oil and consequently increase oil recovery. It could create problems of solid precipitation of asphaltic type that result in damaging formation permeability.

AKNOWLEDGEMENT

We wish to thank Veba Oil Operations Company for giving the chance to the Petroleum Research Centre to explore its capability through the course of study. Special thanks are due to all PRC staff who assisted in conducting the experimental work.

REFERENCES

[1] Yelling, W.F., and Metcalfe, R.S, 1980 (January). Determination and prediction of CO_2 minimum miscibility pressure. *JPT 160-168.*

[2] Glaso, O, 1985 (December). Generalized minimum miscibility pressure correlation. Soc.Pet.Eng. *J 927-934*

[3] DesBrisay, C.L., Gray, J.W., and Spivak, A, 1975 (August). Miscible flood performance of the Intisar (D) field, Libyan Arab Republic. *J. Pet. Tech. 935-943.*

[4] Firoozabadi and Aziz, 1986 (November). Analysis and correlation of nitrogen and lean gas miscibility pressure. *SPE, Reservoir Engineering 575-582.*

[5] Simon, R. and Graue, D.J., 1965 (January). Generalized correlation for predicting solubility, swelling, and viscosity behavior of CO_2 crude oil system. *JPT,102-106.*

[6] Coats, K. H.1980 (October). An equation of state compositional model. *Soc. Pet. Eng .J.363-376.*

[7] Kremesec, V.J., Jr. And Sebastian, H.M.1988 (May). CO_2 Displacement of reservoir oils from Berea cores: laboratory and simulation results, *SPERE 496-504.*

Petroleum Res. J. Vol. 14 (2002): P. 67–82, 15 Figs.

Abu Attiffel Field: Gas Injection Process to Improve the Final Oil Recovery

Emilio Causin, Elio Rossi, Francesco Radaelli* and Ibrahim S. El Ageli**

عملية حقن الغاز لتحسين المسترد النهائي للنفط بحقل أبو الطفل

أميليو كوزين، و اليو روصي، و فرانسيسكو راديلي و إبراهيم س. العجيلي

تم اكتشاف حقل أبو الطفل النفطي، العملاق بحوض سرت الرسوبي بالصحراء الليبية من قبل شركة آجيب عام 1967ف. حيث يتم إنتاج نفط من النوع الخفيف (41 درجة حسب مقياس معهد البترول الأمريكي) من صخور الحجر الرملي القارية عند عمق يصل في المتوسط إلى حوالي 4200 متر تحت مستوى سطح البحر (13,800 قدم).

بدأت عملية حقن الماء بعد سنتين من الإنتاج الأولى للنفط وشمل هذا حفر تسعة (9) آبار للمحافظة على الضغط. يبلغ معدل الإنتاج الحالي للنفط حوالي 91,000 برميل يومياً (14,500م3) وبنسبة مياه تناهز 37% ويتوقع أن تكون نسبة المسترد النهائي حوالي 50%.

ونظراً لزيادة نسبة الماء مع النفط بشكل كبير في السنوات الأخيرة، فقد تم تقييم أسلوب الاسترداد الإضافي بهدف زيادة المسترد النهائي من النفط.

وضمن عمليات الاسترداد الإضافي المألوفة يعتبر حقن الغاز ملائماً لظروف المكمن بحقل أبو الطفل.

أجريت معملياً دراسة أداء غازين مختلفين (ثاني أكسيد الكربون وغاز الفاصل) عند درجة حرارة المكمن وهي 145 درجة مئوية (292 درجة فهرنهايتية) وتحت ضغط 47.6 ميغا باسكال (6897 رطل على البوصة المربعة) وتم الحصول على إمتزاجية ثاني أكسيد الكربون (والتي تكفل أفضل الظروف لتحسين المسترد النهائي للنفط) مع زيت المكمن وتحت ضغط أقل من ضغط المكمن الأصلي إلا أن التجارب المعملية أوضحت حدوث ترسبات بارافينية وتآكل في جميع الإختبارات.

وبالإضافة إلى ما يسببه الغاز الخفيف من ترسبات برافينية في الوسط المسامي ومشاكل التآكل فإنه لم يمتزج مع زيت المكمن عند ظروف المكمن الحالية.

ولقد تم تحقيق تحسن كبير في أداء الغاز الخفيف بإذابة حجم من غاز البترول المسال به وهو ما سمح بالحصول على الإمتزاجية عند ظروف المكمن الحالية (ألف قدم مكعب من الغاز الخفيف مشبع بحوالي 52 برميل من غاز البترول المسال). ومن أجل تأكيد كفاءة الإزاحة المجهرية للنفط، تم إجراء عدة تجارب باستخدام غاز معزز عند ظروف المكمن الحالية. كما تم إختيار عينات لبية ممثلة لتكوين المكمن باستعمال تحاليل جهاز تصوير الرنين المغناطيسي النووي. كذلك تمت محاكاة ثلاثة ظروف مكمنية (تشبع الزيت المتبقي، تشبع الزيت المتوسط، وتشبع الماء المستعصي).

وقد برهنت معظم التجارب كفاءة عالية جداً للإزاحة بالغاز المعزز الذي يتعلق بالمسترد النهائي بينما لعب نسيج الصخر دوراً مهماً عندما درست عينات عند درجة التشبع بالزيت المتبقي.

وأكدت النتائج بأن الغاز المعزز كان أكثر كفاءة من الماء في المسترد النفطي النهائي على مستوى العينات اللبية.

* ENI – Agip Division.
** Agip Oil (Libyan Branch).

Abstract: *The Abu Attiffel oilfield was discovered by Agip in 1967. This field is a giant reservoir located in the Sirt Basin of the Libyan desert. It is producing a volatile oil (41° API) from sandstones of continental environment at an average depth of 4,200 m b.s.l. (13,800 feet).*

Water injection process started after two years of primary oil production, involving 9 injector wells for pressure maintenance purposes. Current field (main area) oil production rate is 91,000 BOPD (14,500 m^3) with a water cut-off of about 37%. The final oil recovery is expected to be around 50%.

Since the water cut-off has dramatically increased in the last years, an EOR approach was evaluated in order to enhance the final oil recovery.

Among the conventional EOR processes, only gas injection was suitable for Abu Attiffel field because of its very severe reservoir conditions.

The performance of two different gases (CO_2 and separator gas) was studied in the laboratory at the average reservoir temperature of 145 °C (292 °F) and pressure of 47.6 MPa (6,897 psia).

CO_2 achieved miscibility (which assures the best conditions for an improvement of the final oil recovery) with the reservoir oil below the original reservoir pressure but paraffinic precipitation and corrosion phenomena occurred in all the tests performed.

Lean gas, besides causing paraffinic deposition in the porous media and corrosion problems, was not miscible with the oil under the current reservoir conditions.

A significant improvement of the lean gas performance was achieved by solubilizing a volume of LPG (liquefied petroleum gas) which permitted the miscibility to be reached under the current reservoir conditions (i.e. one MScf of lean gas enriched with about 52 bbl of LPG).

In order to confirm the improvement of the microscopic efficiency of the oil displacement, several experiments were carried out using enriched gas under current reservoir conditions.

Core plugs representative of the reservoir formation were selected on the basis of Nuclear Magnetic Resonance Imaging analysis.

Three different reservoir conditions (residual oil saturation, intermediate oil saturation and irreducible water saturation) were simulated.

Most of the tests demonstrated the very high displacement efficiency of the enriched gas as regards final oil recovery. Gravitational forces slightly influenced oil recovery, while an important role was played by rock texture when samples at residual oil saturation were considered.

The results confirmed that the enriched gas was more effective than water in the final oil recovery at core scale.

INTRODUCTION

Abu Attiffel field is located in the Sirt Basin, about 400 km SE of Benghazi. It was discovered in 1967 and went on stream in 1972. The present oil rate (91,000 BOPD) is steadily decreasing from an average plateau of 150,000 BOPD maintained until 1993. A peak of 170,000 BOPD was recorded in 1990-92 after an infill drilling campaign. Up to now the cumulative oil production amounts to some 37% of the original oil in place (OOIP), and the expected final recovery is estimated at about 50%.

A water injection project started in 1974 with 9 injectors[1,2] for pressure maintenance purpose. A daily rate of 350,000 bbl of water is presently injected and the field water cut has already reached 37%.

The rate decline and mature status of the field led Agip Oil's management to investigate the feasibility of an Enhanced Oil Recovery project to improve the final oil recovery. The gas injection was the only process suitable under the reservoir conditions of Abu Attiffel field. Carbon dioxide, lean gas and enriched gas were tested with the aim of finding out the most efficient solvent, miscible with the oil at the current reservoir conditions. After the selection of the gas, its performance was evaluated using real core plugs of the reservoir in order to evaluate the "microscopic oil displacement efficiency", in comparison with water injection process.

RESERVOIR CHARACTERISTICS

The reservoir is a west to east elongated horst, approximately 17 km long and 2-4 km wide, limited on all sides by faults and with a low dip of 5° to the north. Its OOIP is estimated at some 620 Mm^3.

The oil production comes from the Upper Nubian Sandstones, a formation of a Lower Cretaceous age whose depth goes from 3886 to 4336 m b.s.l.

The oil-bearing rock is a fine to coarse-grained sandstone with interbedded shale and shaly-siltstones; it ranges in net thickness from 75 to 250 m. The

porosity (8%-16%) is intergranular and was preserved at rather good value by a syntaxial siliceous cementation which reduced the effect of the compaction after the deposition. The horizontal permeability spans from a few md to more than 1000 md, and the k_v/k_h ratio ranges from 0.48 to 1.23. The initial water saturation, which correlates quite well with the local porosity, averages 16%.

At discovery, a bubble point variation with the depth was recognized, but the oil resulted undersaturated at the initial pressure (47.6 MPa) through all the field. The basic volumetric properties and an average composition are listed in Tables 1 and 2, respectively.

The stock-tank crude has a 41° API gravity, its base is paraffinic at high wax content (36.7%) with an upper pour point of 39°C.

Representative gas and oil samples for the study were collected at the separator of the well A-17 (perforated interval: 4,137-4,232 m). They were recombined according to a gas-oil ratio of 245 Sm^3/m^3 to obtain a system saturated at 40.5 MPa at 145°C, *i.e.* at the current field conditions. In fact, a partial reservoir voidage lowered the initial pressure below the original average bubble point.

SELECTION OF THE MOST SUITABLE GAS

Experimental Procedures: The effect of each selected gas, when contacting the reservoir oil, was investigated both at static and dynamic conditions[3] (Fig. 1).

In the first case, the volumetric behavior of several gas/oil mixtures, representing a wide range of

Table 1. Volumetric characteristics of reservoir oil.

Reservoir temperature	145 °C
Reservoir pressure	47.57 MPa
Bubble point pressure	40.46 MPa
Data at reservoir pressure	
Solution gas (Rs)	393.5 Sm^3/m^3
O.R.V.F. (Bo)	2.2623
Reservoir oil density	543 kg/m^3
Reservoir oil viscosity	0.21 mPa s
Data at bubble point pressure	
Solution gas (Rs)	393.5 Sm^3/m^3
O.R.V.F. (Bo)	2.3264
Reservoir oil density	528 kg/m^3
Reservoir oil viscosity	0.17 mPa s

Table 2. Fluid compositions (% MOL).

Components	Reservoir oil	Lean gas	Liquefied petroleum gas	Enriched gas (LGR = 290.3 m^3/MSm^3)
Nitrogen	0.47	0.62	0.01	0.58
Carbon dioxide	3.06	3.76	0.70	3.58
Hydrogen sulfide	-	-	-	-
Methane	61.97	79.51	5.41	75.28
Ethane	8.72	10.43	6.51	10.21
Propane	2.86	3.13	9.29	3.48
I-Butane	0.66	0.63	5.50	0.92
N-Butane	1.10	0.92	10.81	1.49
I-Pentane	0.58	0.29	7.34	0.69
N-Pentane	0.72	0.28	8.19	0.73
Hexanes	1.99	0.27	20.80	1.44
Heptanes	1.94	0.09	13.63	0.86
Octanes (plus)	1.90	0.07	7.00	0.47
Nonanes	1.21	-	2.87	0.16
Decanes	1.16	-	1.22	0.07
Undecanes	0.74	-	0.40	0.02
Dodecanes	0.70	-	0.19	0.01
Tridecanes plus	10.22	-	0.13	0.01

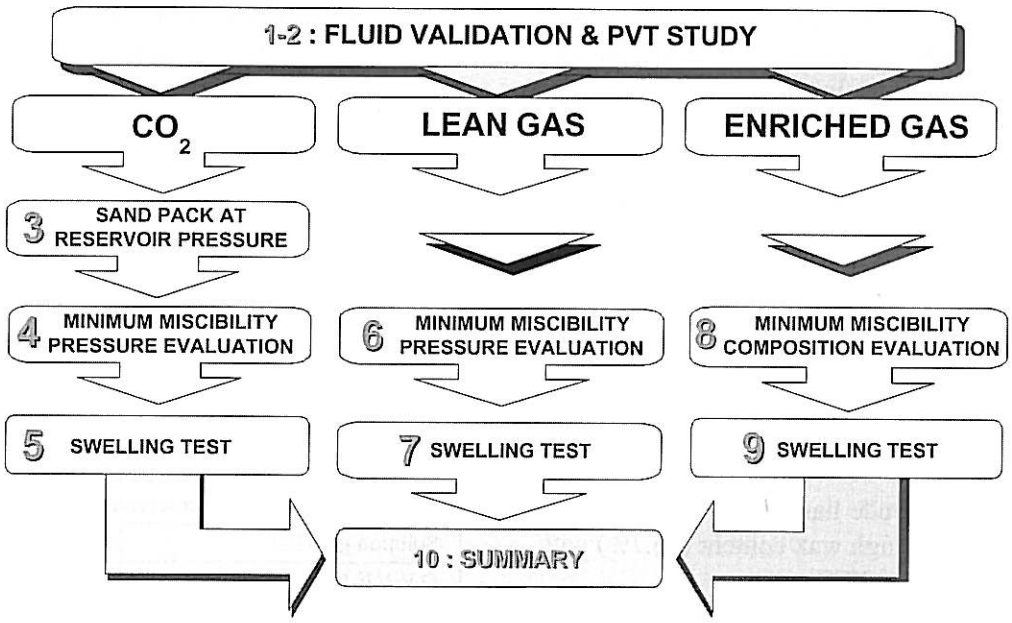


Fig. 1. Scheme of the phase 1 of the gas injection project.

different "injected gas-oil ratios" (IGOR, defined as the volume of gas – referred to standard conditions – added to a unit volume of reservoir oil at the original bubble point), was studied in a double windowed PVT cell. Each mixture was expanded at constant composition for measuring its saturation pressure and its "swelling factor". This last parameter was defined as "the volume of the system at a given pressure divided by the volume of the reservoir oil at the original saturation pressure". Furthermore, each system was identified as "oil" or "condensate", according to the volumetric behavior observed when the pressure was lowered below the saturation point.

The dynamic experiments were performed in a slim tube equipment (Fig. 2), for finding out either the Minimum Miscibility Pressure (MMP)[4] or the Minimum Miscibility Enrichment (MME)[5]. The slim tube had a cross-sectional area of 38 mm² and a length of 18.23 m; the pore volume of the filling sand was 322 cm³ and the absolute permeability to air 3.95 μm².

The rig consisted of two pumps for displacing either the stock-tank or the reservoir oil held in two high pressure vessels. In the thermostatic air bath were put:

- a high pressure bottle filled with gas;

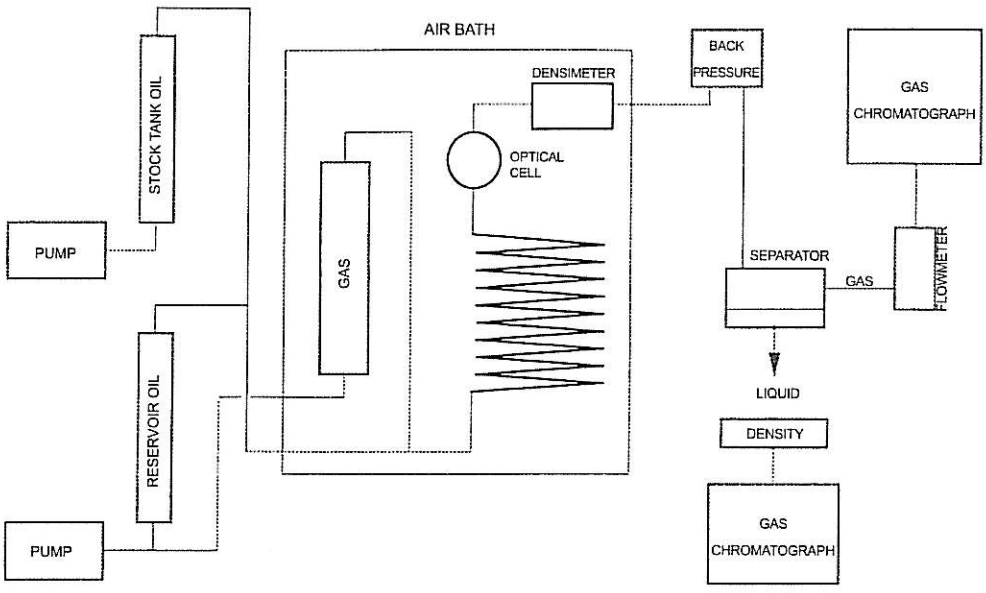


Fig. 2. Scheme of the oil displacement apparatus.

- the slim tube;
- a high pressure densimeter to measure the density of the produced fluid.

Gas and liquid phases were separated in a vessel, working at 15°C and atmospheric pressure. A mass-flowmeter continuously recorded the flow rate of the separated gas, whose chemical composition (up to C_8) was analysed every half an hour by a gas chromatograph set on line. The liquid samples were collected in glass bottles and weighed, as the high pour point of the crude did not allow any reliable volume measurements.

All the tests were carried out at a displacement velocity of 5.0 m/day (equivalent rate: 3.9 cm³/h), and at least 1.2 pore volume of gas was always injected during each experiment.

Phase Behavior of Oil/Carbon Dioxide Mixtures: Figure 3A shows the volumetric behavior of the reservoir oil swollen with CO_2 at different IGORs. The system behaved like an "oil" for IGOR up to 124.6 Sm³/m³ (corresponding saturation pressure: 42.9 MPa). Above it, for IGOR of 173.8 Sm³/m³ (corresponding saturation pressure: 43.8 MPa), the system appeared as a "condensate". The interval enclosed between these two values is the "critical point"zone, which was not investigated.

Five tests at 145°C and 53, 49.1, 42.9, 41.4 and 39.3 MPa were run to find out the MMP. The resulting value was very close to 42.9 MPa, as shown by the plot of the oil recovered (93.6, 93.0. 92.9, 88.2, 81.1% of OOIP, respectively) at CO_2 breakthrough *vs.* pressure (Fig. 4). For pressures beyond this value, the injectant and the oil develop a multicontact miscibility, below it they are immiscible. The MMP found lies inside the transition zone between the "oil" and "condensate" systems outlined with the swelling tests.

It is quite interesting to notice that the CO_2 density (615-720 kg/m³) resulted always greater than that of the reservoir oil (530-540 kg/m³).

In the interval 41.4-49.1 MPa, *i.e.* around the MMP, the CO_2 stripping of the intermediate oil components destabilized the heavy paraffin fractions (C_{25}-C_{60}), and caused a wax precipitation.

At 42.9 MPa a drastic permeability reduction of the sand inside the slim tube was noticed, and the upstream section of the equipment became plugged. The appearance of a solid phase was also observed during the oil swelling tests.

Phase Behavior of Oil/Lean Gas Mixtures: The composition of the lean gas, sampled at the Oil Centre, is listed in Table 2. Four tests at 145°C and 56.9, 53.0, 47.5 and 41.4 MPa were performed to determine the MMP. The oil recovered at lean gas breakthrough was 94.2, 93.4, 89.3 and 46.5% of OOIP, respectively. The plot of these data vs. pressure (Fig. 5) gave a MMP value of 48.1 MPa. which is higher even than the original reservoir pressure. The miscible process was identified as vaporizing gas drive[161].

In the interval 47.5-41.4 MPa, well below the MMP, precipitation of heavy paraffins (C_{30}-C_{60}) was still observed. However, the phenomenon was less severe than that recorded during the CO_2 displacement. In fact, at 41.4 MPa the precipitated waxes caused a permeability reduction only in the

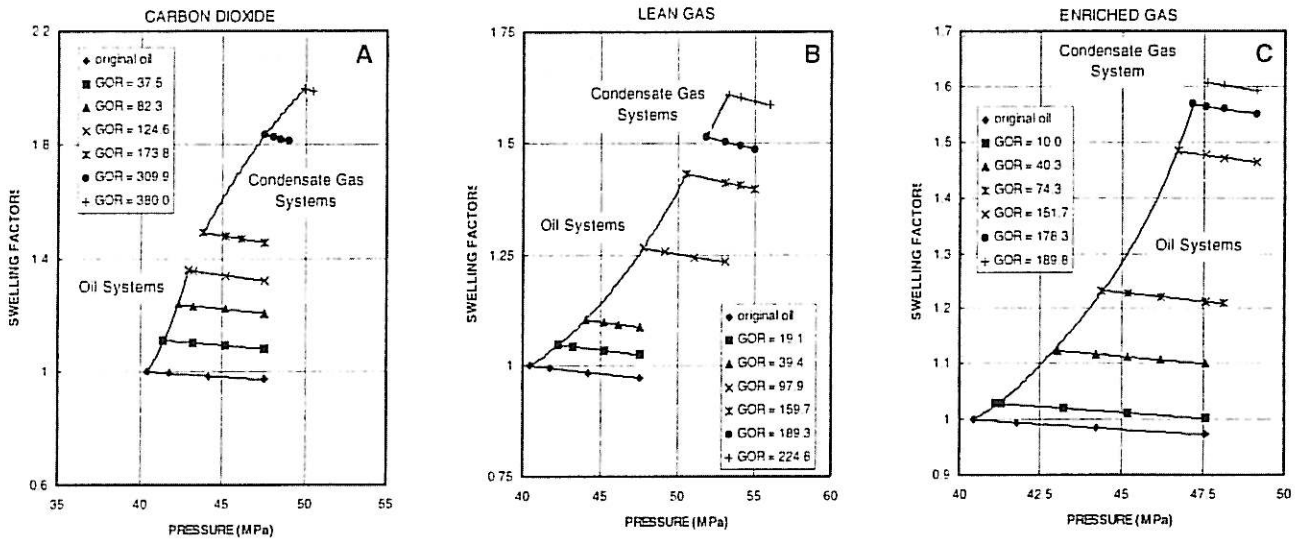


Fig. 3. Swelling factors of different gas/oil systems for several injection G.O.R.

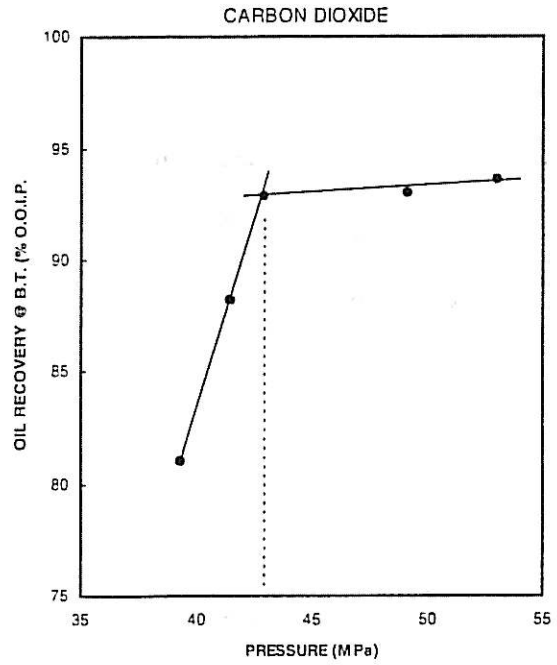


Fig. 4. MMP of carbon dioxide with Abu Attiffel oil.

inlet part of the slim tube and a partial plugging of the upstream section of the equipment.

The swelling tests (Fig. 3B) showed that the systems oil/lean gas behaved as "oil" up to an IGOR of 159.7 Sm^3/m^3 (corresponding saturation pressure: 50.6 MPa). Above it, for IGOR of 189.3 Sm^3/m^3 (corresponding saturation pressure: 51.9 MPa), the system appeared as "condensate".

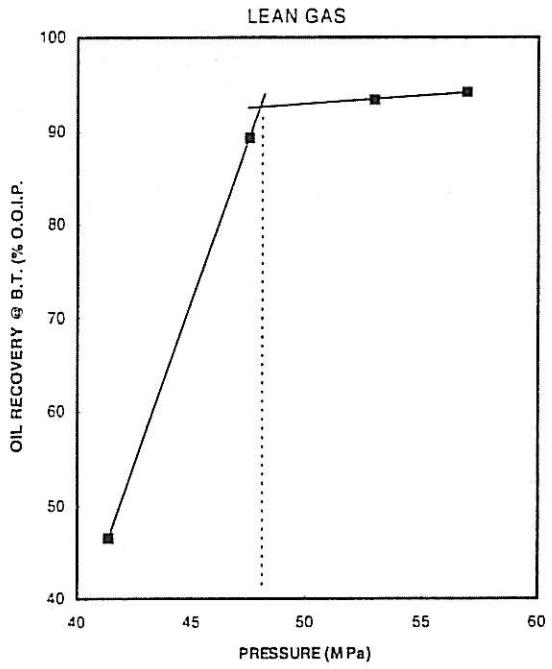


Fig. 5. MMP of lean gas with Abu Attiffel oil.

Lean Gas Enrichment with LPG: Because the lean gas miscibility was attained at too high pressure, it was decided to investigate to what extent it should be enriched with LPG(MME) to obtain a multicontact miscibility. The experiments were run with the equipment and according to the lab procedures employed during the MMP displacements, except the pressure was kept constant at 41.4 MPa to maintain the oil in single liquid phase. Four injectant mixtures, prepared according to different "liquid gas ratios" (LGR, defined as the LPG volume – referred at the sampling conditions 23°C, and 1.3 MPa – added to 10^6 Sm^3 of lean gas) were tested, namely 250, 710, 1000, 1670 m^3/MSm^3.

The results of all these tests were compared with those of the lean gas displacement (LGR=0) performed at the same conditions. The trend analysis of the separated gas composition and the effluent density helped considerably the interpretation. For example, the oil displacement became "piston-like" passing from the lean gas to the richest injectant (LGR=1670 m^3/MSm^3) as shown by the trend of methane concentration in Fig. 6. The same conclusion is attainable also looking at the density (Fig. 7A), whose trend becomes more and more smooth as the injectant is enriched.

The most probable displacement mechanism was a condensing /vaporizing gas drive, with the condensing process prevailing as the gas was enriched[6] .

The MME was quantitatively evaluated plotting the oil recovered at gas breakthrough *vs.* LGR (Fig. 7B). It produced 290.3 m^3/MSm^3.at 145°C and 41.4 MPa (Fig. 7C). The injectant composition, measured after the LPG solubilization in a corresponding volume of lean gas, is presented in Table 2.

Phase Behavior of Oil/Enriched Gas Mixtures: Figure 3C shows the volumetric behavior of the reservoir oil swollen with enriched gas (LGR=290.3 m^3/MSm^3) at different IGORs. The transition zone between "oil" and "condensate" occurred only at high pressure. In fact, the system behaved like a liquid for IGORs up to 178.3 m^3/MSm^3 (corresponding saturation pressure: 47.2 MPa), and like a gas for an IGOR of 189.8 m^3/MSm^3 (corresponding saturation pressure: 47.6 Mpa). The phase transition took place after a minimum change in the system composition, as proved in the following table which reports the chemical analysis of the two mixtures, compared with the original oil and MME gas compositions.

IGOR	Moles (%)									
Sm^3/m^3	CO_2	N_2	C1	C2	C3	C4	C5	C6	C7	C8+
178.3	3.30	0.52	67.95	9.40	3.17	2.11	1.42	1.81	1.49	8.83
189.8	3.30	0.52	68.15	9.43	3.18	2.13	1.42	1.81	1.47	8.59
Original oil	3.06	0.47	61.97	8.72	2.86	1.76	1.30	1.99	1.94	15.93
MME gas	3.58	0.58	75.28	10.21	3.48	2.41	1.42	1.44	0.86	0.74

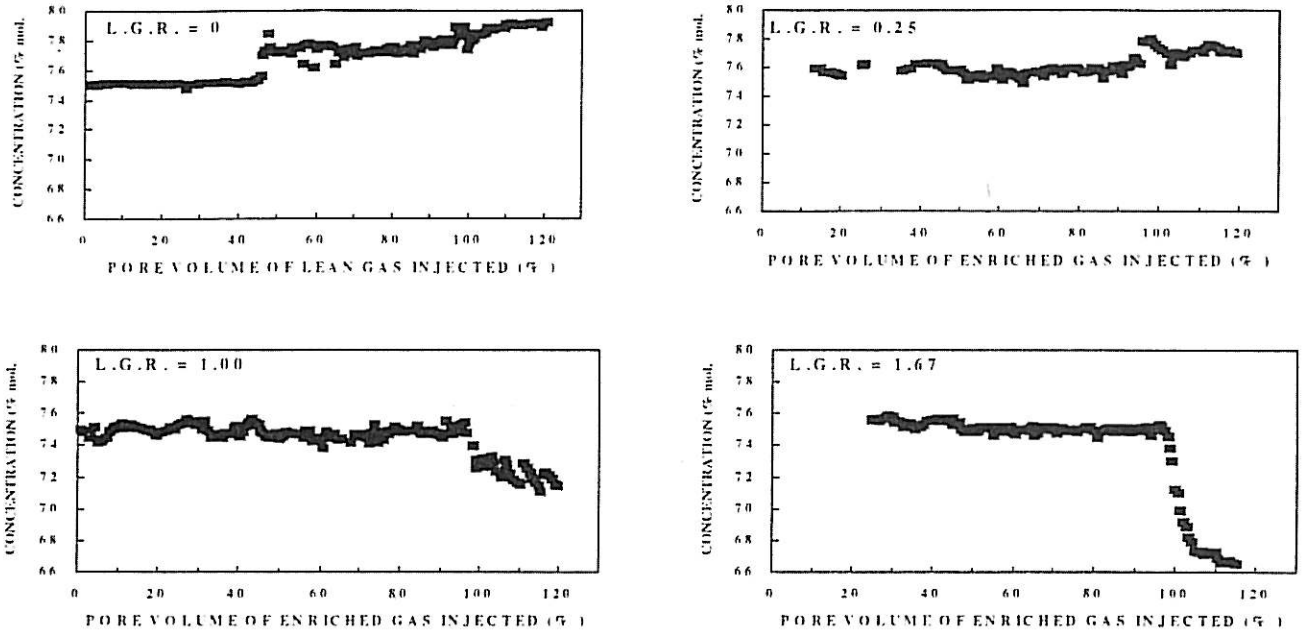


Fig. 6. Separator gas composition (methane concentration trend) for different L.G.R.

On the basis of these results, the enriched gas obtained vaporizing LPG in the lean gas was the most suitable under the current reservoir conditions. With an enrichment of 290.3 m^3/MSm^3 miscibility was attained by, condensing/vaporizing gas drive. Unlike the two other solvents, neither paraffin precipitation nor corrosion occurred in all the tests, therefore this injectant was retained for future field applications.

MICROSCOPIC OIL DISPLACEMENT EFFICIENCY

The experiments previously described had the aim of understanding gas-oil interactions. The effects of the reservoir rock texture and mineralogy, and the impact of water saturation on oil recovery were not taken into consideration.

A set of oil displacement tests was planned in order to determine the "microscopic oil displacement efficiency" of the enriched gas. As known[7] , the efficiency of a displacement process is quantified by the oil recovery factor (E_R), which is defined as the ratio between the volume of oil produced and the volume of oil initially present in the reservoir rock. It depends on the volumetric invasion efficiency (E_V) and the displacement efficiency (E_D) or microscopic efficiency. The oil recovery factor is expressed as the product of macroscopic efficiency multiplied by microscopic efficiency. E_V is evaluated by numerical models, while E_D is determined at core scale using lab experiments described in the following section.

Selection of the Rock Samples: Since no core of the reservoir main area (Upper Nubian Sandstone) was available for this study, some cores of a peripheral well, which was recently drilled for another reason, were used.

A detailed petrographic and sedimentological study was performed in order to recognize the typical facies of the main reservoir area of the Abu Attiffel field. The study showed that the less cemented samples tend to show the best permeability. Moreover, a pore network study enables us to conclude the following:

1) Samples with permeability over 100 md were

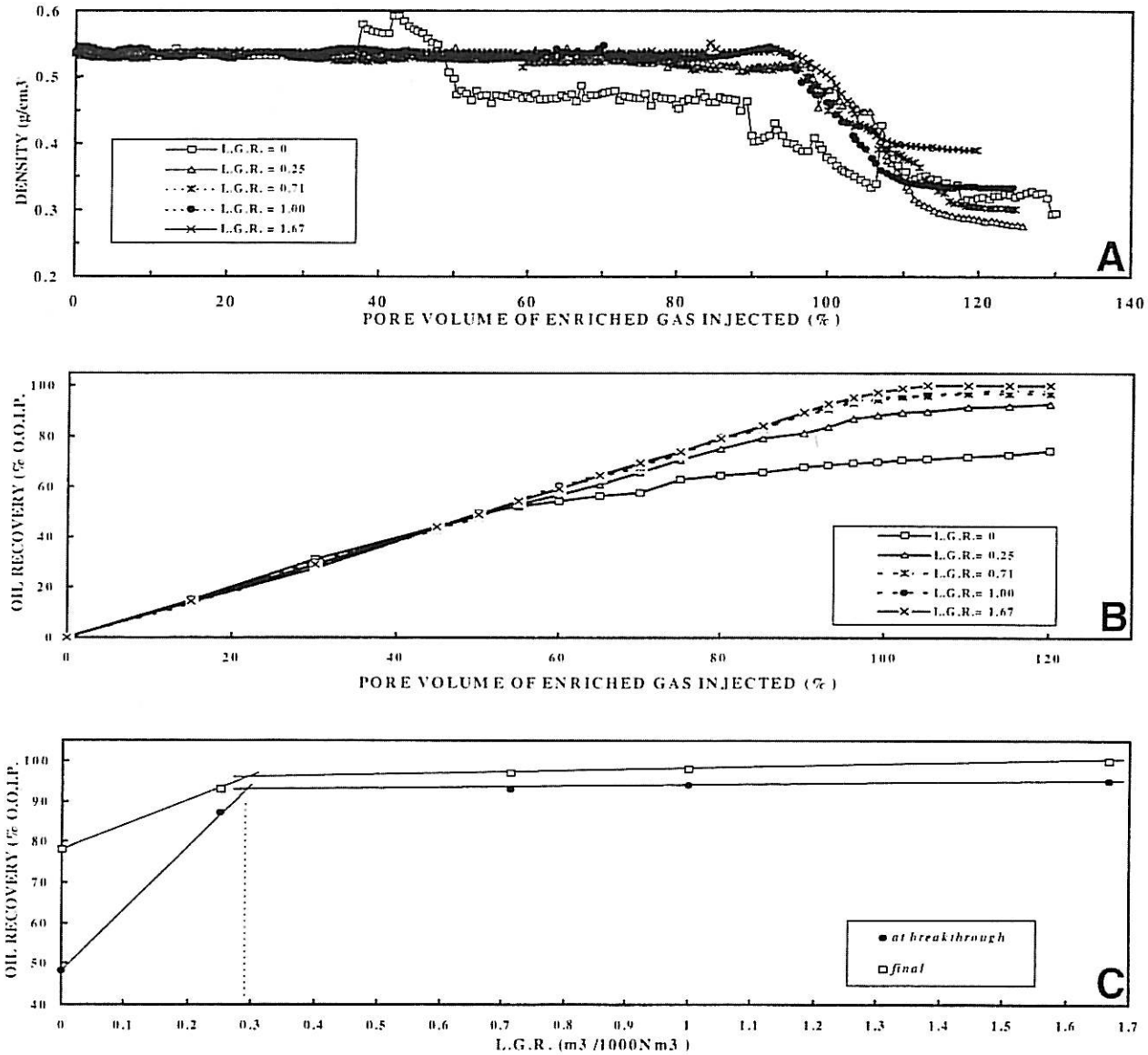


Fig. 7. Effluent density, oil recovery and M.M.E. determination.

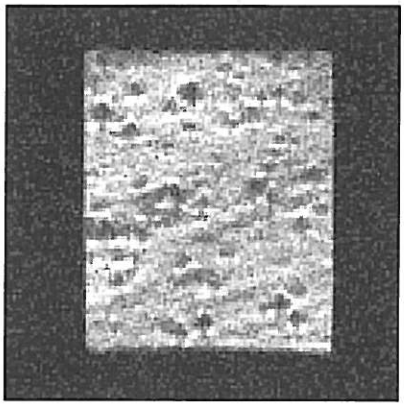
characterized by well- connected, large primary pores and relatively high porosity, with a low content in total authigeneses (quartz overgrowths, kaolinite and chlorite).

2) Samples with permeability ranging from 10 to 100 md were largely influenced by sedimentological features such as cross lamination. Along these features, stronger quartz cementation, more abundant pore-filling kaolinite and compaction-enhancing clay drapes were often observed; this deteriorates the pore structure which creates permeability barriers on a microscale.

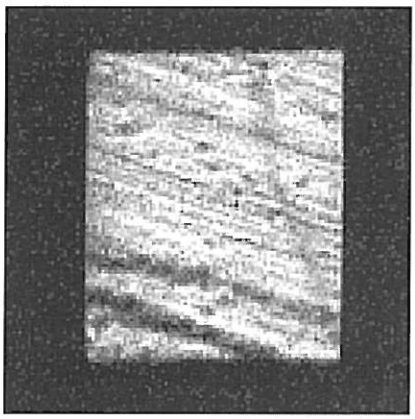
Finally, a routine core analysis study was performed on plugs of 5 cm diameter and 5-6 cm length. After saturating the selected plugs with water, Nuclear Magnetic Resonance Imaging equipment (MRI) was used to evaluate the type of heterogeneity of their internal texture and fluid distribution, without destroying them.

Analysis of the MRI images (the white zones of the images show the greatest water saturation. Water saturation decreases as the colour changes from white to black) highlighted four types of rock samples among the selected plugs:

- *Type 1. Homogeneous samples with subrounded non-porous zones.* The texture observed is probably due to cementation by patchy carbonates, commonly observed in Upper Nubian Sandstones; the other possibility is the presence of large-size quartz grains, but this is less likely, considering the normal grain-size of sandstone(Fig. 8).



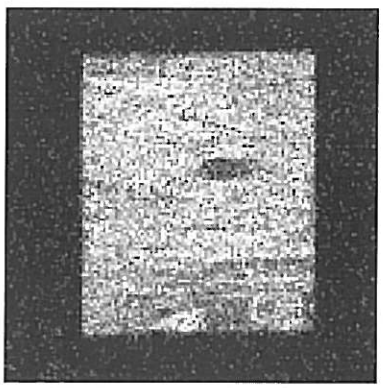
Quartz+heavies	82 %
Feldsparts	0.5 %
Pseudo matrix	0.5 %
Quartz overgrowth occlusive	1.5 %
Quartz overgrowth part. occlusive	3 %
Carbonate occlusive	1 %
Chlorite	3 %
Kaolinite	8.5 %



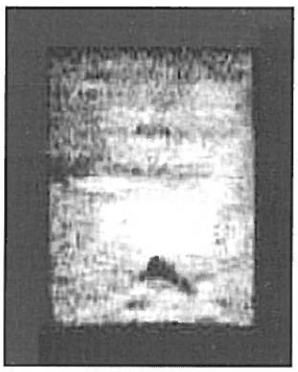
Quartz+heavies	77.5 %
Orthomatrix	1 %
Matrix rim	0.5 %
Quartz overgrowth occlusive	2 %
Quartz overgrowth part. occlusive	14.5 %
Kaolinite	4.5 %

Fig. 8. MRI images of rock type 1 and 2.

- *Type 2. Laminated samples.* The cross lamination, which is either well- developed or barely visible, is highlighted by more or less saturated laminae; this is due to a reduction in grainsize and the presence of depositional or diagenetic clays which produce a local permeability barrier. The presence of laminae with very low fluid saturation may be due to the preferential precipitation of carbonate cements along these laminae. This is also demonstrated by the precipitation of carbonate cements along these laminae. This is also demonstrated by the occurrence of subrounded non-porous zones in the laminae (Fig. 8).
- *Type 3. Homogeneous sample.* Only faint depositional structures are present and saturation is fairly homogeneous. The dark, isolated, low-saturated structure is probably a clay clast (Fig. 9).
- *Type 4. Heterogeneous rock with crude lamination.* This type of sample is quite common at the basal part of fluvial cycles, where uniformity of grainsize, cementation and occurrence of clay clasts is at a maximum. High porosity zones with very large pores can be isolated into a relatively



Quartz+heavies	78 %
Quartz overgrowth occlusive	2.5 %
Quartz overgrowth part. occlusive	18.5 %
Kaolinite	1 %



Quartz+heavies	67.5 %
Orthomatrix	32.5 %

Fig. 9. MRI images of rock type 3 and 4.

less porous network with non-porous zones due to clay clasts or cementation (Fig. 9).
All the samples were water-wet.

OIL DISPLACEMENT TESTS

Experimental Procedure: All the oil displacements using water and enriched gas were carried out at a high pressure and high temperature rig shown in figure 10[8]. The selected core plugs were washed and saturated with formation water (209 g/l salinity) and brought to irreducible water saturation conditions using a synthetic oil and centrifugation. After MRI analysis all the samples were mounted in a suitable high pressure and high temperature core-holder inserted in a thermostatic air bath. 5-10 pore volumes (PV) of recombined oil were pumped through the plug at a flow rate (which varied according to the petrophysical parameters of the sample) of 2.4-3.2 m/day in order to measure the oil permeability under residual water saturation (Swi).

All the displacements were carried out under a capillary regime[9,10] in order to simulate the flow rate present in the bulk of the formation as accurately as possible under the current reservoir conditions. For the fluids being studied, interfacial tension and density values at reservoir temperature and at different pressures were experimentally determined. Table 3 shows the results obtained. In particular, the interfacial tension between water-oil, gas-water and gas-oil systems was determined using "pendant drop apparatus" [11,12] .

Water Injection: The oil recovery through water injection and water-oil relative permeability was determined following an unsteady state method, whereby water was injected (10-20 PV) at the same flow rate as recombined oil, and oil production and pressure drop at the core ends were recorded. The relative permeability values at the end points were directly calculated from experimental data. The relative permeability curves were obtained using a calculation code based on an implicit method developed by Watson[13] .

Enriched Gas Injection: In the case of oil displacements using enriched gas, the following three different rock saturations were simulated:

- *Residual oil saturation (to simulate complete water-flooded zones).* To obtain these experimental conditions, the enriched gas was injected through samples which were previously flooded by water.
- *About 50% of oil saturation (to simulate zones under the current average oil saturation).* The plugs in Swi conditions were saturated with recombined oil. A known volume of water was injected in order to obtain the desired oil saturation. Finally, enriched gas was injected.
- *Irreducible water saturation (to simulate non-water-flooded zones).* To simulate these reservoir zones, the core plug brought to Swi conditions was saturated with recombined oil and then flooded with enriched gas.

RESULTS

Oil Displaced by Water: The scope of this step was to estimate residual oil saturation after the water-flooding process using more realistic conditions (reservoir conditions) than possible, when the conventional laboratory approach is adopted. The resultes of five tests are given in Table 4.

The lowest oil recovery, after the water-flooding process, of sample 41 (rock type 2) was due to its rock texture characterized by low permeability layers.

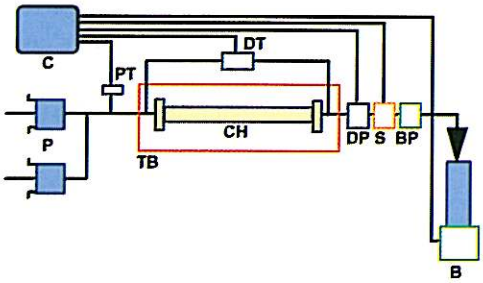
These results were compared with those obtained under laboratory conditions in previous petrophysical studies. As figure 11 shows, the final oil recovery obtained during tests under reservoir conditions was lower. The main conclusion drawn was that the efficiency of the water-flooding process under

Table 3. Interfacial tension between different systems.

Pressure	Oil		Enriched gas		Interfacial tension (mN/m)		
(MPa)	Density kg/m³	Viscosity (mPa. s)	Density kg/m³	Viscosity (mPa.s)(°)	Oil-water	Gas-water	Gas-oil
47.6	562.5	0.23	297.5	0.0386	24.0	32.3	<0.1(°°)
44.2	557.8	0.22	286.5	0.0367	25.2	33.4	<0.1
41.8	553.4	0.21	-	-	-	34.5	-
41.1	552.1	0.20	275.1	0.0349	27.0		<0.1

Table 4. Results of oil displaced by water.

Oil recovery									
Sam. no.	Pore Volume (ml)	Liquid perm. (md)	Swi (%)	Sor (%)	@Break-through (%)	Final (%)	Kro @Swi	Krw @Sor	Capillary number (Nc)
41	13.41	53	18.6	31.9	43.1	60.85	0.007	0.011	$4.33*10^{-8}$
170	15.78	37	10.4	16.6	66.5	81.43	0.4	0.39	$3.67*10^{-8}$
34	14.58	39	4.1	20.4	64.4	79.59	0.3	0.16	$3.98*10^{-8}$
37	15.37	18.3	16.6	19.9	39.0	76.62	0.062	0.042	$3.78*10^{-8}$
63.5	13.10	5.7	7.1	27.8	54.2	70.33	0.95	0.82	$4.45*10^{-8}$



S fluid separator
BP back pressure regulator
B balance
C computer
PT pressure transducer
P pump
TB air thermostatic bath
CH core holder
DT differential pressure transducer
DP digital densimeter

Fig. 10. Sketch of the experimental flooding rig.

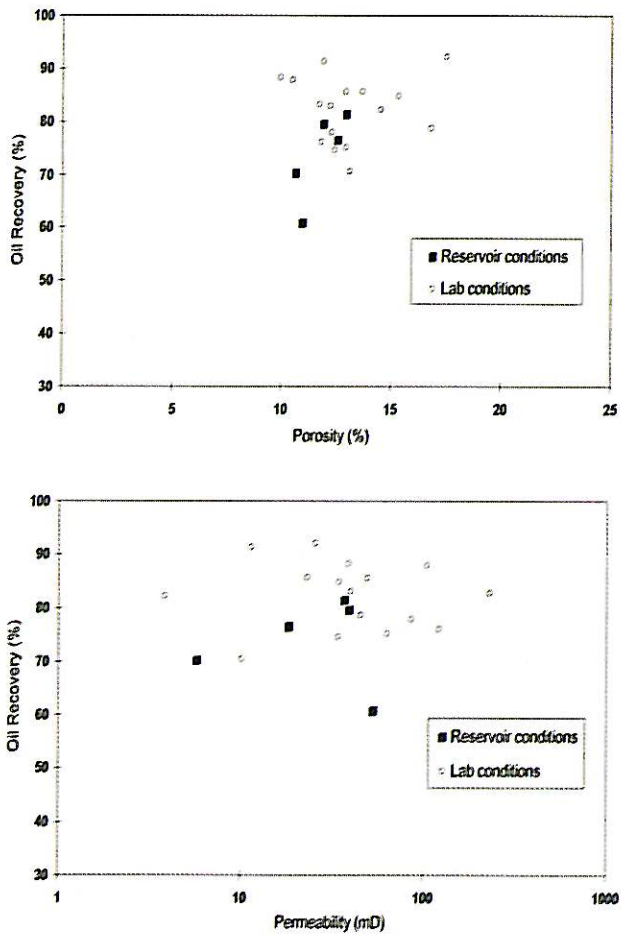


Fig. 11. Oil recovery by water-flooding *vs.* porosity and permeability.

reservoir conditions was poorer than that obtained following the conventional approach.

Oil Displaced by Enriched Gas: Four tests were carried out for each of the three different oil saturations which characterized the rock samples at the beginning of gas injection.

Samples under residual oil saturation. The main results obtained are summarized in Table 5. The following points characterized these oil displacements:

- the final oil recovery was achieved after the injection of less than 1.5 PV of enriched gas and its value was greater than 95% in samples with the lowest permeability;
- oil production began after significant water (mobile phase) production. Figure 12 shows an example where the cumulative fractions of oil and water produced are plotted together with the cumulative gas produced (associated and injected gasses);
- gas stripping of the oil intermediate components (C_{13}-C_{19}) took place in all the displacements;
- samples with greater liquid permeability had an early gas breakthrough with a consequent low oil recovery value (less than 75%);
- rock heterogeneity greatly influenced additional oil recovery; the most homogeneous samples gave the lowest oil recovery compared to other more heterogeneous ones, probably because the residual oil was spread over a larger rock volume;

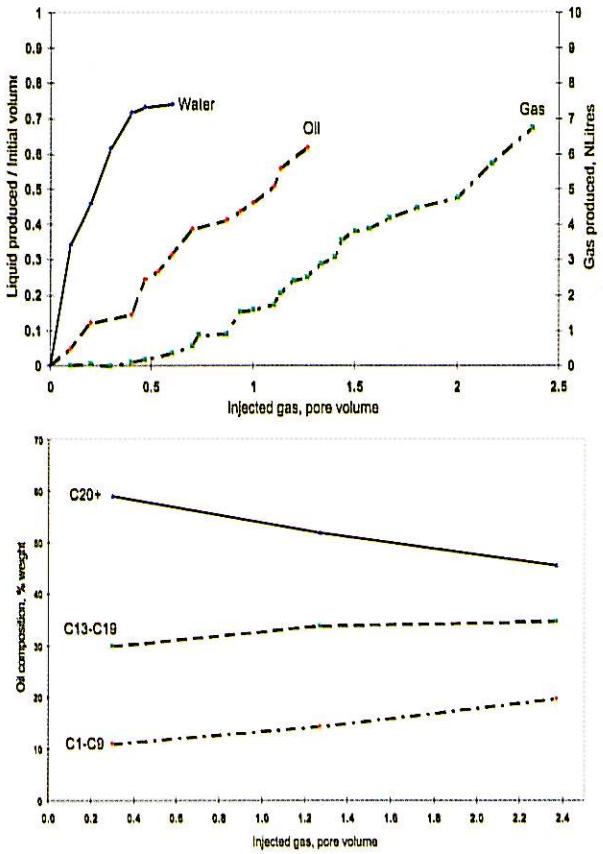


Fig. 12. Rock sample under residual oil saturation: oil displacement by gas, fluid production and composition of produced oil.

- the volume of enriched gas needed to cover a unit volume of reservoir ranged from 11,400 to 1,900 Nm^3/m^3, which, at reservoir conditions, considering a deviation factor (z) of the gas of 1.0834, became 5.3-7.5 m^3/m^3.

Samples under intermediate oil saturation. The oil displacement results are shown in Table 5. The following conclusions were drawn:

- final oil recovery ranged from 63 to 97% within a 1 PV of enriched gas injected;
- water production began before oil, probably because of a more favorable relative permeability of the gas-water system compared to gas-oil system (the rock was water-wet). Figure 13 shows an example where the cumulative fractions of oil and water produced are plotted together with the cumulative gas produced (associated and injected gasses).
- gas stripping of oil intermediate components took place in all displacements;
- the composition of the gas flashed from the oil produced showed an enrichment of light components (C_1-C_9);
- two displacements, carried out on cores in vertical position, gave an incremental oil recovery which ranged from 3 to 8%;

Table 5. Oil recovery after the injection of the enriched gas.

Sample no.	Rock type	Porosity (%) @Reservoir conditions	Liquid perm. (md) @Reservoir conditions	Oil saturat. (%) @Reservoir conditions	Gas volume Reservoir oil vol. (Nm^3/m^3)	@Reservoir conditions	Final oil recovery (% OIP)
Residual oil saturation (Sor)							
170	1	12.9	37.0	16.6	1944	7.44	74.43
63.5	1	10.6	6.0	27.6	1382	5.29	95.5
34	3	11.9	39.0	27.6	1743	6.67	61.7
37	2	12.5	18.0	21.5	1479	5.66	95.5
Intermediate oil saturation (So 50%)							
170	1	12.9	37.0	40.4	1036	3.96	63.1
70	2	11.6	31.0	51.2	466	1.78	95.3
68	2	12.8	7.0	51.7	457	1.75	88.5
151.8	2	12.4	16.0	49.1	565	2.16	96.9
68 Vert.	2	12.9	7.0	47.9	539	2.06	91.0
170 Vert.	1	11.6	37.0	46.8	922	3.53	68.4
Irreducible water saturation (Swi)							
32	4	10.9	30.0	88.5	482	1.84	94.1
100	2	12.7	15.0	93.5	349	1.34	98.0
66.5	1	10.4	33.0	82.8	474	1.81	99.1
193.5	1	12.6	55.0	93.5	288	1.10	99.0

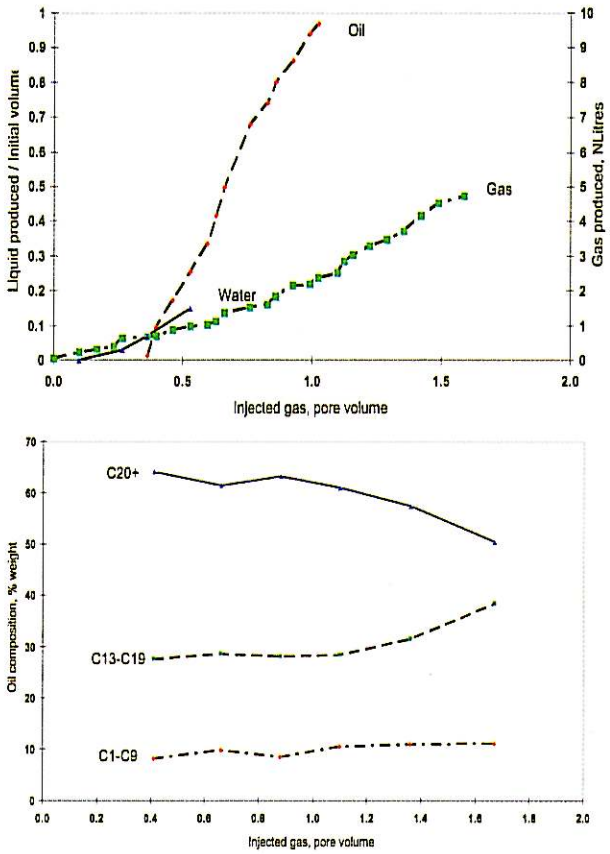


Fig. 13. Rock sample under intermediate oil saturation: oil displacement by gas. Fluid production and composition of produced oil.

- the volume of enriched gas needed to cover a unit volume of reservoir ranged from 450 to 1050 Nm^3/m^3, which, at reservoir conditions, considering a deviation factor (z) of the gas of 1.0834, became 1.70-4.0 m^3/m^3.

Samples under irreducible water saturation. The oil displacement results were shown in Table 5. The following conclusions were drawn:

- final oil recovery exceeded 94% in all the tests and is not greatly influenced by petrophysical parameters and rock texture. Figure 14 shows an example where the cumulative fraction of oil produced is plotted together with the cumulative gas produced (associated and injected gasses);
- gas stripping of oil intermediate components took place in all displacements;
- the composition of the gas flashed from the oil produced showed an enrichment of light components (C_1-C_9);
- the volume of enriched gas needed to cover a unit volume of reservoir ranged from 300 to 500 Nm^3/m^3, which, at reservoir conditions, considering a deviation factor (z) of the gas of 1.0834, became 1.1-1.9 m^3/m^3.

The volume of enriched gas injected needed to recover a unit volume of reservoir oil was plotted against the oil saturation of the rock. In figure 15 the values with oil recovery greater than 90% have been highlighted. As one can see, the oil recovery values of rock samples with low oil saturation are greatly affected by rock heterogeneity. This means that, at field scale, the microscopic efficiency of oil displacement using enriched gas for well water-flooded zones (near Sor conditions) will be difficult to estimate, without good knowledge of the rock textures of these zones. For non-water-flooded zones, we can estimate that a 1 m^3 of reservoir oil volume to be recovered will require less than 400 Nsm^3/m^3 of enriched gas with an E_D value greater than 90%.

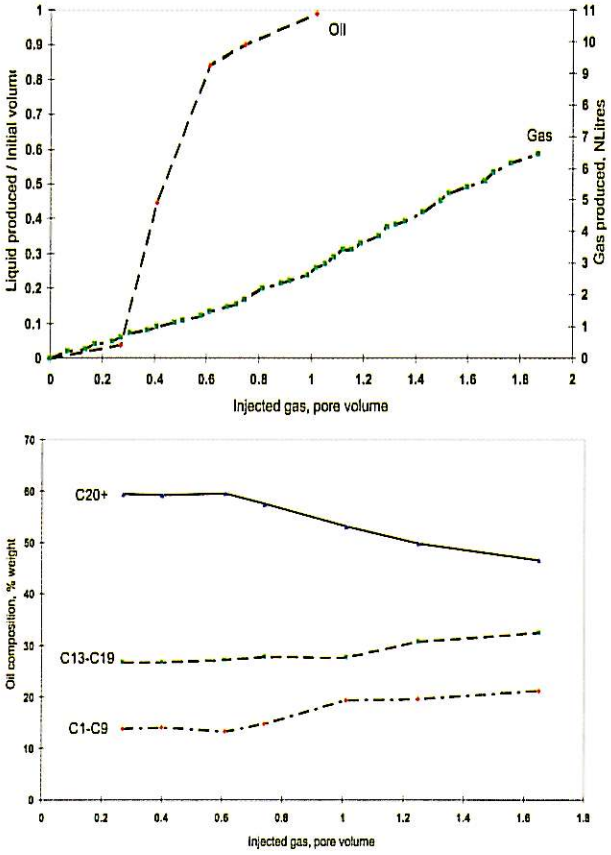


Fig. 14. Rock sample under irreducible water saturation: oil displacement by gas. Fluid production and composition of produced oil.

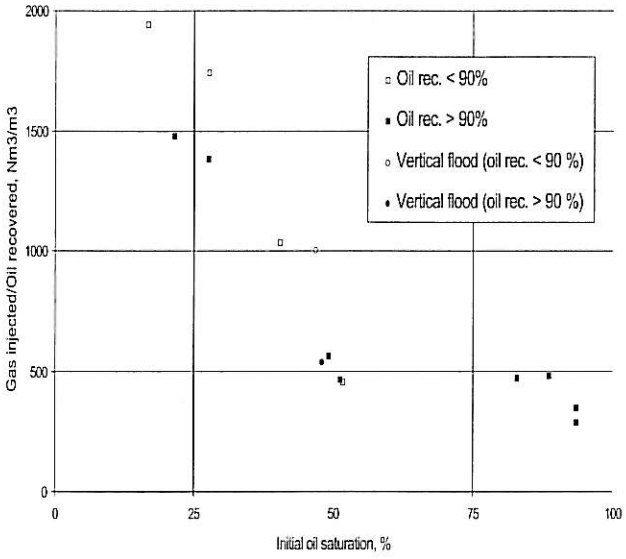


Fig. 15. Gas volume required to recover one cubic meter of reservoir oil at different oil saturations of the rock.

CONCLUSIONS

The behavior of three injectants, potentially available in the area, was investigated under Abu Attiffel reservoir conditions, namely:

Carbon Dioxide. It does not appear as the most suitable solvent for field applications. In fact, it developed miscibility, even though at a pressure level (42.9 MPa) a little higher than the current reservoir pressure (40.5 MPa), with precipitation of heavy paraffins noticed both during the displacements in slim tube and the swelling tests. Moreover, a large corrosion took place in some parts of the lab. equipment. The handling of these problems at field scale should affect considerably the operating costs.

Lean Gas. It is still an inadequate solvent because it becomes miscible only at 48.1 MPa, a pressure even higher than the original one (47.6 MPa). Moreover, paraffin precipitation and corrosion were again noticed during the experiments.

Enriched Gas. Obtained vaporizing LPG, available on the field, in the lean gas. With an enrichment of 290.3 m^3/ Msm^3 miscibility was attained by condensing/vaporizing gas drive. Unlike the two other solvents, neither paraffin precipitation nor corrosion occurred in all the tests, therefore this injectant was retained for future field applications.

Most of the tests presented a very high oil recovery value, which means a high efficiency of oil displacements using enriched gas.

Owing to miscibility between oil and enriched gas, gravitational forces only partly influenced final oil recovery, whereas the rock's internal rock texture greatly influenced oil recovery when residual oil saturation conditions were reached in the formation. For higher oil saturations, the rock texture effect was far less evident.

The enriched gas volume needed to recover a unit volume of oil under reservoir conditions was estimated at between 2,000 Nm^3/m^3 (minimum oil saturation – Sor) and 300 Nm^3/m^3 (maximum oil saturation – Swi).

The highest value of final oil recovery through enriched gas injection was obtained under irreducible water saturation conditions.

Finally, as one would expect, comparison of the results of the oil displacement tests by water and by enriched gas, carried out under Swi rock conditions, shows that enriched gas injection was more efficient than water injection in terms of the "microscopic displacement efficiency". In fact, oil recovery for enriched gas injection reached 99% against about 80% (maximum) for water-flooding.

ACKNOWLEDGEMENTS

The authors thank the management of Agip Oil, Libyan Branch, and ENI (Agip Division) for their permission to publish this paper. They extend their appreciation to all the colleagues at the Corporate E&P Laboratories who contributed to this work.

REFERENCES

[1] Erba, M. *et al.*, 1983. Bu Attiffel Field – A synergetic geological and engineering approach to reservoir management, paper PD6 presented at 11th World Petroleum Congress, London.

[2] Safsaf, S.R. and Michelotti, G., 1985 (April 16-18). Improved oil recovery by water flooding in Libyan oil fields operated by Agip (N.A.M.E.) Libyan Branch, paper presented at 3rd European Symposium on IOR, Rome.

[3] Causin, E., Radaelli, F., Terzi, L. and El-AGeli, I.S., 1997 (October 20-22). Bu Attiffel field (Libya): Gas Injection Project – laboratory approach, paper EAGE 038 presented at 9th European Symposium on Improved Oil Recovery, The Hague, Netherlands.

[4] Yellig, W.F. and Metcalfe, R.S., 1980. Determination and prediction of CO_2 minimum miscibility pressure, *JPT*, 160-68.

[5] Godbole, S. P., Thele. K. J., and Reinbold, E. W., 1992 (October 4-7). EOS modeling and experimental observation of three-hydrocarbon-phase equilibria, paper SPE 24936 presented at 67th Annual Technical Conference and Exhibition, Washington.

[6] Zick, A. A., 1986. A combined condensing/ vaporizing mechanism in the displacement of oil by enriched gas, paper SPE 15493, presented at 61st Annual Technical Conference and Exhibition, New Orleans, LA.

[7] Chierici, G. L., 1994. *Principles of Petroleum Reservoir Engineering* **–2**, Springer-Veralg.

[8] Causin, E. and Rossi, E., 1995 (15-20 June). Relative permeability at reservoir conditions, paper presented at THERMIE Workshop on IOR and EOR Technology in Europe, Beijing and Urumqi, China.

[9] Mohanty, K. K. and Miller, A. E., 1991(September). Factor influencing unsteady state permeability of a mixed-wet reservoir rock, SPEFE, 349-358.

[10] Schechter, D. S. *et al.,* 1994. Low IFT drainage and imbition, *J. Petr. Science and Eng.*, 283-300.

[11] Andreas, J. M. *et al.*, 1938. Boundary tension by pendant drop. *J. Phys. Chem.*, 1001.

[12] Hansen, F. K. and Rodshrud, G., 1991 (January). Surface tension by pendant drop. I. A fast standard instrument using computer image analysis. *J. Coll. Int. Sci.*

[13] Watson, A. T., *et al.*, 1988 (August). A regression-based method for estimating relative permeabilities from displacement experiment, *SPERE*, 953-958.

Petroleum Res. J. Vol. 14 (2002): P. 83–92, 9 Figs.

The Mabruk History or How to Develop a Challenging Field

Daniel Chaussumier* and Benoît Ludot**

تاريخ حقل المبروك أو كيف يتم تطوير تحديات الحقل

دانيل سوزيومايير و بينوت لادوت

يتكون حقل المبروك الواسع من أربعة تراكمات للنفط بغربي حوض سرت الرسوبي وتوجد أفضل خصائص المكمن بحقل المبروك، غرب، حيث أنه الحقل الوحيد قيد التطوير حالياً.

تتكون صخور المكمن بالحقل من رواسب جيرية على عمق حوالي 3500 قدم، ترجع إلى عصر الباليوسين. وقد سلطت الدراسات الجيولوجية الضوء على الإختلافات الحادة بين سحنات مفصولة ومعقدة نتج عنها التعرف على العديد من الصخور وأكثر من عشرة أسطح تماس بين الماء والزيت. ونظراً لضآلة سمك المكمن (45 قدم) والنفاذية فإن قابلية الإنتقال منخفضة، كما أن أداء الآبار العمودية بصفة عامة ضعيف جداً.

توالت عدة شركات مشغلة لهذا الحقل منذ نهاية الخمسينات ولكن البداية الفعلية كانت عام 1995 ف مع شركة CPTL كمشغل. وشمل البرنامج التطويري لهذا الحقل مرحلة النموذج التجريبي والتي استغرقت مدة سنتين قبل الإنتهاء من برنامج النضوب. وتم حتى فترة إنعقاد هذا المؤتمر (1999) إستخراج حوالي 16 مليون برميل، ويصل المعدل الحالي للإنتاج حوالي 15000 برميل يومياً يتم إستخراجها من 35 بئر إنتاجية. كما يتم المحافظة على ضغط المكمن بحقن الماء عن طريق 23 بئر. وللتعامل مع الإنتاجية الضعيفة وعدم التجانس العالي تم إستعمال تقنيات حفر متطورة متعددة الصرف والضخ (Esp, PcP).

بدأت محاكاة المكمن للتنبأ بالمناطق ذات المردود المتدني، ويستعمل تنعيم المحاكاة الشبكي لتمثيل المعالم الجيولوجية بطريقة تؤثر تأثير على أداء المكمن.

Abstract: *The Great Mabruk field is made up of four oil accumulations located in the Sirt Basin. West Mabruk, where the best reservoir characteristics were encountered, is the only one currently developed.*

The reservoir, located at a depth of 3500 feet, is made up of carbonates of Palaeocene age. The geological studies highlight steep variations of facies together with a complex compartmentalization, resulting in the definition of numerous rock types and more than ten oil water contact (OWC).

Owing to the small thickness (45') and owing to permeability, the transmissibility is low and the performance of vertical wells is generally very poor.

Since the late fifties several companies have followed one another as operator but the real start-up of the field took place in 1995 with CPTL as operator. The development included a two-year ‹‹pilot›› phase prior to finalizing the depletion scheme. To date almost 16 million stb have been recovered and the current rate is around 15000 bopd from 35 producers. Reservoir pressure is maintained by 23 water injectors.

Sophisticated techniques concerning drilling (multi-drains) and pumping (PCP, ESP) were pioneered to cope with the low productivity and

* Totalfina,
** CPTL

the high heterogeneity. Reservoir simulation was initiated to predict the areas to be poorly swept. Fine simulation grids are used to represent geological features in a way that captures their impact on reservoir performance.

BRIEF REVIEW OF THE HISTORY

The Great Mabruk field is made up of four oil accumulations located in the Sirt Basin (Libya), namely North Mabruk (discovery well #1), Central Mabruk (discovery well #2), East Mabruk (discovery well #3) and West Mabruk (discovery well #6). Figures 1 and 2 show the location of the field and of the different panels.

It is noteworthy that West Mabruk, which was the last to be discovered, is the only one currently developed. This suggests that the characteristics encountered in the other three were really discouraging. Effectively several companies have followed one another as operator since the late fifties.

Between 1959 and 1961, Exxon drilled 26 wells and implemented a five spot water injection pilot in the NE part of West Mabruk. Following corrosion problems and early water breakthrough (250 m spacing), they gave up rapidly.

Sirt Oil resumed the development in 1982, shot a 3D seismic, drilled four wells and abandoned. Since the beginning, the original oil in place (OOIP) estimate decreased from 1 Gstb (including 0.6 Gstb in West Mabruk) to half of this value.

However TOTALFINA, SAGA and the National Libyan Oil Corporation (NOC) were not put off by the challenge. The subsidiary CPTL was created and the real start-up of the field took place in 1995 with CPTL as operator. The development included a two-year ‹‹pilot›› phase prior to finalizing the depletion scheme.

To date around 16 million stb have been recovered from West Mabruk. The current rate is 15000 bopd from 35 producers. Pressure maintenance is ensured by 23 water injectors. A large part of the wells (all the recent ones) are horizontal or multi rains. With some additional wells, the recovery is expected to reach 125 million stb for a water cut of 90%, 29% OOIP. Moreover, it is planned now to shoot a 3D seismic in the East and Central Mabruk accumulations with the objective of launching the development of these panels.

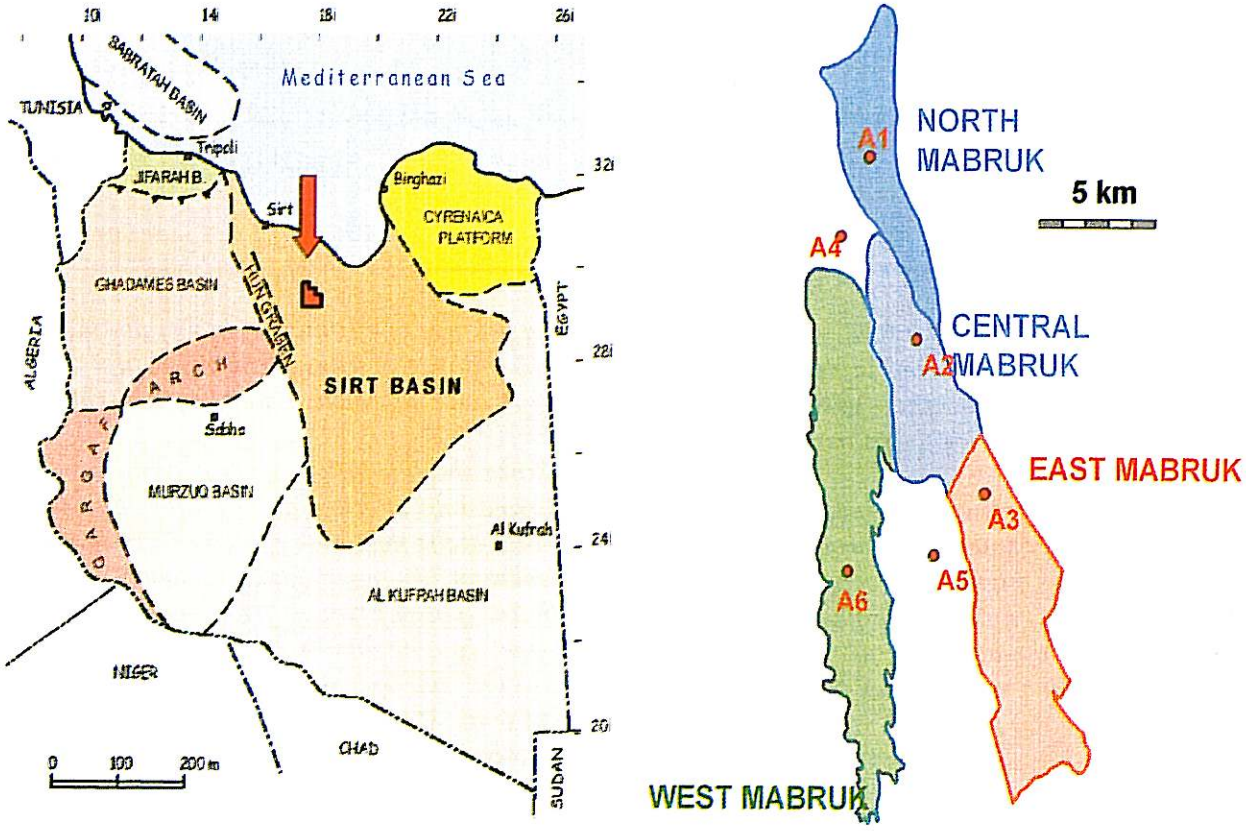


Fig. 1. Location map.

The purpose of this paper is to describe the problems posed by these fields and how the determination of three companies got over them.

GEOLOGICAL BACKGROUND

The reservoir is located at a depth of 3500' (3000 feet ss, 900 mss). It is made of carbonates pertaining to the so-called upper Mabruk member of the Heira Formation, of Palaeocene age, which overlies the Dahra Formation (Upper Cretaceous).

The structure is an elongated NS anticline truncated by numerous NW/SE faults (Fig. 2). The dip is low (around 3° on the flanks). The hydrocaron column does not exceed 500 feet (150m) and the oil accumulation extends over a surface of roughly 15 km x 3 km.

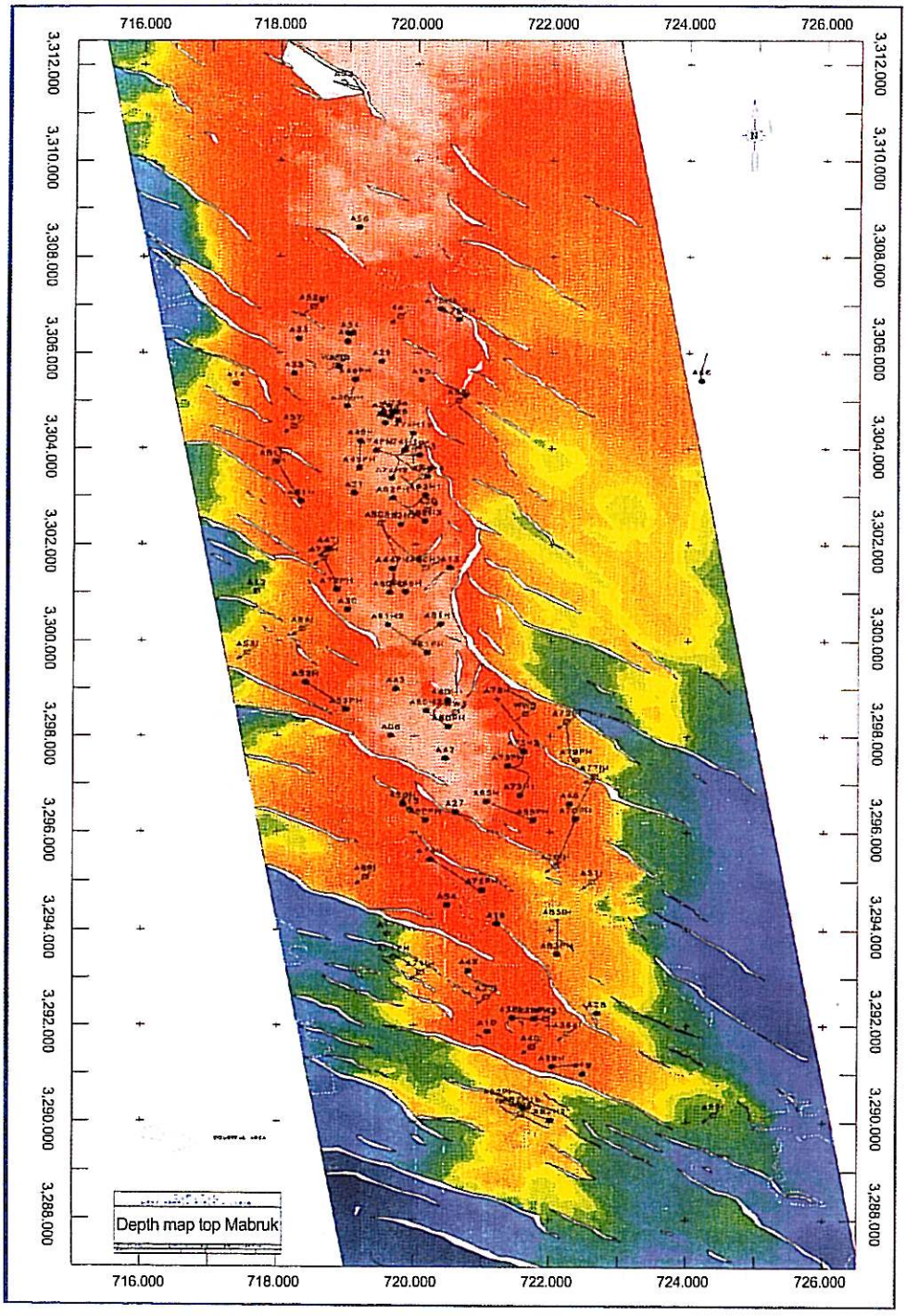


Fig. 2. Structural map at top Upper Mabruk.

The interpretation of the 3D seismic, shot in 1982, proved very difficult and some parts of the structure (crest and eastern flank) have remained "blind" for years,. It is only the use of recent tools (correlation maps) that allowed an interpretation everywhere (interpretation supported by the drilling of new wells in the "blind zones").

However, significant uncertainties concerning the structure and the fault pattern are still remaining today. Among other things, it is not possible to assess definitely the number of isolated panels from the current seismic data.

The gross thickness of the reservoir averages 90 feet (27 m), distributed in three layers: from top to bottom, A2, B and C (Fig. 3). The C layer exhibits much poorer properties (very low N/G) than A2 and B, which both contain most of the oil in place. The average net thickness is 45 feet (14 m).

The facies changes from the north (micritic skeletal limestone) to the south (dolomitic limestone). In fact, the Mabruk reservoir is characterized by its heterogeneity resulting in sharp facies changes.

Porosity, which varies between 16% and 30%, averages 23% over the field. It decreases from the crest to the flanks.

There is no clear relationship between porosity and permeability. Estimated from test data, permeability is generally low: median around 20 mD. However it can be enhanced locally owing to fissuring. The permeability thickness varies among the tested wells between 0.1 D.foot and 15 D.feet, the median being 1 D.foot.

PVT AND OOIP

Oil samples were taken in two wells, located at both ends of the field, north and south. In both cases, the oil is largely undersaturated with a dissolved GOR of only 5 v/v. Bubble point is 130 psi for an initial pressure of 1180 psig at 2530 feet ss (81 bars at 771 mss). However, the oil seems lighter in the south (39.4°API) than in the north (34.7°API). This has an impact on the viscosity, which is higher (3cp) in the north than in the south (2cp). The reservoir temperature is 135°F (57°C). The initial oil FVF is 1.05 v/v and the compressibility 9.1 10^{-6} psi^{-1}. The formation water has a rather high salt content (TDS=63 g/l). Its viscosity is 0.5 cp.

As explained above, the compartmentalization of the field is complex. A consequence is that no less than eleven different OWC were recognized. The OOIP of West Mabruk has been estimated at 430 million stb. The HCPV being 875 million stb this corresponds to an average connate water, saturation of 48%. The mobile oil is 276 million stb this OOIP is almost equally distributed between layer A2 (221 million stb 51%) and layer B (195, million stb, 45%). There are only 17 million stb (4%) in layer C.

DEVELOPMENT PLAN

Recap on Reservoir Characteristics: A brief review of what was described above shows that almost all the characteristics are unfavorable to a development:

- The transmissibility through the reservoir (kh/ì) is low, due to the poor permeability, the small thickness and the (relatively) high viscosity of the oil.
- The natural energy of the system is low. The compressibility is small and (almost no dissolved gas) there is no active aquifer.
- In case of water drive, the mobility ratio is higher than one.
- The reservoir is highly heterogeneous and, moreover, unpredictable. In some areas it is fractured.
- The structure is divided in many compartments.

Solutions Contemplated for West Mabruk: To cope with the difficulties described above, the following solutions were found. It is noteworthy that some of these solutions were pioneered in Libya.

- Owing to the lack of natural energy (low compressibility, no aquifer influx), the recovery process involves the implementation of a water flood. The low transmissibility implies reducing the distance between producers and injectors (to maximize the rate that can flow through the reservoir). Therefore, peripheral injection was complemented by pattern injection.
- To get decent rates per well, horizontal drains were drilled for both producers and injectors. Owing to the presence of local barriers between layers and to cater for the heterogeneous nature of the reservoir (i.e. to increase the chance to encounter a zone with good facies), some wells count several drains (up to four).
- The reservoir pressure and the well PI being low, it is important to lower the BHFP in the producers as much as possible (while keeping above the bubble point of 130 psi). Owing to the shape of

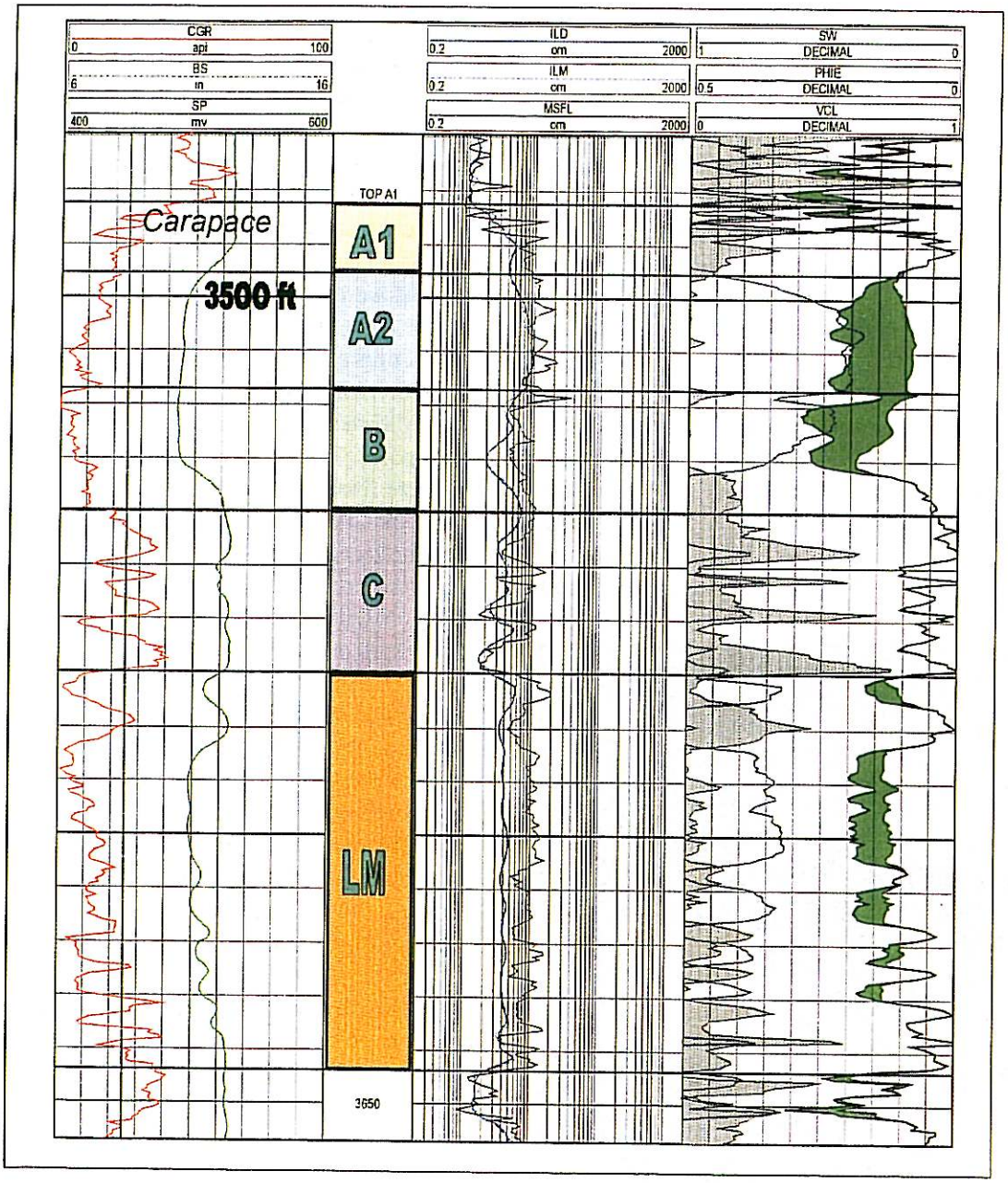


Fig. 3. Reservoir layering.

the well, it is not possible to achieve this objective while using beam pumps in horizontal wells. The use of PCP (Progressive Cavity Pumps) and ESP (Electrical Submersible Pump) allowed a significant reduction of the BHFP and an increase of the production rates.

The reservoir heterogeneity, the field compartmentalization and the low transmissibility imply planning for a large number of wells, which has a significant impact on the CAPEX and also the OPEX. Therefore it was deemed necessary to have a tool allowing the simulation of a development plan to optimise this number.

A reservoir simulator was built. It was based on the reinterpretation of the old 3D seismic (elimination of the "blind zones"). A sedimentological study was carried out to predict the facies distribution. A comprehensive SCAL work was also performed.

The reservoir model was validated through the match of the production history (pressure and water cut development by well). It was then used for the predictions and the optimization of the development plan: number, location of the wells and distribution between producers and injectors to accelerate the recovery while improving the sweep.

THE RESERVOIR MODEL

Grid and Compartmentalization: The grid of the reservoir model comprises a total of 30360 blocks (110x92x3), of which 13255 are active. it is oriented along with the main faults direction (Fig. 4). Corner point geometry was used to capture the impact of the throw of the faults on the communication within or between layers. There are three layers, corresponding to the geological units A2, B and C. The size of most cells is 160m x 160m (525 feet squared).

The field compartmentalization was reviewed with the aim of simplifying. In other barriers words, barriers were kept only when justified by pressure and/or contacts considerations. Various data concerning the OWC can be obtained from the wells: FWL (Free Water Levels, encountered in only two wells), LPO (Lowest Proven Oil) and HPW (Highest Proven Water).

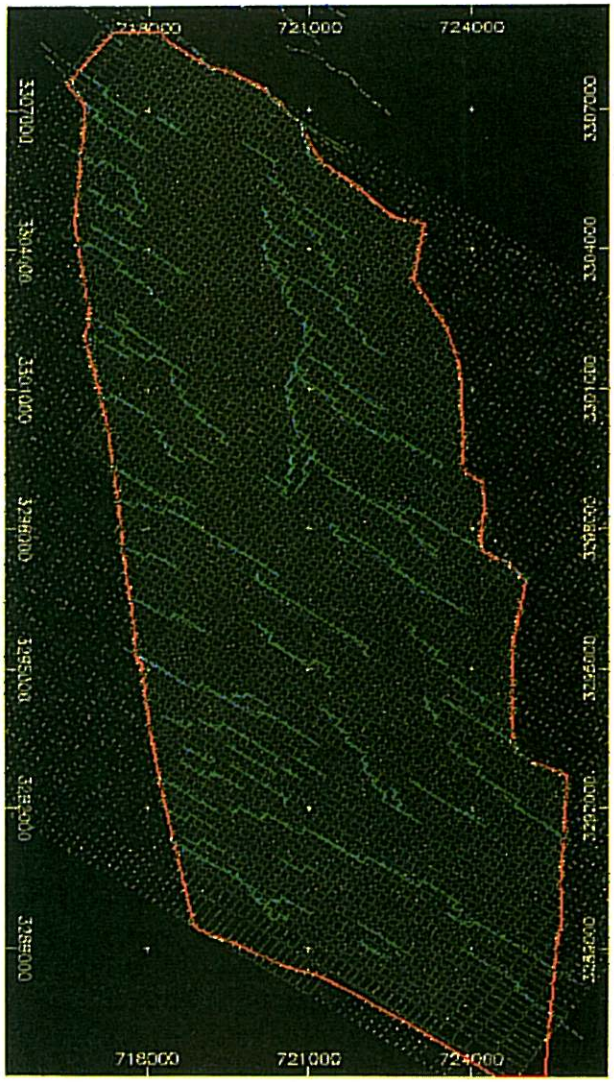


Fig. 4. Model grid.

Previously the western and eastern flanks of each panel were generally assumed to be isolated owing to differences in contacts. However pressure ,data following the field start up suggest sometimes a clear communication between both flanks. The following explanation is proposed to reconcile contacts with pressure data. It is based on the assumptions that:

- the western flanks are truncated by NW/SE barriers and the reservoir properties are vanishing westwards so that they do not communicate with the eastern flanks;
- oil migration comes from the east.

When oil fills the structure up, water is expelled from the west to the east until the WOC reaches the spill point. Thereafter, water remains trapped in the western flank and if oil continues to accumulate, the WOC will be, deeper on the eastern flank. Following this theory, it is possible to have a single panel with different contacts on both flanks provided that the, contact on the western flank correspond to the depth of the spill point.

The simplification of the compartmentalization resulted in the diminution of the number of isolated panels to five.

The oil /water contacts are identical in the three layers A2, B and C. However, they are different on both flanks of the structure. Moreover, because of the truncation of the western flanks, there may be several contacts per panel on this side. The final number of different contacts is eleven.

Petrophysics: The porosity and net/gross maps are derived from log data. There is about one control point per square kilometer.

To determine the permeability variation throughout the field it was decided to rely just on the test data. Permeability thickness could be measured in around 30 wells. This corresponds to an average distance of 1200 m between data points. Then, a mapping software was used to build a kh map.

However, this map had to be significantly altered to match the pressure history. Permeability anisotropy, with a mere 30% improvement along the SE/NW direction, proved helpful in the match of pressures and water cuts. This anisotropy can be related to the presence of natural fissures parallel to the main faults. On the whole, permeability had to be increased by about 60%. This increase can also be partly explained by a relative permeability effect: most of the tested wells are in the transition zone and what is measured is the effective permeability rather than the absolute permeability. The main features of the final kh map

are the presence of two ‹‹good›› zones at both ends of the field and a worsening towards the eastern flank. The average (absolute) permeability among the tested wells turns out to be around 60 md, which yields an average permeability thickness of 2.6 D.ft in the whole field.

A comprehensive sedimentological study was performed to describe the various facies and their distribution throughout the oil accumulation. Several lithofacies were defined. Taking into account the effects of diagenesis they became ten rock types pertaining to five categories. In every part of the field there are at least five different rock types present. On the other hand some exist only in certain areas (the south for the dolomites).

However, the difficulty in deriving reliable relationships between porosity and permeability suggests that the actual number of rock types could be largely more than ten. Then, as the number of rock types increases, another difficulty arises with the number of available plugs per rock type, which is too small to derive reliable averages.

Several solutions were tested with the model and the one which produces the best history match consists in inputting a single set of curves for capillary pressure and for relative permeabilities. Theses curves are based on a Swi of 35%. Plotted on a Swi vs ö graph together with the SCAL measurements, this value corresponds approximately to the average field porosity of 23%.

Regarding the shape of the capillary pressure curve, the analytical expression of Brooks Corey was used with a pore size distribution index(ë) of 2 and threshold pressure of 1 psi. The resulting distribution of water saturation vs depth compares reasonably well with the values derived from the logs.

As far as rel perms are concerned, the SCAL experiments, carried out on preserved cores show a mixed or oil wettability together with a fair displacement efficiency. Analytic expressions (Corey) were used, which fit the experimental points. The single set of curves is based on Swi of 35% and Sorw of 21.5%, which yields a displacement efficiency of 67%. The corey exponents are No=3 (typical of intermediate wet behaviour) and Nw=2 (typical of oil-wet behaviour).

PVT: In West Mabruk two types of oil were identified: a 34.7° API in the north and a lighter one in the south (39.4°). The main difference concerns the viscosity, which is higher (3cp) in the north than in the south (2cp). Both types of oil are displayed in the present model.

History Match: The history available for the match extends over four years since the production startup in February 1995. The data to match are the pressures and the water cut development in all the producers.

The largest effort was devoted to the match of the RFT measurements which are considered to be the most reliable among the acquired data. A fair to good match was obtained in most of the cases. Regarding RFT, it is worth mentioning that no significant pressure differential between layers was ever observed in any well, which supports the assumption of effective vertical communication.

PBU/PFO data were available for a large number of wells. The match obtained with these data does not appear as good, which can be explained by the uncertainty concerning the determination of the average pressure in the well drainage areas.

Finally, BHFP, measured through sonologs, were available for all the producers and could be matched by tuning the well productivities. However, in a few cases, we had to assume a sharp decrease of the PI with time, which can be attributed either to a local "double porosity/double permeability" behaviour[1], or to decrease in permeability close to the wellbore, due to the closure of micro fissures caused by the pressure drawdown.

A fair to good match of the water cut development was also achieved in each producer. However, at the end of May 1998, only 28% of the producers had a significant water cut for a field recovery of just above 3% OOIP.

The parameter that influences most the match is the absolute permeability. Inputting locally a SE/NW anisotropy (+30%), justified by the presence of fissures in the same azimuth, proved helpful. Figure 5 illustrates the water cut match obtained for the field.

Prediction Runs: Once validated by the history match, the reservoir simulator was used to:

- optimize the number of producers and injectors;
- define the trajectories of the multi-drains to improve the sweep efficiency;
- locate the injectors to bring an effective pressure support;
- evaluate the impact of the water injection capacity on the production profile;
- assess the reserves and determine the production profiles.

Figure 6 shows saturation maps drawn out by the model at two different times.

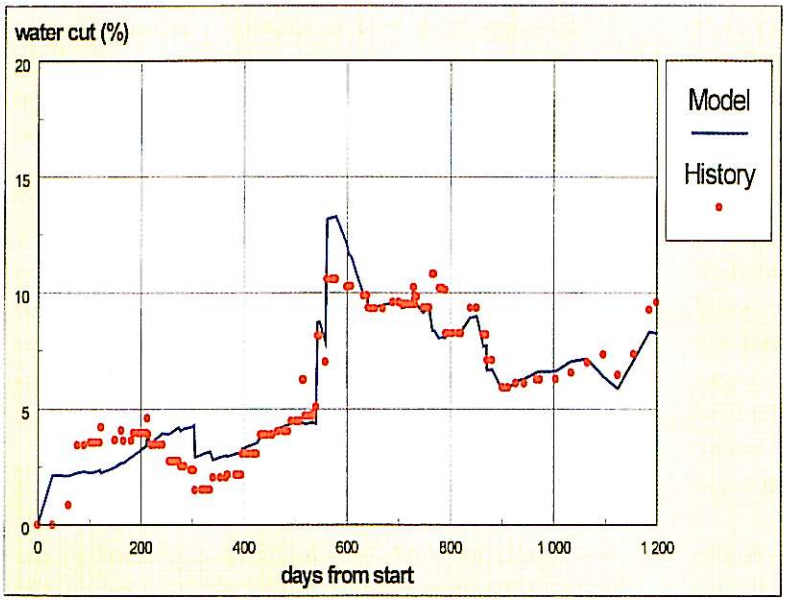


Fig. 5. Water cut match.

WELL ARCHITECTURE AND DRILLING TECHNIQUES

With the introduction of the horizontal wells in Mabruk field in 1995, TOTAL petroleum engineers faced a new challenge: conciliate the complex technology involved in the horizontal drilling and the drastic budget limitations.

TOTAL drillers, geologists and reservoir engineers worked together to select the technical options the most adapted to Mabruk requirements, helped by the worldwide experience gained by TOTAL in horizontal drilling through its subsidiaries. The different technologies

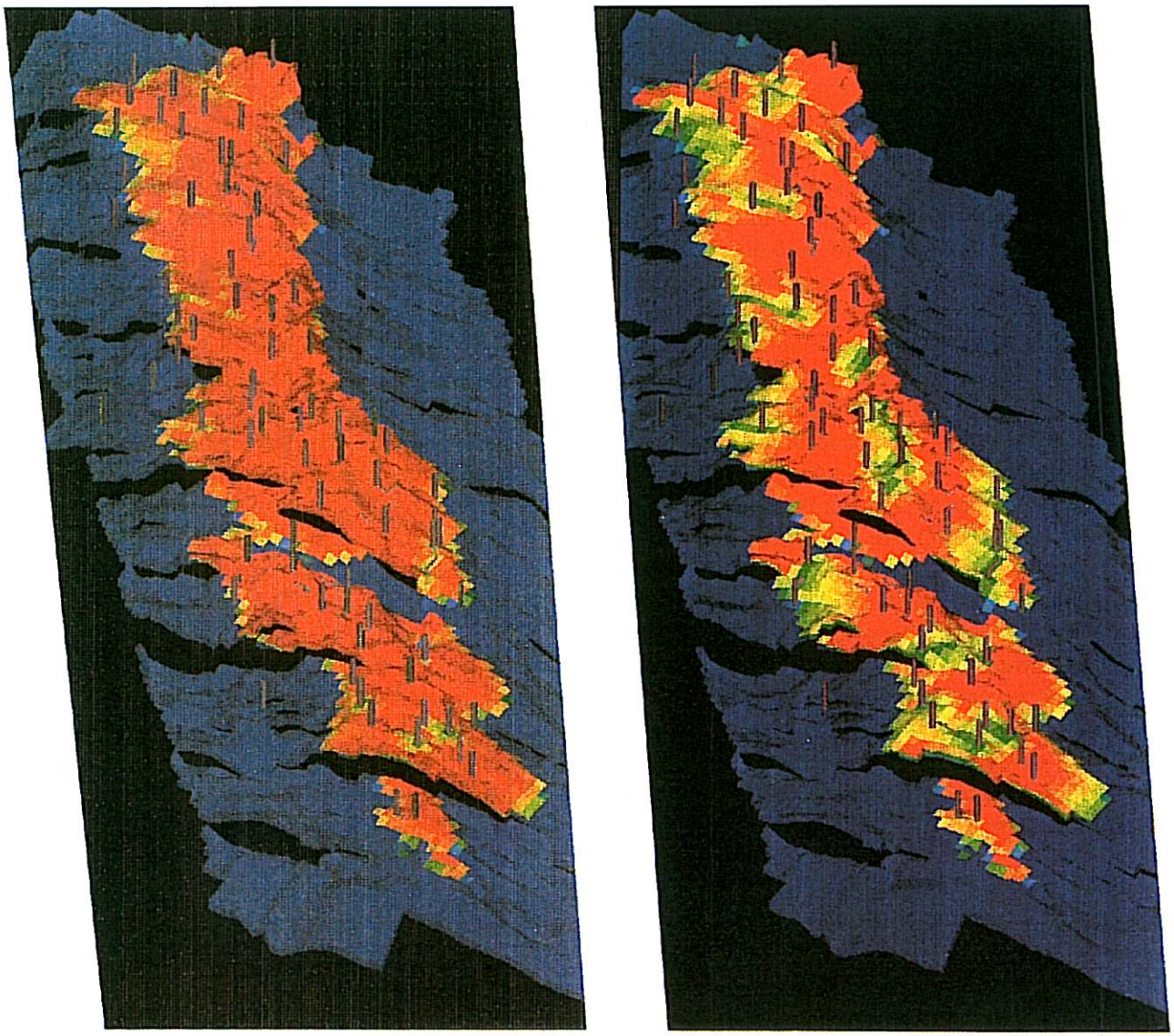


Fig. 6. Saturation maps.

provided by the Services Companies, as Survey tool MWD, geological steering, directional drilling, drilling bits... were integrated into a homogeneous package to result in a viable and cost-effective project. Thirty horizontal wells were drilled by CPTL in West Mabruk field between 1995 and 1999, including twenty-one, oil producers and nine water injectors. Today, a horizontal well costs around 20% higher than a vertical well when the Productivity Index is multiplied by about two.

The multi-drain technology was introduced in Mabruk field at the end of 1996 to be used as:

1. Delineation tool. The additional drain, drilled first, could be drilled in area where the seismic interpretation was doubtful. If the zone was not interesting, the drain would be plugged back and the main drain would be drilled as planned.
2. Enhance oil recovery tool. Additional drains should increase the reserve, increase the drainage efficiency and the well PI and reduce the CAPEX by reducing the well concentration in the field.

Multi-drains in Mabruk field are planar, i.e. all the drains are drilled at the same plane in the same reservoir. They are completed open-hole with commingle production assisted by artificial lift ("level 1" of multi-lateral technology).

The well architecture, given in figure 7, derives from the horizontal well design:

- The 12¼" section is drilled vertical. The 95/8" surface casing is set below the loss zone of AMUR
- A 8½" pilot hole can be drilled to Mabruk reservoir. The hole is then plugged and sidetracked. The KOP is around 50 feet below the 9⅝" casing shoe.
- The 8½" build up is drilled in medium radius (9°/100 feet) to reach the tight top layer of the reservoir (CARAPACE) at around 70°. inclination where the 7" production casing is set.
- The drain hole diameter is 6". The first drain is drilled as a standard horizontal well and any additional drain starts from an open hole side track.

With the benefit of C.P.T.L. experience in horizontal drilling, the open-hole multi-drain technology (including open-hole side track, re-entry...) was rapidly mastered. Nine multi-drain wells were drilled in Mabruk field with two up to four drains (see Fig. 8 A74H first quadrilateral well drilled in Libya) for a cost increase of 5% to 10% by branch. Conversely, the multi-lateral technology increased the well production by 50 to 100%, and reduced well concentration in the field by increasing the drainage area.

ARTIFICIAL LIFT OPTIMIZATION

An aggressive program of artificial lift is being also implemented to optimize the horizontal well production, otherwise limited with the beam pump located in the vertical section far above the reservoir. Submersible Electrical Pump (ESP) and, for the first time in Libya, Progressive Cavity Pump (PCP), were run in high deviated sections close to the pay zone, increasing typically a well production by up to 50% (Fig. 9).

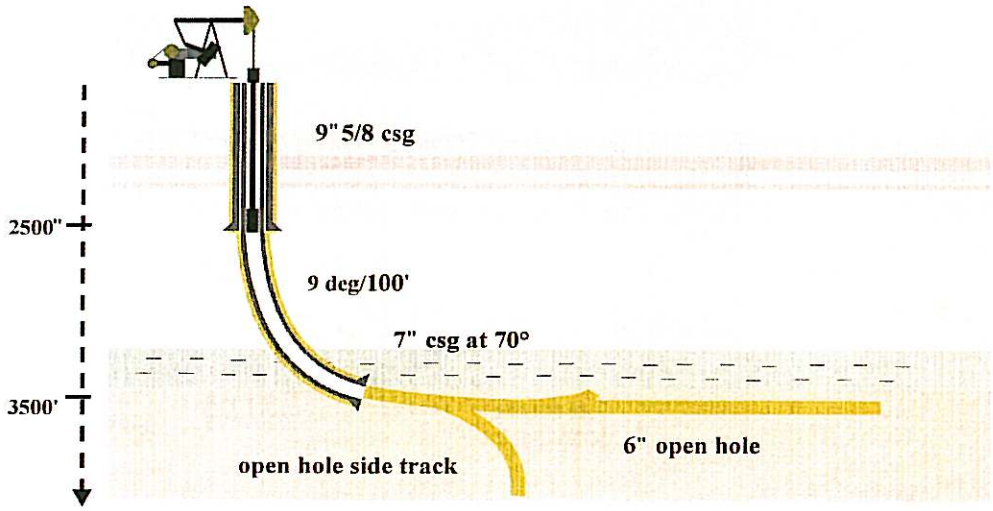


Fig. 7. Multi-drain well architecture.

* The early time data are governed by the capacity of high permeability medium (e.g. fracture network) connected to the well and the late time data by the transmissibility between this medium and a lower permeability/high capacity medium (e.g. matrix)

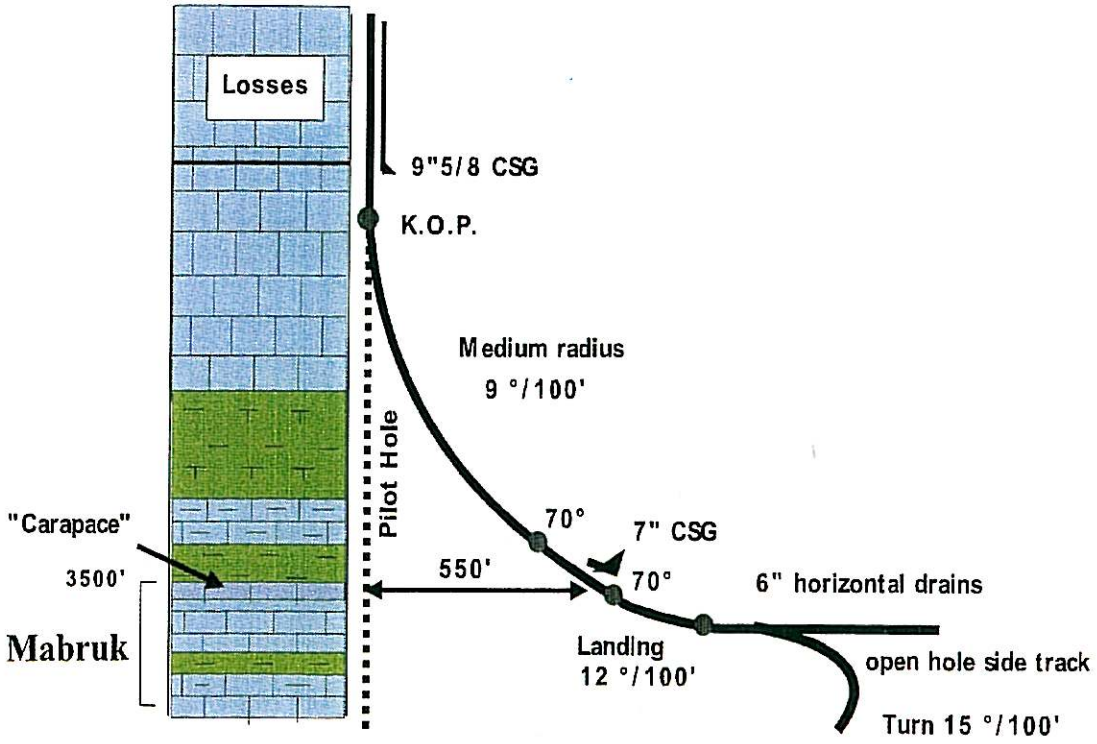


Fig. 8. A74H quadri-lateral well.

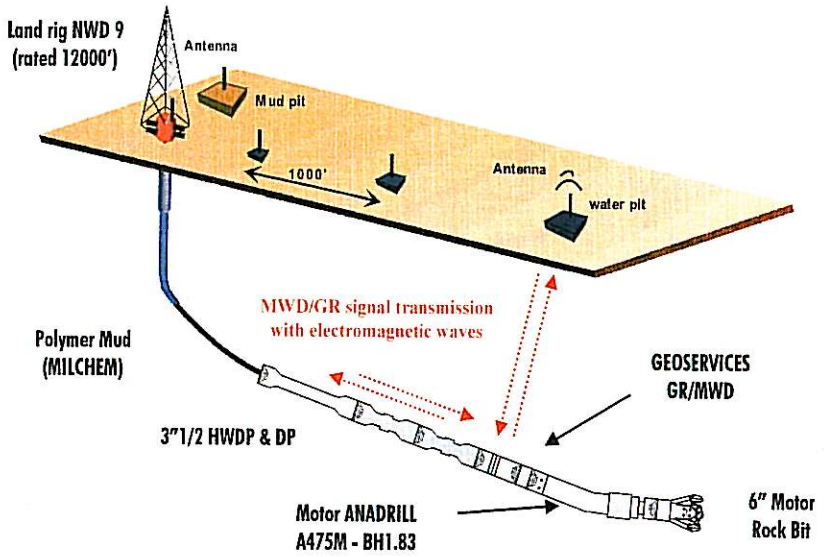


Fig. 9. Artificial lift optimization.

Petroleum Res. J. Vol. 14 (2002): P. 93-96

4D Case History in North Kuwait

Tim Perrin*

دراسة حالة بشمال الكويت باستعمال التحليلات السيزمية ذات الأربعة أبعاد

تيم بيرين

حقول النفط كاملة التكوين وخاصة بعض الشاسع منها على اليابسة في منطقة الشرق الأوسط قد تحتوي على مئات من آبار النفط تم حفرها على مسافات بينية متساوية الأبعاد.

وقد تكون هناك معلومات بتروفيزيائية وجيولوجية مفصلة ومعروفة عن كل موقع، ولكن هذه البيانات تكون صحيحة لمسافات قصيرة تتجاوز نصف قطر حفرة البئر بقليل، مما يتسبب في تفسيرات مشكوك بينها للمسافات الهائلة بين مواقع الآبار.

يعزز الحصول على المعلومات السيزمية ذات الثلاثة أبعاد وما لازمه من تفسير للمكمن ثقة مهندسي المكامن عند تفسيرهم نموذج بنية وطبقية المكمن بشكل كبير. وعند التخطيط لإدارة المكمن يميل في أغلب الأحيان مهندسوا المكمن إلى النمذجة العشوائية للإنتاج ومعدلات تدفق الحقن. إلا أن نماذجهم تتضمن العديد من المتغيرات والتي بعض منها غير معروف بدرجة عالية من الثقة، ونتيجة لذلك لا يوجد حل فريد لهذه المشكلة وتبقى الشكوك موجودة.

إن المعلومات السيزمية، لكونها تقييم محدد لنتاج مجموعة من الصفات المميزة، تعطي لقطة سريعة للمكمن في وقت معلوم من تاريخ المكمن. ويمكن إشتقاق التغير في البيانات السيزمية عند المكمن بادخال لقطة سريعة ثانية وثالثة وطرح مجموعة من البيانات الأخرى. وتمثل هذه التغيرات السيزمية التغير المطلق في خواص المكمن إلا أنها أقل وضوحاً من معلومات قاعدة بيانات البئر.

وبالإمكان عند هذه النقطة مقارنة نتائج نمذجة المكمن ببيانات الإختلافات السيزمية المقاسة وتحديث نموذج المكمن عن الحاجة. وبعد إعادة متكررة للنمذجة المتقدمة والتحسين بمضاهاة التجاوب السيزمي المقاس عن قرب يمكن توضيح نموذج مقبول للمكمن. ومن هنا تكمن إمكانية لتخطيط مواقع آبار أخرى وبدرجة عالية من الثقة بناء على تنبؤات تدفق الموائع وليس على أساس المسافات البينية المتساوية.

INTRODUCTION

Mature oilfields, especially some of the large onshore oilfields in the Middle East, may have hundreds of oil wells drilled, often on a regular grid. There may be detailed petrophysical and geological information known for each location. But this information is only valid over a short radius from the well bore. Therefore, uncertainty exists over the considerable distances between the well locations.

Acquisition of high resolution, 3D seismic data, and the subsequent interpretation of the reservoir, improves the confidence of the reservoir engineer's structural and stratigraphic model of the reservoir

*Schlumberger Geco-Prakla

enormously. Co-krigging of seismic attributes and well data can further improve the well model.

Reservoir engineers often turn to Stochastic modeling of production and injection flow rates to plan the management of the reservoir. However, their models include a large number of variables, some of which are not known with absolute confidence, and as a result there is not a unique solution to the problem and uncertainty exists.

Seismic data, a deterministic evaluation of the product of a combination of attributes, provides a snapshot of the reservoir at a defined time in the reservoir's history. By introducing a second or third snapshot, and subtracting one data set from another, the changes in the seismic data at the reservoir are derived. These seismic changes represent absolute changes in the reservoir characteristics, albeit with lower resolution than well based data.

At this point it is possible to compare the results of reservoir modeling with measured seismic difference data set, updating the reservoir model as necessary. After numerous iterations of forward modeling and refinement, a close match to the measured seismic response will indicate a reliable reservoir model. Clearly there is then potential to plan further well locations with confidence on the basis of fluid flow rather predictions rather than on a simple geometric grid basis.

GEOLOGICAL SETTINGS

The Albian Mauddid Carbonate reservoir in the Sabiriyah Oilfield of North Kuwait, is situated on broad north-south trending anticline on the Kuwait Arch.

The Mauddud Formation is a slope facies carbonate, which is preceded by fluvial sediments of the Burgan Formation, and overlain by basinal mudrocks of the Wara Formation. The Mauddud has a lower series of layered elastic and carbonate facies, and an upper series of carbonate facies, which progress, from compacted clay bearing layers at the base to cleaner carbonates at the top.

The Mauddud reservoir is approximately 90 m thick in the Sabiriyah Field. It is at 2100 m depth, has average porosity of 21% and average permeability of 31 millidarcies. There is, however, a high permeability layer 3-6 m thick which is thought to account for over 40% of fluid of injected water.

THE KOC WATERFLOOD EXPERIMENT

KOC were planning a water flood experiment in the Sabiriyah Field of North Kuwait in preparation for future wide scale injection programs. It consisted of an inverted 5-spot pattern, one water injection well surrounded by 4 production wells, making a square with sides approximately 600 m long.

4 D CONCEPT

Geco-Prakla made a series of presentations to KOC in 1996 and 1997 to demonstrate the concept of 4D seismic. Fluid movement caused changes in seismic attributes, which can be measured by carefully planned repeated 3D surveys, which are then subtracted from each other to reveal the lateral extent and magnitude of change.

Seismic data is a measure of the reflection coefficient between different layers of rock deep in the earth. It is directly related to acoustic impedance, and, therefore, to a selection of rock and fluid parameters, including the velocity, bulk moduli, density, porosity, water saturation, Poisson's ratio, temperature and pressure. Depending upon the situation several or all of these factors may be important.

FEASIBILITY OF 4D SUCCESS

It was decided that the Gassman Equations relating to the rock physical parameters were the most suitable for the reservoir conditions present in North Kuwait. Feasibility studies using these equations predicted potential time lapse results for several locations in Kuwait. Clastic reservoirs were expected to have up to 10% change in p-wave acoustic impedance, whereas carbonate reservoirs such as Sabiriyah were expected to have changes in acoustic impedance of up to 5%, and this assumes maximum potential replacement of oil with water.

With such a small potential change in acoustic impedance in carbonate reservoirs, the level of non-repeatable noise in the data set becomes significant. It was anticipated that this is likely to be up to 2% even in high-resolution good signal to noise data.

To verify the results of the feasibility studies, it was agreed to perform a small baseline 3D survey and a follow up survey. An area with high oil production was desirable as this would lead to early

results. The site of the KOC Water flood experiment was selected as a suitable area.

THE 4D EXPERIMENT

The layout of the 3D seismic surveys consisted of a static template of 8 parallel receiver lines 200 m apart with 60 traces at 50 m. Orthogonal and symmetrical to the receiver lines were 8 source lines 200 m apart with 60 source points at 50 m. An unweighted inline geophone array was used for the receivers, and a relatively heavy source effort was used to combat surface noise from roads and installations etc.

The Vaseline 3D survey was acquired in May 1997 prior to the start of water injection. By November 1997 when the repeat survey was recorded there had been 3 months of injection at a rate of about 10,000 bbls/day. The 3D data sets were processed by Geco-Prakla in Germany, under the direction of Roland Marschall.

The refraction static and velocity field were derived for the first data set and applied to both data sets. Whilst the same processing route was applied to both data sets there are going to be small differences due to determinist processes such as deconvolution, where different levels of noise will result in a different operator.

The final product from each data set was a 3D migrated cube, which had L1-norm deconvolution, followed by BORN-inversion for the high frequency part of acoustic impedance (AI). These acoustic impedance cubes were different to produce the final acoustic impedance difference cube.

Transit time changes through the reservoir due to velocity changes after water replacement result in spikes in the acoustic impedance difference cube, which are removed by median filtering.

The result at this stage is a map showing the change in acoustic impedance due to replacement of oil by water in the Mauddud Formation. This map can be calibrated as a saturation map, or fluid flow map.

RESULTS

The experiment proved that time lapse seismic could detect changes in reflection coefficient to map saturation changes within the reservoir.

The heterogeneity of the reservoir was shown by the saturation maps, and agreed closely with KOC own independently derived water cut maps.

Saturation maps derived from the 4D results can be used to plan future well locations, rather than simple geometric placement, resulting in higher efficiency and savings from reduced number of wells.

CREDITS

Geco-Prakla would like to thank Kuwait Oil Company for their permission to present material contained in this paper.

Processing and development work directed and performed by: Professor Roland Mershell, Chief Geophysicist, Geco-Prakla, Hanover, Germany.